Het verkeerskundig
laboratorium
voor studenten

ITS EDU LAB

Ramp metering: a microscopic control approach

A case study in the Netherlands

S. R. Klomp

28 April 2020

Rijkswaterstaat
Ministerie van Infrastructuur en Waterstaat

TU Delft

Colophon

Author	S. R. Klomp
Email	stefan32klomp@gmail.com
Graduation Committee	Prof. dr. ir. S. P. Hoogendoorn Chairman TU Delft, CiTG, Transport & Planning
	Dr. V. L. Knoop Daily supervisor TU Delft, CiTG, Transport & Planning
	Dr. ir. H. Taale External supervisor Rijkswaterstaat, dienst WVL TU Delft, CiTG, Transport & Planning
	Dr. J. A. Annema Secondary supervisor TU Delft, TPM

Published by	ITS Edulab, Delft
Date	28 April 2020
Status	Final report
Version number	1.0
Information	Henk Taale
Telephone	+31 88 798 2498

ITS Edulab is a cooperation between Rijkswaterstaat and Delft University of Technology

TU Delft

Rijkswaterstaat
Ministerie van Infrastructuur en Waterstaat

SUMMARY

INTRODUCTION

Congestion numbers are rising in the Netherlands. This leads to more travel time losses, increased pollution and increased safety risks. Thus, increased congestion leads to more social costs. Therefore, reducing congestion is desirable from a policy perspective.

Reducing congestion levels can be done in several ways. For example, efforts can be made to reduce road traffic demand. However, this proves to be difficult. Moreover, technology improvements in the connected and automatic vehicle sector might solve various congestion problems. Unfortunately, it is very questionable if and when these vehicles will have a high penetration rate on the roads. This could easily be decades from now. Therefore, this is not the solution to reduce congestion right now and any futuristic technologies are not considered in this research.

Besides the solution directions mentioned above, dynamic traffic management systems try to mitigate congestion levels as well. There are several alternative dynamic traffic management solutions, but most of them rely heavily on the compliance of drivers on advisory messages, either en-route or before the route has been determined. A dynamic traffic management alternative that does not rely on the compliance rate as much, is the ramp metering installations alternative.

Ramp metering installations try to prevent congestion on the main lane by controlling the flow of on-ramp vehicles merging onto the main lane. In various scientific studies, ramp metering installations have found to be effective. Mostly, the current ramp metering control concepts can delay congestion to emerge for approximately 15 minutes by cutting up platoons (groups) of merging vehicles into single merging vehicles. These single merging vehicles have a better chance of finding an appropriate gap in a time frame than multiple vehicles do. The current ramp metering control strategies are of a macroscopic nature, meaning they make use of average main lane flows to determine the flow that can be allowed onto the main road from the on-ramp. This means that the probability of a merging vehicle not being able to merge onto the main lane without causing a traffic jam is decreased. Nevertheless, the control structure is still dependent on probabilities. The question arises if this probability can be taken out of the equation. If this can be performed successfully, congestion might be prevented entirely due to the merging vehicles always having a required gap at disposal.

So, even though the current ramp metering algorithms already improve the situation, there might still be room for improvement. Namely, by getting rid of this probability factor by fitting on-ramp vehicles in measured gaps on the right lane of the main road. This fitting of the on-ramp vehicles in measured gaps, is called a microscopic ramp metering control approach. All this leads to the following research question in this thesis: **To what extent could a microscopic Ramp Metering (RM) control approach lead to less travel time delays compared to current alternatives?**

CURRENTLY USED RAMP METERING ALGORITHM

The currently used macroscopic ramp metering algorithm in the Netherlands is the Rijkswaterstaat ramp metering algorithm. This control structure makes use of both feed-forward and feed-back control. Primarily though, the feed-forward control is used in order to determine the upcoming flow of the main road. Considering the measured flow on the main road, a red time between two green phases for the traffic light is calculated. This waiting time in seconds is calculated by dividing 3600 by the difference between 6000 and the measured upcoming flow. However, if this red time is greater than 15 seconds or the measured upcoming flow is equal to or exceeds 6000 vehicles per hour, the maximum red time of 15 seconds is selected.

This red time is updated every 60 seconds. In other words, every 60 seconds an average main lane flow is determined by detector loops on the main road upstream of the ramp metering installation. Normally, the distance between the beginning of the merging area between the on-ramp and the main road and the location of these detector loops is 500 meters. However, for the considered site, this is only 200 meters. Therefore, a distance of 200 meters is used in this research.

After a single vehicle has received a green traffic light, loop detectors just downstream of the traffic light detect when to turn the traffic light back to yellow and red. When these loop detectors are triggered and the traffic light does not show the colour that should be shown, the traffic light colour will be changed accordingly.

The current Rijkswaterstaat ramp metering control structure is only activated when the flow on the main lane is higher than a certain threshold value or when the average main lane speed drops below a critical value. The flow related threshold value is currently 1500 vehicles per lane per hour. The ramp metering installation is deactivated again when the flow on the main lane is lower than the flow related threshold value. Furthermore, the ramp metering installation can be deactivated if a congestion is measured. This could also happen when a traffic jam that originated upstream of the controlled on-ramp spills back to the ramp metering site. However, deactivation due to congestion upstream of the controlled on-ramp is outside the scope of this research and is therefore not taken into consideration.

METHODOLOGY

The research question is answered by investigating the effects on the key performance indicators for ramp metering installations. This investigation is performed by means of simulations in a microscopic traffic simulation tool, 'the Open Traffic Simulator', which is developed by researchers at the Delft Technical University. The main key performance indicator to compare the microscopic ramp metering control approach with the currently used macroscopic ramp metering control and with the no control alternative, is are the travel time delays for the entire system. Furthermore, the travel time delays for the various origin-destination routes are identified as key performance indicators. To compare various microscopic ramp metering control parameter settings among each other, a successful merger percentage and a percentage of vehicles that had to wait too long will be examined. A vehicle is found to have been waiting for too long when the waiting time of that vehicle while being first in the queue exceeds 15 seconds. This is the maximum red time between two green phases in the Rijkswaterstaat ramp metering algorithm presently being used in the Netherlands.

A specific site will be analysed. This site has a three lane main road, since this is common in the Netherlands. Furthermore, a single lane on-ramp in order to have a single traffic light is recommended. Moreover, the off-ramp upstream of the controlled on-ramp should be considered as well, since vehicles taking this off-ramp can provide gaps on the right lane of the main road. These gaps in

turn can be filled by merging vehicles from the on-ramp. A site that does meet these requirements, is the A13 Delft-North on-ramp in the direction of Rotterdam. The network characteristics in terms of, for example, the truck percentage, vehicle demand, distance between several nodes and length of the on-ramp, will be used to draw up the network in the simulation tool.

In order to come up with the microscopic ramp metering control structure, several scientific papers regarding current macroscopic ramp metering installations have been consulted. Furthermore, opinions of experts have been reviewed and personal ideas have been used.

The main idea behind the microscopic ramp metering control approach is to let on-ramp vehicles merge into measured gaps. To do this, first the location of the gap measurement detector locations has to be determined. This requires some information. Basically, the acceleration distance of the on-ramp vehicles before the merging manoeuvre and the travelled distance of the measured gap have to be known. To determine the travelled distance of the gap, the acceleration time of the merging vehicle and the speed of the main lane has to be known. The speed of the measured gap is assumed is assumed beforehand and not individually measured in this research for the sake of simplicity. Additionally, to compute the acceleration distance and acceleration time of the merging vehicles, the desired merging speed and the acceleration trajectory of the merging vehicles has to be known.

Since the determination of the gap measurement location is fundamental for investigating the quantified effects of changing the macroscopic nature of ramp metering installations into a microscopic one, an experiment to gain insight in the acceleration trajectories of the on-ramp vehicles has been performed. This was done by filming the current ramp metering installation at the considered site, extracting vehicles trajectories from the video footage and then determining the maximum acceleration and used power by these accelerating vehicles. After that, a normal distribution for the maximum acceleration was fitted around these data points, which in turn is given as an input in a simulation tool.

MICROSCOPIC CONTROL STRUCTURE

The maximum acceleration of trucks and passenger cars differ greatly. In order to fit these vehicles in the gaps accurately, a gap detector loop for both groups was placed at different locations. Unfortunately, the field experiment only had enough data to fit a distribution around the maximum acceleration for passenger cars. Therefore, a normal distribution was fitted for the trucks, based on a different mean value, which was taken from another study, but including the same standard deviation value as for the passenger cars. For both normal distributions, a maximum and minimum was provided to prevent negative maximum acceleration or unrealistically high maximum accelerations.

Due to this difference in the average acceleration, a prolonged red time has been scheduled for a waiting passenger car if it follows up a truck. This is done to ascertain that the same gap is not used twice due to double measurements following the two different gap detector loop locations, while it can only fit one vehicle. Thereby, it is also ensured that a passenger car is not obstructed by a truck when it has to accelerate to get to the measured gap in time. In this thesis, the required minimum gap for trucks and passenger cars is assumed to be equal for the sake of simplicity.

Just as in the Rijkswaterstaat algorithm, detector loops downstream of the traffic light are located to observe when the traffic light needs to turn back to yellow and red. Similar to the currently used ramp metering algorithm, the microscopic ramp metering approach gives green for only a single vehicle at a time. Moreover, the microscopic ramp metering installation uses an activation and deactivation measured flow threshold as well.

Unfortunately, the simulation tool causes traffic congestion when the ramp metering installation has been active for some time and the measured flow drops just below the deactivation threshold value. This is the result of all waiting vehicles being led onto the merging area simultaneously, while there is insufficient space to let all vehicles merge onto the main lane without harsh braking manoeuvres. This in turn leads to congestion. Therefore, it was chosen to not deactivate the ramp metering installations at all, unless the flow on the main road reaches below 500 vehicles per lane per hour and the speed is in the free flow speed branch of the fundamental (traffic flow) diagram.

RESULTS

Several conclusions can be drawn regarding the results. The main conclusion is that the developed microscopic ramp metering control approach could lead to less travel time delays compared to the no control and current Rijkswaterstaat alternatives. However, how much travel time can be saved depends on several factors. These factors include:

- The presence of a semi-permeable lane demarcation, preventing merging manoeuvres from the main road onto the right lane of the main road;
- The speed limit;
- Truck percentage on the on-ramp;
- The main lane, on-ramp and off-ramp demand.

Concerning some numbers of the average saved travel time per vehicle for the entire system, it was found that the microscopic ramp metering control approach could increase the average travel time savings for the entire system up to 36 seconds compared to the currently used Rijkswaterstaat algorithm. The exact value depends on the used combination of microscopic settings. When a more robust combination of microscopic settings is chosen, an average travel time saving of 13 seconds per vehicle was observed. The Rijkswaterstaat ramp metering algorithm already saves 25 seconds on average, making the proposed microscopic ramp metering approaches potentially save either 38 seconds or even 61 seconds in comparison to the no control alternative.

Regarding the presence of semi-permeable lane demarcation, it was found that all simulated alternatives benefit from its implementation. The lane demarcation used in this thesis starts at the end of the off-ramp and continues all the way to the end of the merging area between the on-ramp and the main road. This semi-permeable lane demarcation is present at several other sites in the Netherlands. The largest gain with the presence of the lane demarcation is found for the microscopic control approach. Due to reducing the probability of a measured gap being filled by a non-merging vehicle, it helps preserving measured gaps. Therefore, the merging vehicles have an increased chance of having a gap at their disposal, reducing the probability of a congestion kicking in.

Furthermore, the main lane flow is a decisive factor. When this flow is not high enough to enforce the maximum waiting time for the on-ramp vehicles during an activated Rijkswaterstaat ramp metering installation, the travel time savings of the microscopic ramp metering control approach decreases in comparison to the currently used algorithm. This is due to the fact that the microscopic ramp metering approach mainly saves travel time for the on-ramp vehicles, while minimising the extra delays for the main lane vehicles at the same time. In the base case scenario in this research, the main lane demand might be higher than in the real life situation. This is a result of having to use a higher main lane demand than recalled in the traffic data database to cause congestion in the simulation tool. Thus, the actual

average travel time savings for the microscopic ramp metering approach might be less than found in this research.

Moreover, the off-ramp demand is an important factor in the success of the microscopic ramp metering approach. A sufficient off-ramp traffic demand is required to get gaps on the right lane of the main road frequently enough. In the base case scenario, the used off-ramp demand was lower than the real life situation, since a higher off-ramp demand ratio caused congestion at the off-ramp in the simulation tool, interfering with the simulation results. An increase in the number of on-ramp vehicles should also benefit the microscopic ramp metering control approach, since the travel time savings for the on-ramp vehicles compared to the Rijkswaterstaat algorithm are higher than for the main lane vehicles when the main flow is high.

Additionally, the truck percentage on the on-ramp is a crucial factor while determining the success of the microscopic ramp metering approach. A truck percentage higher than 5% (e.g. 10%) results in less travel time savings on average. Apparently, the current microscopic ramp metering algorithm works better with passenger cars than with trucks. This could have multiple reasons. For instance, the gaps are measured further upstream, giving the trailing vehicle of the gap more time to close the gap. However, another likely contributor is that trucks need larger gaps than passenger vehicles, which is not present in the current microscopic ramp metering approach. Therefore, it is recommended to investigate if using a larger minimum required gap time for trucks would increase the effectiveness of the microscopic ramp metering control approach for trucks.

The speed limit is also an important factor. When the speed limit is adjusted to $80\frac{km}{hour}$ or $120\frac{km}{hour}$ instead of $100\frac{km}{hour}$, the microscopic ramp metering approach performs considerably worse. This could be a consequence of the fact that the required minimum gap times to merge changes with the speed of the vehicles. This minimum required gap time was not adjusted according to the speed limits (or measured main lane speed) in this research. Furthermore, the speed on the main lane can fluctuate more with a higher speed limit, increasing the probability of a mismatch between the merging vehicle and the measured gap when using an assumed main lane speed. Moreover, it was concluded that the location of the gap measurement loop detectors was not entirely correct in these adjusted speed limit scenarios, concluding from the low successful merger percentage. Getting the location of the gap measurement detectors right is very important when using this microscopic approach. Thus, it is recommended to adjust the minimum required gap time for different main lane speeds. Additionally, it is suggested to measure the speed on the main lane of the leading vehicle of the measured gap and use that speed as the travelling speed of the gap to improve upon the developed algorithm.

Furthermore, the average acceleration of the on-ramp vehicles should be accurately known in order to correctly place the gap measurement loop detectors. In the chosen simulation tool however, the average acceleration fraction of the maximum acceleration seems to be too high, considering the results of the acceleration field experiment. This was not adjusted to leave the standard driver behaviour scripts by OpenTrafficSim (OTS) intact. It might be worth investigating the results of a similar project when using a steeper decline in the acceleration during the acceleration trajectory of the on-ramp vehicles.

CONCLUSION

To summarise, the microscopic ramp metering approach seems to be effective in reducing travel time delays. Moreover, the developed algorithm still has room for improvement. It is believed that a combination of the already existing Rijkswaterstaat control structure and the microscopic ramp metering approach could provide the best algorithm. This would be accomplished by using the Rijkswaterstaat algorithm when the flow on the main lane is between the activation flow of 1500 vehicles per lane per hour and some threshold value and using the microscopic ramp metering approach when the flow on the main lane is above this threshold value. This threshold value could be chosen in such a way, that it is equal to the flow value when the average waiting time with the microscopic ramp metering approach is equal to the average red time for the Rijkswaterstaat algorithm. When using a required minimum gap time of 1.8 seconds in the base case scenario for the microscopic approach, this results in a flow of 1867 vehicles per lane per hour. This way, the microscopic ramp metering approach would be used when this algorithm provides the highest average flow of on-ramp vehicles onto the main road. The Rijkswaterstaat algorithm would be used when this algorithm supports the highest flow from the on-ramp onto the main lane. Regarding the average travel time delays for the main lane vehicles, this was found to be very similar for the two algorithms. Thus, the largest benefits for the entire system when using these ramp metering installations are gained by limiting the delay for the on-ramp vehicles.

ACKNOWLEDGEMENTS

I would like to thank my committee, Victor Knoop, Henk Taale, Jan Anne Annema and Serge Hoogendoorn for helping me performing this research and writing this report. They have provided valuable insights and have supported me throughout the process. Additionally, I would like to thank Wouter Schakel for helping me with programming in the simulation tool. Without his help I would have had a much harder time to get to the eventual code. Furthermore, I would like to give a special thanks to Johan Groenenwold, Erik van de Laak and the other employees at Rijkswaterstaat for the comments they gave me during interviews and conversations.

Moreover, I want to thank my family, Luuk, Mirjam and Judith for standing by me throughout this research, but also throughout all my academic years. The same can be said about my friends, Iris Vendrik, Rick Overvoorde, Remco Troquete, William van Lindonk, Ilias Bouhannouche and Marcel Kool. Especially the first four mentioned friends, who were all in the same study phase as me. A special thanks to William van Lindonk for helping me to conduct the acceleration experiment.

Lastly, I would like to thank my girlfriend, Miranda Meuldijk, for standing by me throughout the entire master phase and supporting me all the way. Additionally, she helped me relax a bit when I was analysing my research too much and when I was overthinking my simulation runs. She made sure I was not working all day long. Especially during the busy finishing weeks, she has been a bright spot in my life.

CONTENTS

LIST OF FIGURES

LIST OF TABLES

ACRONYMS

AMOC Advanced Motorway Optimal Control . . . 12
CORSIM CORridor SIMulation . . . 16
DRIP Dynamic Route Information Panel . . . 2
DTM Dynamic Traffic Management . . . 2
MI&W Ministry of Infrastructure and Water-management . . . 2
IDM Intelligent Driver Model . . . 23
ITS Intelligent Transport System . . . 18
KPI Key Performance Indicator . . . 23
MITSIM MIcroscopic Traffic SIMulator . . . 16
MOTUS Microscopic Open Traffic Simulation . . . 16
MPC Model Predictive Control . . . 19
MSE Mean Squared Error . . . 23
OD origin-destination . . . 25
OTS OpenTrafficSim . . . vii
PARAMICS PARallel MICroscopic Simulator . . . 16
RM Ramp Metering . . . iii
RMI Ramp Metering Installation . . . 1
TTS Total Time Spent . . . 12
VISSIM Verkeer In Steden SIMulatiemodel . . . 16
VoT Value of Time . . . 1
VSL Variable Speed Limit . . . 2

1 INTRODUCTION

This chapter contains an introduction to the research. This includes some background information on the current traffic state in the Netherlands and an introduction to Ramp Metering Installations (RMIs). Furthermore, a figure that shows the research structure is provided. Lastly, an overview of the remaining report structure will be presented.

1.1 CONGESTION, ITS CONSEQUENCES AND CURRENT MEASURES

The number of registered cars in the Netherlands has been increasing over the last years. For example, at the first of January last year (2019), the Netherlands had 12.7 million registered motorised vehicles. This was an increase of 227 thousand compared to the first of January 2018 (CBS, 2019). Alongside this increase in registered motorised vehicles, congestion numbers (length times duration) have been steadily increasing since 2015. In 2018 for example, an increase of 20% has been observed (ANWB, 2018). The total number of traffic jams, the total congestion kilometers and the total travel time losses are all increasing. Additionally, the records for most total congestion kilometers in both the morning and evening peak have been broken in 2019 (NOS, 2020b).

Congestion leads to several unwanted effects. The most obvious consequence of congestion is that vehicles are not able to drive at free flow speed anymore. This causes an increase in the travel times. Travel times that are higher than the free flow travel times are so called travel times losses. The social costs of these travel time losses can be calculated by multiplying the average travel time delay per vehicle by the traffic volume, multiplied by the Value of Time (VoT) (Goodwin, 2004). Last year, just in the Netherlands alone, traffic congestion cost freight traffic 1.4 billion euros (Panteia, 2019). However, congestion has more negative consequences than only an increase in the travel times (Calthrop and Proost, 1998).

One of these additional negative externalities is that congestion also influences the number of road accidents. It is believed that congestion leads to more accidents than free flow road conditions. However, the severity of the accidents decreases in congestion conditions due to lower speeds. Therefore, it is concluded that congestion actually leads to less social costs, since especially fatalities drive the social costs of road accidents (Schefer and Rietveld, 1997; Theofilatos and Yannis, 2014; Yau, 2004).

Furthermore, road congestion has a negative effect on the environment. In Barth and Boriboonsomsin (2009), it is concluded that (very) low speeds contribute more to the emission of carbon dioxide than regular free flow highway speeds of 80 $\frac{km}{h}$, 100 $\frac{km}{h}$ and even (but to a lesser degree) 130 $\frac{km}{h}$. Furthermore, congestion results in increased PM_x emissions. This increase poses health risks, as concluded by Levy et al. (2010).

In order to reduce these negative consequences, efforts are being undertaken to reduce congestion. Several ways to prevent congestion at all or to mitigate the severity have been thought up and some of them have been tested or have even been implemented. Reducing congestion can be achieved by different approaches.

A relatively straightforward approach to combat congestion is to add on to the existing infrastructure. However, this proves to be an approach that faces a lot of resistance. Besides the fact that some congested roads do not have enough room to expand, adding on to the existing infrastructure is undesired by various political parties. The political arguments against building more infrastructure are mostly of an economic or environmental nature (Van der Berg, 2017; Papageorgiou and Kotsialos, 2002).

1.1.1 Demand approach

Another measure that could be taken in order to mitigate congestion problems is reducing the traffic demand. This could be accomplished by achieving a modal shift. In this case, that means reducing the number of cars on the road by moving drivers to opt for other transport modes, like trains for instance. The Ministry of Infrastructure and Water-management (MI&W) has explicitly expressed their interest in making travellers take the train more often in an effort to reduce the negative impact of travelling on the environment (Rijkswaterstaat, nd). In the first half year of 2019, the number of train passengers increased more than expected. In essence, it seems that the goal of having more train passengers is being achieved. However, regardless of the increase in train passengers over the past period, there are no signs of a decrease in the road congestion numbers, as stated in the beginning of this chapter. Moreover, if the growth in the number of train passengers continues at this rate, it is expected that in 2027 the capacity on the tracks can not be increased anymore (NOS, 2019a,b).

Another way to reduce the road travel demand is making drivers change their departure time and/or route pre-trip. In order to be able to change the routes before leaving, the travellers need to know the traffic situation. This information can be obtained by the traffic information on the radio and via traffic information apps, like Google Maps. Travellers could also opt for adjusting the departure time. Even though these data gathering options have already been enrolled for quite some time, congestion in the Netherlands is still increasing.

A policy that has not been implemented yet, but would accommodate in changing route and/or departure time choices, is dynamic road pricing. In Eliasson and Mattsson (2006), it is concluded that road pricing indeed works and that the total time spent in the traffic system decreases. However, road pricing has been proven to be politically difficult for decades. Therefore, it currently seems unlikely that road pricing will be the solution to tackle road congestion in the near future (Giuliano, 1992; Vereniging Zakelijke Rijders, 2017).

1.1.2 Dynamic traffic management approach

Besides these demand approach solutions, Rijkswaterstaat and research institutes like the Delft University of Technology have also been thinking of solutions to reduce congestion levels with en-route adjustments instead of pre-trip adjustments as mentioned above. The overarching term for this solution direction is called Dynamic Traffic Management (DTM).

One of these en-route DTM measures is the application of Dynamic Route Information Panels (DRIPs). These panels inform the drivers on which route to take and/or which not to take due to congestion. In Hoogendoorn (1997), it is found that this is an effective measure to reduce congestion. However, the compliance rate of drivers needs to be sufficient in order to obtain these results.

Implementing a Variable Speed Limit (VSL) is effective in reducing the backward propagation movement of wide-moving jams. This is done by lowering the speed limits by means of dynamic information panels (Bergan and Bushman, 2004; Bertini et al., 2006). However, just like the DRIPs measure, this solution is heavily dependent

Figure 1.1: Ramp metering system in the Netherlands, A2 Maarssen-oost (Middelham and Taale, 2006)

on the compliance of drivers (Hellinga and Mandelzys, 2011). The effectiveness will be reduced if drivers do not follow the posed variable speed limits.

Ramp Metering (RM) algorithms attempt to delay or even prevent traffic congestion by reducing the inflow on the main lane from an on-ramp. Additionally, the congestion levels are decreased by splitting up the platoons of merging vehicles into single merging vehicles (Chaudhary and Messer, 2000). A traffic light is used to accomplish both of these means. This way, the number of possible conflicts by the absence of a large enough gap to fit all merging vehicles is decreased. In the Netherlands, Rijkswaterstaat is responsible for implementing RMIs (Middelham and Taale, 2006). An example of such an RMI in the Netherlands can be seen in Figure 1.1. Additionally, an overview of how RM works in general, is shown in Figure 1.2. A more in-depth analysis on the working of RMIs is provided in Chapter 2.

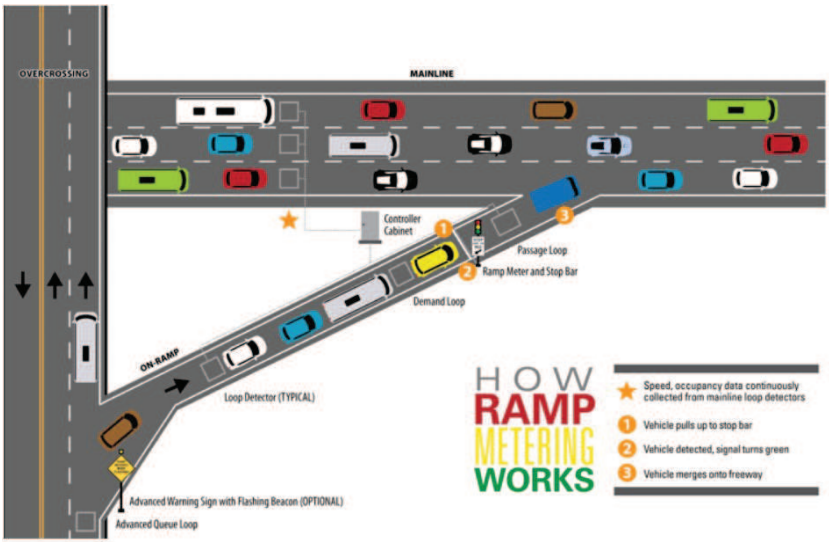

Figure 1.2: The working of a Ramp Metering Installation, simplified (NOACA, 2016)

1.1.3 Autonomous and connected vehicles

A final solution direction to reduce road congestion is in the field of autonomous and connected vehicles. Decreasing congestion numbers would be achieved, since autonomous and connected vehicles would be able to drive more closely to each other, increasing the capacity on the road. Furthermore, the rise of autonomous and connected vehicles would decrease the number of road accidents, consequently decreasing the number of congestion that arises as a result of road accidents (Darbha et al., 2018; Talebpour and Mahmassani, 2015).

However, realising the (full) integration of these autonomous and connected vehicles is difficult and hard to control by government institutions like MI&W and Rijkswaterstaat. The (full) integration could be decades away, especially, since certain laws would have to be changed and cyber threats have to be eliminated (Kohler and Colbert-Taylor, 2014; Parkinson et al., 2017). Unfortunately, the congestion problems are already present today. Therefore, until the (full) integration of autonomous and connected vehicles is accomplished, efforts should be made in order to find a solution that can be implemented in the short term. Thus, although autonomous and connected vehicles could be a very powerful solution, this is not the solution to reduce congestion problems in the near future.

1.2 PROBLEM STATEMENT AND RESEARCH OBJECTIVE

Concluding from the previous section, DTM is the best solution direction in order to reduce traffic congestion in the short term. However, two of the three aforementioned approaches in the DTM solution direction are of an advisory nature. These solutions are using DRIPs and implementing a VSL. The effectiveness of these alternatives rely heavily on the compliance of drivers (Hoogendoorn, 1997; Kang et al., 2004; Papgeorgiou and Messmer, 1991). In Bonsall and Joint (1991) it is shown that just 35% of all drivers fully follow up the traffic management advice. This exact percentage may be different though, since the precise compliance rate depends on several factors and can hence not be predicted definitely. Yet, concluding from interviews with employees at Rijkswaterstaat and the Delft University of Technology, the actual compliance rate in the Netherlands for DRIPs is probably lower. Similarly, drivers in the Netherlands tend to not fully comply with the speed limits as provided by VSL and dynamic road information panels. Drivers tend to lower their speed later and to a lesser degree than suggested by the dynamic road information panels. Summarising, the effectiveness will be limited as long as the drivers do not follow the messages more strictly.

RMIs seem to have a higher compliance rate. This is not only found in scientific papers, but this is also empirically observed during this research. This is probably due to the fact that drivers would have to run a red traffic light if they would not comply with an RMI. Therefore, an RMI is a more powerful instrument than a VSL and than DRIPs. Nonetheless, the effectiveness of current RM algorithms shows room for improvement, as stated in Chapter 2. Consequently, the objective of this research is to explore the effects on the travel time delays of a microscopic RM control approach compared to the current alternatives.

In order to investigate the effects of a microscopic RM control approach on the travel time delays, the acceleration distribution, including the average acceleration, of the on-ramp vehicles at RMIs in the Netherlands has to be known. This is necessary to predict the relative travelled distance of the measured gap on the main lane to the merging vehicle. Currently, this acceleration distribution is not known yet. Thus, an experiment will be performed in this research to obtain an acceleration distribution.

1.3 RESEARCH QUESTION

As mentioned before and as will be mentioned in Chapter 2, it is proven that ramp metering works, but there might still be improvements possible. Therefore, further research is desired. The research described in this report will revolve around the following research question: **To what extent could a microscopic Ramp Metering (RM) control approach lead to less travel time delays compared to current alternatives?** In order to be able to answer this research question in a structured way, the following sub-questions are defined:

1. What combination of characteristics of the microscopic Ramp Metering (RM) control approach attains the best travel time savings results?
2. How does the microscopic Ramp Metering (RM) control approach stack up against the no Ramp Metering Installation (RMI) control alternative?
3. How does the microscopic Ramp Metering (RM) control approach compare to the currently used macroscopic Rijkswaterstaat Ramp Metering (RM) control approach?

1.4 RESEARCH SCOPE

As can be seen in the previous section, the research revolves around highways with an on-ramp. When considering highway congestion, the underlying network has to be considered as well, since too much spillback from the on-ramp would lead to extra congestion on that network. However, to simplify testing of the control strategies, the underlying network will not be taken into account in this research. The traffic flow from the on-ramp onto the main road will be taken into account. When considering this traffic volume, at least comparisons between the achieved on-ramp traffic flows for the various control alternatives can be conducted.

Furthermore, an isolated on-ramp will be tested for the sake of simplicity. This means that adjacent on-ramps and bottlenecks will not be simulated. Moreover, only one site will be tested due to time constraints. It could be that using another layout for a site gives different results. The chosen site in this study will be in the Netherlands, since the research is in name of two Dutch organisations. These are the Delft University of Technology and Rijkswaterstaat.

As can be derived from the previous sections in this chapter, the conducted research that is described in this report only considers RMIs as a solution for the current congestion problems. The newly proposed RM control structure, as described in Chapter 4, will be tested against the current Rijkswaterstaat RM control (as described in Chapter 2) and no control at all. All situations will be simulated and the results of these simulation runs will be the means of comparison between the three alternatives.

1.5 RESEARCH AND REPORT STRUCTURE

The research described in this report has been performed in multiple stages. The chronological order is shown in Figure 1.3 and is displayed from top to bottom. Furthermore, the outgoing arrows indicate which subsequent processes are affected by the results of that process. The literature review and the expert interviews are processes that were undertaken during the entire research. Moreover, the chapters wherein the findings of a process can be found, are also included in the rectangles.

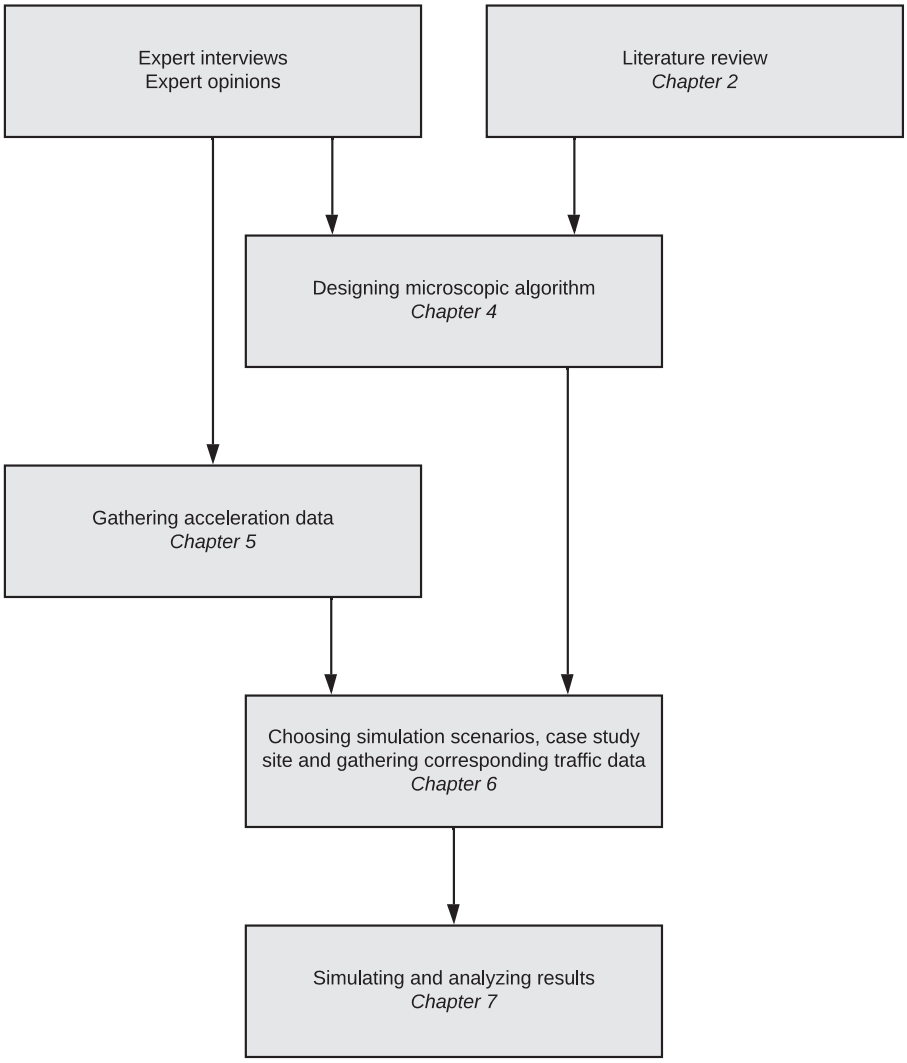

Figure 1.3: Research structure

However, not all chapters are mentioned in Figure 1.3. All in all, two chapters are not present in Figure 1.3. The first missing chapter is chapter 3, which describes the methodologies used in this research. The second missing chapter is the final chapter of this report. This chapter includes the conclusion, recommendations and the discussion.

Thus, this report will continue on after this first chapter with chapter two, which entails a literature review and the research gap. Thirdly the used research methodologies will be outlined. Fourthly, the developed microscopic ramp metering algorithm will be explained. Fifthly, a chapter elaborating upon determining the acceleration distribution in the Netherlands will be included. Sixthly, the simulation setup of this research will be described. Seventhly, the results regarding multiple scenarios will be outlined. Finally, a chapter regarding the conclusion and recommendations following the research will be outlined.

2 LITERATURE REVIEW

Now that the goals of the research have been introduced and scoped in Chapter 1, this chapter discusses the literature that will be used for performing the study. How this literature review has been performed, will be explained in Chapter 3. Firstly, literature on the goals of Ramp Metering Installations (RMIs) will be covered. Secondly, scientific literature regarding control strategies will be discussed. Thirdly, literature on the currently used macroscopic RM algorithm will be outlined. Finally, scientific literature about the simulation software will be covered.

2.1 RAMP METERING

RMIs are located at on-ramps. Since the inflow of the main road together with the on-ramp lane can easily exceed the capacity of the downstream area, traffic jams can be commonly expected around such areas (Ahn et al., 2010). Thus, on-ramps are responsible for a large number of traffic jams. Therefore, taking a closer look at these road sections could lead to an increase in total travel time savings. In these merging areas especially, a lot of possible conflicts (between the merging vehicles and the vehicles on the main lane) arise (Chin and Quek, 1991; Yang and Ozbay, 2011). Reducing the number of possible conflicts and its severity, thus making the traffic drive more fluently, would decrease the traffic oscillations and would consequently result in less congestion. A lot of these conflicts occur due to the lack of gaps that are large enough to fit the merging vehicles on the main lane. In other words, there are no gaps available in the stream, which are sufficiently large to allow the vehicles from the on-ramp to merge without enforcing a braking manoeuvre to another vehicle on the main road (Knoop et al., 2018). Therefore, synchronising the inflow with the gaps in the main lane flow is considered to be an interesting solution direction. Since this is what RM tries to do,n RM could reduce the total congestion numbers, if it is working properly.

The goal behind any RM algorithm is to prevent (or delay) the onset of congestion, preventing the capacity drop, on the "protected" road. As can be seen in the fundamental diagram in Figure 2.1, the free flow branch extends to the critical vehicle density (K_{ko}) and critical speed (V_{ko}) values. These values are called critical, since a traffic congestion will emerge when the vehicle density exceeds this critical density value, causing the speed to drop below the critical speed value. As the density on the road increases towards K_{ko}, the speed will gradually decline until at some moment K_{ko} is reached and the speed suddenly drops to the congested branch of the diagram. Once this happens, the density will have to be reduced towards $K_{go,min}$ before the pre-congestion flows on the free flow branch can be attained again. Translated to practice, this entails that the goal of any RMI algorithm is to maintain the density on the "protected" road somewhere between $K_{go,min}$ and K_{ko} in a way that maximises the flow, while the probability of congestion emerging is minimised. In traditional RM algorithms this goal is reached by limiting the flow from the on-ramp to a sufficient level, thus shaving the peak.

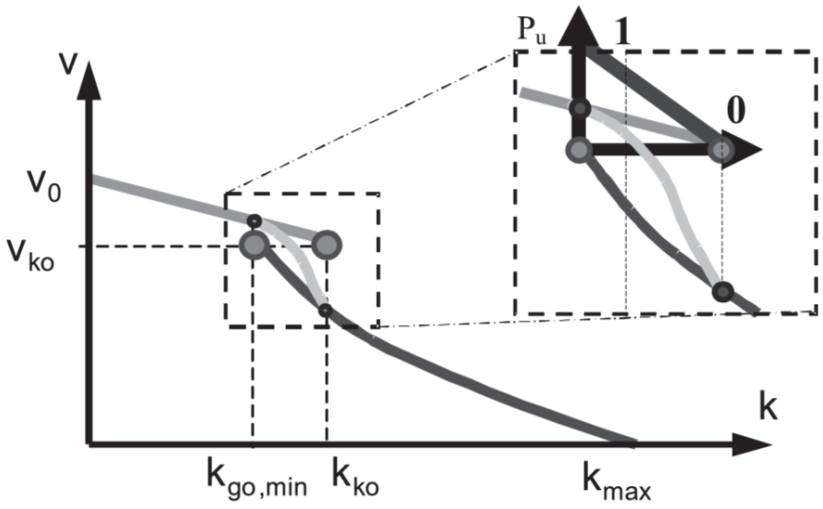

Figure 2.1: The fundamental diagram in the speed-density plane by (Wu, 2002)

Instead of using the density as a criterion for determining the inflow, some algorithms use a flow level. This does not alter the principle, but may affect the results of the algorithm, as will be shown in the remainder of this section. Summarising, RM algorithms attempt to delay or even prevent traffic congestion by reducing the inflow on the main lane from an on-ramp and by splitting up the platoons of merging vehicles into single merging vehicles (Chaudhary and Messer, 2000). Rijkswaterstaat is responsible for implementing RMIs in the Netherlands (Middelham and Taale, 2006). An example of such an RMI in the Netherlands can be seen in Figure 2.2.

Figure 2.2: Ramp metering system in the Netherlands, A2 Maarssen-oost (Middelham and Taale, 2006)

Ramp metering has been found to be effective in multiple studies. In most cases, RM is able to postpone the congestion tipping point and sometimes even to prevent congestion at the specific site altogether. In Persaud et al. (2001) for example, this effectiveness is underlined.

2.2 CURRENT RAMP METERING STUDIES

Although RM has been found to be an effective measure in reducing congestion to at least some extent, it is clear from the variety of algorithms that an universally optimal solution has not been found yet. The first control structures were not traffic responsive. They were traffic demand responsive, where the traffic demand was predetermined based on predictions regarding the traffic demand (Wattleworth, 1965). Although these already had some positive results, there was plenty of room for improvement. As a result, various traffic responsive RM control strategies have been designed and tested throughout the years. In Table 2.1, a selection of these approaches is displayed. Herein, question marks indicate that no concluding remarks were found in scientific literature.

Table 2.1: Control strategies overview

	Macroscopic	Feed-forward	Feed-back	Real-life tested	Highway tested	Effectiveness	Robustness
ALINEA	Yes	No	Yes	Yes	?	+	++
Zhang	Yes	Yes	Yes	?	?	++	+
AMOC	Yes	?	Yes	Yes	Yes	++	+
RWS	Yes	Yes	Little	Yes	Yes	+	+

2.2.1 ALINEA

An example of an RM algorithm is called ALINEA. This control structure was proposed in a paper by Papageorgiou et al. (1991). A strength of this algorithm is that it uses feed-back control. Feed-back control strategies are less sensitive to prediction errors. Feed-back control strategies measure the output flow of a system and adjust their control accordingly. This is in contrast to feed-forward control systems, which use predictions of the output. These predictions are made by combining the upstream measured traffic flow and the flow that is let onto the main road from the on-ramp. This upstream measured traffic flow is used as an input when determining the on-ramp flow let onto the main road to achieve the desired output. Furthermore, ALINEA uses the occupancy instead of the flow, since the critical occupancy is less sensitive to fluctuations in external variables, like weather conditions, than the flow.

In order to accomplish the mentioned control structure, ALINEA uses only one loop detector downstream of the merging area, at which the occupancy is measured. Then, knowing the critical occupancy of the road downstream of the on-ramp, the metering rate of the on-ramp is determined. Usually, the measurements and the control are updated every 60 seconds. The first time it was put in practice was in Paris, where a minimum green phase of 10 seconds was used in a cycle of 40 seconds. It was found that the control algorithm is effective in preventing congestion and preserving the capacity (Papageorgiou et al., 1991).

Summarising, ALINEA is a simpler control strategy than some of the other mentioned control strategies in this chapter. It uses downstream data instead of upstream data, which requires predictions Therefore, ALINEA is more robust. It only uses one loop detector and it is easily adjustable to real life sites (Papageorgiou et al., 1991).

2.2.2 Combined feed-back and feed-forward

Zhang and Ritchie (1997) combines the benefits of a feed-forward strategy with the robustness of a feed-back control strategy. Their overall proposed control strategy is a feed-back structure. However, a second layer is added to this control structure, which consists of a feed-forward neural controller. Using the proposed algorithm

that combines the feed-back structure with the second layer feed-forward part, the control structure tries to maintain the density at or below the desired level.

When considering the results in the isolated neural network that was formulated in Zhang and Ritchie (1997), it was concluded that the proposed control structure performs quite well in regard to maintaining the density at the set threshold. Furthermore, when compared to ALINEA for instance, the maximum density that was reached on the road is lower. Moreover, the drop in density and flow is less pronounced. Therefore, it is concluded that the control strategy proposed in Zhang and Ritchie (1997), albeit being more complex, performs better than ALINEA as proposed in Papageorgiou et al. (1991) when it comes to maintaining a capacity flow, without an increased risk of breakdown.

2.2.3 AMOC

Apart from isolated on-ramp settings in which ALINEA operates, there is also Advanced Motorway Optimal Control (AMOC) for RM, presented in Kotsialos et al. (2001). AMOC is a software tool that delivers an optimal RM control for a specific situation. The algorithms as a result of AMOC are used to coordinate a (ring) road and all on-ramps to that road. It does so, by taking small discrete time steps (e.g. 10 seconds) to update the algorithm and by dividing the (ring) road up into road stretches of a value in the order of magnitude of 500 meters.

AMOC works together with local RM strategies, like ALINEA, in order to get a better overall performance for the whole (ring) road. AMOC has been tested at the ring road of Amsterdam (the A10) as well. The control sample time for this real life experiment was set at 60 seconds. The experiment was conducted during the evening peak (1600h - 2000h). The results showed that implementing the AMOC strategy led to a decrease of the Total Time Spent (TTS) in vehicle-hours. When comparing the implementation of AMOC with no control at all, it was found that AMOC led to a decrease in the TTS by 20% to 40%. Furthermore, the total time horizon and spatial presence of the congestion is decreased by implementing AMOC. This is an improvement which is not necessarily captured in the TTS (Kotsialos et al., 2001).

2.3 CURRENT RIJKSWATERSTAAT RAMP METERING ALGORITHM

The final control strategy that will be considered, is the control strategy that is in place at different sites in the Netherlands. The algorithm that is currently in use at Rijkswaterstaat includes multiple measuring points. There are detector loops both upstream and downstream of the merging area on the main lane. Furthermore, there are measuring points just in front of the stop line, upstream of the stop line, downstream of the stop line and at the beginning of the on-ramp (Rijkswaterstaat, 2013). This is represented in Figure 2.3.

The speeds and flows are measured by the detector loops. When loop detectors of the traffic light signalling systems Motorway and Traffic Management system are present, these could be used as well (Rijkswaterstaat, 2013).

The RM control strategies are activated when the main lane flows are greater than a threshold value. However, the traffic lights located next to the on-ramp will only be activated when the flows on the on-ramp are sufficient. That is, because there is no point in regulating the flow from the on-ramp onto the main lane if the demand from the on-ramp is not too high (Rijkswaterstaat, 2013).

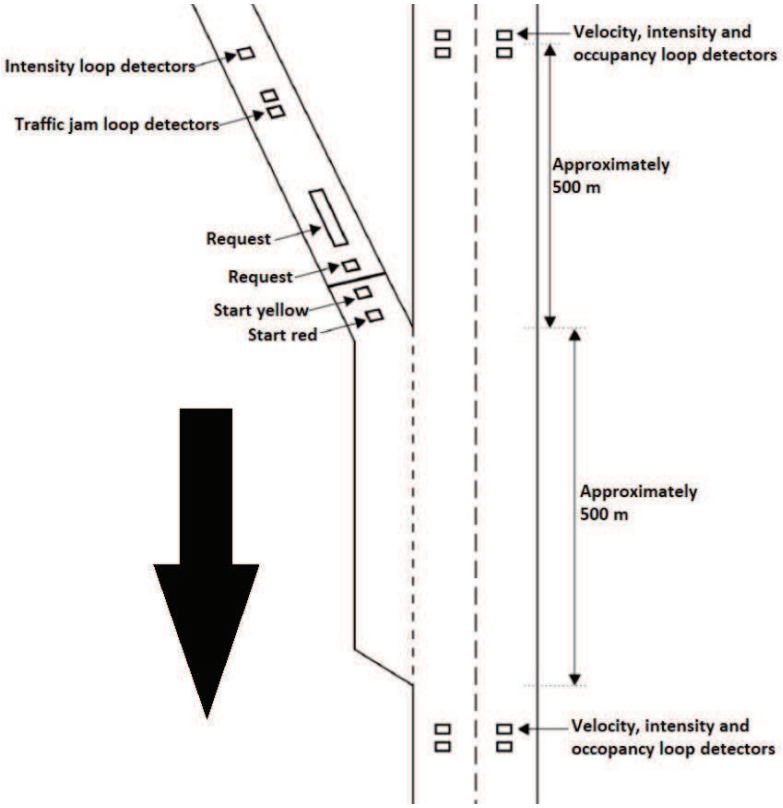

Figure 2.3: Currently used algorithm layout (Rijkswaterstaat, 2018)

The RMI control strategies can be deactivated if one of these criteria are met:

1. When the speeds are higher than a deactivating threshold value;
2. When the measured flows are lower than a deactivating threshold value;
3. When the measuring points do not provide updates for an excessively long period of time;
4. When the on-ramp is full of vehicles and a 'congestion' is caused on the on-ramp.

Furthermore, the control strategy determines the number of traffic light cycles based on the flows on the road. Usually, one vehicle receives a green light per cycle per traffic light. When a green light is shown, the vehicle will start accelerating to enter the main road from the on-ramp. When two lanes and two traffic lights are present at the on-ramp, the traffic lights for both lanes get green simultaneously. Therefore, in a double lane RMI, the traffic lights grant access to two vehicles per green phase (Rijkswaterstaat, 2013).

Lastly, the current macroscopic Rijkswaterstaat RM control strategy checks if too many vehicles pass the traffic light at the on-ramp in a single cycle. If so, the cycle time of the next cycle is increased, delaying the next vehicle from entering the main lane (Rijkswaterstaat, 2013).

2.3.1 Research gap

Concluding from the considered different RM control approaches in the previous section and the currently used Rijkswaterstaat algorithm in the Netherlands, implementing an RMI is effective in reducing travel time delays. There is no consensus on the best RM control strategy regarding whether to use feed-back of feed-forward control structures. However, all currently known research use

either average flows or occupancy rates. It is unknown what would happen when microscopically measured gaps are used as an input for letting an on-ramp vehicle pass the RMI. Therefore, the effects of changing the macroscopic nature of RMIs to a microscopic nature is the research gap that is filled in this research. This gap led to the main research question, being: **What are the quantified effects of changing the macroscopic nature of current ramp metering systems in the Netherlands to a microscopic nature?**

2.4 NECESSITIES AND GOALS WHEN CONSIDERING A RAMP METERING INSTALLATION

When designing a new control strategy for RM installation in the Netherlands, certain goals and necessities have to be considered. Rijkswaterstaat (2018) has drawn up a document that consists of all the necessities in order to implement a new RM algorithm in the Netherlands. Furthermore, the goals of implementing an RMI are mentioned.

The main goal, as mentioned in multiple papers (e.g. in Zhang and Ritchie (1997)), is to preserve free flow conditions on the main road as long as possible. This is also stated in Rijkswaterstaat (2018). Furthermore, Rijkswaterstaat (2018) mentions that limiting rat routing is also a possible outcome of installing an RMI.

When considering to implement an RMI in the Netherlands, three phases have to be completed. These phases are:

1. Check if an RMI could improve the overall system traffic flow and check if installing an RMI is possible from a civil engineering perspective;
2. Perform a dynamic traffic simulation in order to weigh the costs and benefits;
3. Determine if installing an RMI is worth it.

The five civil engineering factors that have to be considered when installing an RMI at a certain location are:

- Enough acceleration length behind the stop line before merging area;
- Enough space for merging of two lanes into one if applicable;
- Enough waiting capacity in front of the RMI;
- Placing the RMI with eye for visibility and safety;
- Enough room at the roadside for roadside assets.

When considering installing an RMI at an on-ramp, a minimum distance after the stop line is necessary to accommodate for a suitable merging speed. Rijkswaterstaat (2018) mentions three aspects concerning this distance:

1. The minimum acceleration length for personal vehicles from the stop line up to the desired merging point;
2. The minimum acceleration length for trucks from the stop line up to the desired merging point;
3. The minimum required space between the lane reduction area and the beginning of the gore.

In Rijkswaterstaat (2018), formulas to determine the above mentioned minimum lengths are provided. The formula to determine the minimum distance between the stop line and the start of the merging area will be discussed.

It is assumed that a passenger vehicle has a velocity of $0\frac{km}{hour}$ and is located very closely behind the stop line. It is assumed that the passenger vehicle will merge onto the main lane approximately 100 meters downstream of the start of the merging area. In order to be able to merge onto the main road by then, the passenger vehicle should have reached a velocity of 0.85 times the activation main lane speed norm. When this merging speed is determined, the required acceleration length can be found in Guangchuan et al. (2016). Herein, an overview of aggressive and conservative acceleration lengths is listed. Furthermore, this can be compared to the acceleration length for passenger vehicles provided in Rijkswaterstaat (2018).

The formula for the minimum required acceleration length for a truck has some similarities with the required acceleration length for passenger cars. However, trucks only require to have reached a velocity of 0.85 times the activation main lane speed norm at the end at the end of the merging area. When this speed has been calculated, the required acceleration length can be found in Yang et al. (2016a). Herein, an overview of the acceleration lengths for trucks is provided. Furthermore, this can be compared to the acceleration length for trucks provided in Rijkswaterstaat (2018).

The minimum required space between the lane reduction point and the beginning of the gore depends on:

- Distance between the stop line and the beginning of the lane reduction area;
- Length of the lane reduction area itself;
- Length of the gore.

It is important to accommodate for situations when the RMI is turned on and when it is switched off. Assuming that the expulsion arrows are not located in front of the stop line, a distance of at least 60 meters is required with a minimum arrow configuration of $50\frac{km}{h}$.

The length of the lane reduction area itself normally consists of an expulsion area (which is a demarcation on asphalt, where vehicles are not allowed to drive) of circa 30 meters, a parallel road stretch of 15 meters and a retraction line, which is dependent on the angle of the on-ramp relative to the main road. For regular on-ramps, this will approximately be 30 to 60 meters.

The length of the gore is normally approximately 100 meters, which brings the total minimum required space between the lane reduction area and the beginning of the gore to approximately 235 to 265 meters (Rijkswaterstaat, 2018).

Existing on-ramps however, might not have this space. In that case, a justified decision will have to be made. Aspects that should be considered, are:

- The expected effectiveness of the RMI on the traffic flow;
- The vertical alignment of the on-ramp;
- The proportion (heavy) trucks;
- The length of the on-ramp;
- The horizontal alignment of the on-ramp.

Currently, strict regulations for the assessment is not available. However, it has been found that on-ramps with a too short distance between the stop line and the gore, an uphill slope and a large share in (heavy) trucks, pose high accident risks.

2.5 SIMULATION SOFTWARE

There are numerous microscopic simulation models. Some widely used ones are:

- AIMSUN (AIMSUN, 2020; Young et al., 2014)
- CORridor SIMulation (CORSIM) (Halati et al., 1997; Sun and Kondyli, 2010)
- MIcroscopic Traffic SIMulator (MITSIM) (Chen et al., 2010; Sun and Elefteriadou, 2010)
- Microscopic Open Traffic Simulation (MOTUS) (Schakel, 2015)
- OTS (Van Lint et al., 2017, 2020)
- PARallel MICroscopic Simulator (PARAMICS) (Cameron et al., 1994; Dijkstra, 2011)
- Verkeer In Steden SIMulatiemodel (VISSIM) (Chou and Nichols, 2014; Group, 2020)

Out of all these aforementioned microscopic driver simulation tools, MOTUS and VISSIM are calibrated for the Netherlands. Furthermore, in Van Beinum (2018) and in Hidas (2005), it is stated that MOTUS and VISSIM are preferred for modelling driving behaviour around highway-ramps. Since this research revolves around merging from an on-ramp onto the main lane of a highway, this is a major advantage. Additionally, the fact that these are calibrated for the Netherlands, makes them the preferred microscopic simulation models.

3 METHODOLOGY

The various methodologies used in this research will be outlined in this chapter. Every other chapter, except for Chapter 1 and Chapter 8, will therefore refer to the methodologies described in this chapter. Firstly, the literature review methodology will be discussed. The actual literature review is found in Chapter 2. Additionally, some findings of the literature review were also already presented in Chapter 1. Additionally, throughout the entire research, interviews have been conducted. This will be briefly mentioned secondly. Thirdly, the design method to come up with the microscopic ramp metering control structure is outlined. Fourthly, the used simulation tool, the OpenTrafficSim (OTS), will get a short introduction. Finally, the data gathering process will be explained.

3.1 LITERATURE REVIEW

In order to prevent wasting time "reinventing the wheel" when it comes to inventing a new RM control structure, a literature review, among other things, has been conducted in this research. The literature review in this research has one main goal. The other goals as described by Neuman (2014) are also applicable in the literature review in presented in Chapter 2. Firstly, the main goal of the literature review of this research is to "learn from others and stimulate new ideas". Since a new RM control structure will be developed in this research, it is useful to learn from existing RM control structures, both successful and unsuccessful. This provides in what adjustments might work and which will probably not work. Secondly, a goal of a literature research is to "demonstrate a familiarity with a body of knowledge and establish credibility". A third goal of a literature study is "to show the path of prior research and how a current project is linked to it". A fourth and final goal of a literature study is "to integrate and summarise what is known in an area".

Furthermore, Neuman (2014) defines six types of literature reviews. In the literature review posed in Chapter 2, the two present types are:

- *Context review:* This type of literature review connects the research topic to a broader knowledge spectrum in the research field. This is primarily done when a research builds upon already existing knowledge on the matter.
- *Methodological review:* This type of literature review compares different research methodologies that could be used in the specific study. This is present in Section 2.5 when considering different microscopic driver simulation models.

The majority of the used literature is published in journals. Besides these journal papers, web articles and course materials have been consulted as well. Most scientific papers used in the literature review in Chapter 2 were found using Google Scholar. However, search engines Scopus and Science Direct were also called upon. For the various already existing RM control structures, keywords like "ramp metering" were used. Besides finding papers by using the search engines, forward and reverse snowballing has also been used in order to come up with more relevant papers.

As mentioned above, Chapter 2 contains the literature review. Additionally, some of the literature review findings are also presented in Chapter 1.

3.2 INTERVIEWS

Another way to gain insight in current RM systems, is conducting interviews with experts on Ramp Metering. These expert can be twofold, namely theoretical (e.g. researchers at a University) or practical (e.g. RMI control managers). Besides discussions with members of the committee, an interview with Johan Groenewold from Rijkswaterstaat and a discussion with Erik van de Laak from Rijkswaterstaat were performed to gain insights in possible improvements. This way, a qualitative assessment on what might work and what most likely will not work can be performed without trying every single possible iteration in a simulation environment (Boyce and Neale, 2006).

It was stated that the current control strategy faces challenges in regards to the robustness of the loop detectors. This should be taken into account, since improving the robustness of these loop detectors increases the frequency the control strategy can be activated. However, in this study this was not taken into consideration, since all RMI alternatives rely on these loop detectors. It is assumed that all RMI alternatives therefore would face the same difficulties in real life to a similar degree, thus there would be no significant differences on this regard between those alternatives.

Furthermore, it was discussed that it is of the utmost importance that the measured gaps stay gaps until the actual merging point. This way, the idea for implementing a semi-permeable lane demarcation to prevent merger manoeuvres from the main road onto the right lane of the main road was proposed. The implementation of such a lane demarcation is therefore tested in this research. Additionally, the point that there are differences in the acceleration statistics between various vehicle groups was brought up. Therefore, two different vehicle groups will be simulated. All these obtained insights were used in the development of the system, which is outlined in Chapter 4 and in Chapter 6.

3.3 DESIGN METHOD

A specific design method for Intelligent Transport Systems (ITSs), including RMIs, is described in Knoop et al. (2018). The design method described five steps that need to be taken in order to come up with a possible solution to an existing traffic problem.

The first step of the design method is the 'problem recognition and description' step. The goal of this step is to capture the problem with the current situation and to describe the desired situation. In other words, what is undesired in the current situation and what should the situation ideally be. It is important to be complete and to remain realistic in the formulation of the two situations (Knoop et al., 2018).

After this first phase, the problem has to be described in traffic flow terminology. In order to accomplish this, firstly the cause of the problem should be known. Usually, this cause could be defined in different steps of a chain that leads to the undesired current situation. It is important to choose a cause that can actually be influenced (Knoop et al., 2018).

When the cause is identified, the necessary measurements that have to be executed can be identified in the second step. This is based on the cause, current situation and the desired situation. Furthermore, the conditions in which an intervention is expected to work can be formulated in this phase (Knoop et al., 2018).

Thirdly, a problem analysis in control engineering terms can be drawn up. In this step, a mathematical formulation of the control goal will be provided. Furthermore, all present signals in the system will be identified. Moreover, the constraints in mathematical terms of the control system will be drawn up (Knoop et al., 2018).

The fourth step involves selecting the control approach. There are various options, such as feed-back and feed-forward. The difference between both options is that feed-back control uses measured outputs of the system and then determine the control strategy, where feed-forward uses a prediction of the future state and then determines the control strategy. Feed-back is more robust than feed-forward, but its disadvantage is that outdated data is used (see Chapter 2) (Knoop et al., 2018). Other control strategies that could be used are Model Predictive Control (MPC), knowledge-based methods and domain-specific methods.

The fifth and final step of the design method is the operationalization step. In this step, the developed control strategy will be tested and possibly adjusted when it does not work as desired yet. Questions that can be used in order to determine whether or not the control strategy has to be adjusted, are:

1. Do the conditions under which the controller is expected to work occur as frequently as expected?
2. If the conditions are met, does the controller indeed solve the cause of the problem? Does it take the appropriate action?
3. If the conditions are met but the controller does not solve the problem, does it remove the cause (as previously identified in the problem analysis part)? If it removes the cause, are there other causes that play an important initially overlooked role?
4. Are there other disturbances in the system, which have been initially overlooked?

The actual design development is outlined in Chapter 4.

3.4 ACCELERATION DISTRIBUTION ESTIMATION AT RAMP METERING INSTALLATIONS IN THE NETHERLANDS

One of the crucial parts of implementing a microscopic approach to RM is determining the location of the gap measuring detector loops on the main road, as will be discussed in Chapter 4. Crucial information in determining the correct placement of the gap measurement detector loops is, for example, accurate information on the acceleration behaviour of drivers. However, information regarding the acceleration behaviour at RMIs in the Netherlands is not available in academic research yet. Of course there is information on average or maximum acceleration characteristics, but most (if not all) of the available analyses have not been conducted in the Netherlands. Furthermore, these analyses were not performed at RMIs and the acceleration behaviour of the drivers might be different at these locations.

Essentially, a distribution of Dutch drivers acceleration at RMIs is not available yet. When a single acceleration value for all vehicles in a specific group (e.g. passenger cars) is assumed, the lack of probability enables the microscopic RM control structure to predict the acceleration of the merging vehicles perfectly to the meter. However, not all drivers within one vehicle group have exactly the same acceleration. Accordingly, not implementing a distribution around the acceleration of drivers within a single vehicle group could lead to an overestimation of the power of a microscopic ramp metering control approach. Since this is not desirable when assessing whether changing the current macroscopic nature of RMIs to a microscopic one is beneficial, an acceleration distribution is of utmost importance. An acceleration distribution is also not present in the standard driver behaviour models in the most common microscopic simulation models, including the chosen microscopic simulation model (i.e. OTS) for this research.

Considering all this, a field experiment was conducted to come up with a distribution around the acceleration of merging vehicles that are controlled by an RMI in the Netherlands. The following sub-sections will describe the execution of this field experiment and how this led to the experiment results. The process and results of the field experiment will be outlined in Chapter 5.

3.4.1 Gathering and preparing the raw data

Firstly, raw data on how vehicles accelerate has to be collected. This is done by filming the on-ramp of the A13 Delft-North in the direction of Rotterdam (southeast) with a stationary camera, placed on the Sint-Jorispad, near the Brasserskade bridge (see Figure 3.1). This site was chosen, because it entails a single lane on-ramp downstream of the the traffic light all the way to the end of the on-ramp, which makes sure that a filmed vehicle will not disappear behind another merging vehicles overtaking other the filmed vehicles. In other words, by making sure only one vehicle is accelerating at a time, it is ensured that individual vehicles will be more easily identified. Moreover, thanks to the bridge over the highway, it was fairly easy to film the accelerating vehicles. Furthermore, since the vehicles were filmed from behind and the drivers were unlikely to notice the filming installation from the other side of the bridge, the driver behaviour was most likely not influenced by the presence of the filming camera. The moment of data collecting was on Tuesday the 5th of November 2019 during the evening peak between 15:30h and 18:00h.

Figure 3.1: Filming location for the acceleration distribution field experiment (Google, 2020c)

Then, before the acceleration of multiple filmed vehicles can be determined, the video data is cut into single frame data. This is done by means of a program called **FFmpeg** (FFmpeg, nd). This program has been executed by running a windows-bat file with the following command-line: ***ffmpeg.exe -i*** *'videoname'.'videoformat'* ***-r*** *'frames per second'* ***image%****'number of digits in the naming of the frames'****d.jpg***.

Next, these frames have been combined into vehicles trajectories with the help of a MATLAB-code, provided by dr. Victor Knoop (MathWorks, 2020). A vehicle trajectory is a line in a (distance, time) plot that shows the movement of a vehicle. An example is shown in Figure 3.2.

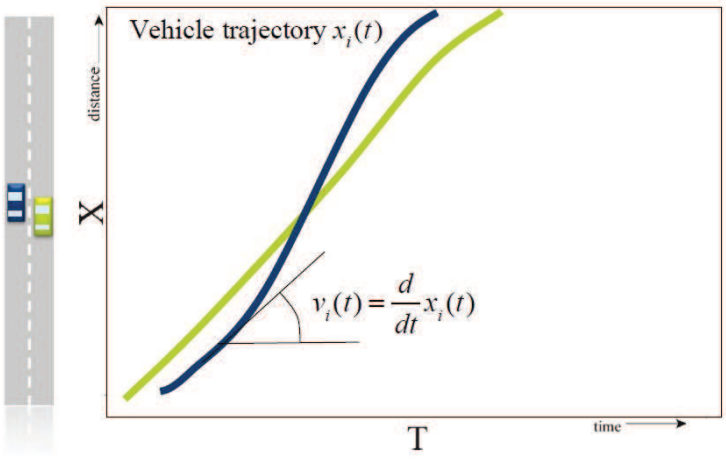

Figure 3.2: Vehicle trajectory example (Knoop et al., 2018, p.239)

When considering all the obtained trajectories, only the acceleration part is useful for this experiment. Therefore, only vehicles with a low speed (i.e. a more or less horizontal trajectory near the stop-line of the RMI) will be taken into account. The pixel-data of this trajectory is determined by hand, by looking at the border between the coloured trajectory and the shadow of the vehicle in an image manipulation program called GIMP 2.10.14 (GIMP, 2019).

However, the computed trajectories show the time and distance in pixels instead of in seconds and in meters. So, a conversion from pixel data to seconds and to meters has to be made. This is made possible by a fellow student named William van Lindonk. He drove a passenger vehicle with a known and constant speed for the entirety of the on-ramp. With this knowledge and the hand derived pixel data that corresponds with that specific vehicle trajectory, a conversion from pixels to meters has been configured for all frames that show that the vehicle is located at the on-ramp. Moreover, the number of frames per second in the video is known. This leads to the conversion of the time data in frames to time data in seconds.

3.4.2 Estimating vehicle trajectories

Considering all mentioned steps in the previous sub-section, distance data points in meters and time data points in seconds can be determined for a number of individual vehicle trajectories. This is done by determining the speed in the next time step with the calculated acceleration in the current time step.

$$v_{t+1} = v_t + a_t dt \tag{3.1}$$

Consequently, the position of the vehicle in the next time step can be determined by adding the travelled distance for this time step to the next to the current position.

$$x_{t+1} = x_t + \frac{v_t + v_{t+1}}{2} dt \tag{3.2}$$

This way, calculated trajectories can be determined. Thus, the acceleration at every time step has to be calculated. Physics formulae provide the opportunity to determine the acceleration for every time step. The effective acceleration at every time step is assumed to be the minimum value of the calculated acceleration regarding the physics formulae and a, to be fitted, individual maximum accepted acceleration value. Then, these data points provide the opportunity to fit an acceleration curve that is based on physics formulae. An assumption in the process is that air resistance (or drag) is the only form of resistance the vehicle encounters. The entire list of formulae and corresponding mathematical steps can be found in Appendix B. All variables that are used in this report are summarised in Appendix A. In the main text, only the most important equations will be shown.

Firstly, the power of objects can be calculated by multiplying the force with the speed.

$$P = Fv \tag{3.3}$$

Secondly, the force of an object can be calculated by multiplying the mass by its acceleration.

$$F = ma \tag{3.4}$$

Thirdly, the effective force of an object can be calculated by subtracting the resistance force that applies to the object from the powered force. In this case, the powered force comes down to the force accumulated by the car engine. The resistance force is assumed to only consist of air resistance (or drag) in this research.

$$F_a = F_e - F_{\text{res}} \tag{3.5}$$

Fourthly, the double value of the air resistance (or drag) can be calculated by multiplying the drag coefficient by the density of the air, the area of the object that encounters the air resistance and the speed squared. In order to get to the actual air resistance that applies to the object, the answer to the previously explained double value of the air resistance should be divided by two.

$$F_t^r = \frac{1}{2} C_d \rho A v_t^2 \tag{3.6}$$

Combining these physics formulae, the acceleration at every time step can be determined by dividing the used acceleration force for the considered time step by the mass of the vehicle.

$$a_t^f = \frac{F_t^a}{m} \tag{3.7}$$

By using a maximum between this value and a to be fitted individual maximum accepted acceleration value, the vehicle acceleration trajectory can be computed. This is done by fitting the best combination of the individual maximum accepted acceleration (a_{max}) and the used power (P_{used}) per individual vehicle. These to be fitted variables are kept constant for the entirety of an individual vehicle trajectory.

Some assumptions that have to be made in order to draw up an individual vehicle trajectory by fitting the individual values for the a_{max} and the P_{used}, using the equations stated above, are:

- A maximum possible delivered power for a passenger car is assumed;
- The mass of a passenger car is assumed;
- The vehicle is assumed to have a starting speed equal to 0 $\frac{m}{s}$;
- The vehicle is assumed to have a starting distance of 0 meters.

Considering the previously mentioned conditions and the gathered data points for a single vehicle, the drawn up vehicle trajectory can be compared with the actual measured data points. By minimising the sum of the squares (Mean Squared Error (MSE)) of the difference between the calculated vehicle trajectory data points and the actually measured data points for vehicle n, an as accurate as possible vehicle trajectory can be fitted (see Equation 3.8). This formula is only applicable for the time steps that have both a calculated position ($x_{t,n}^{calc}$) and an observed position ($x_{t,n}^{obs}$).

$$\text{MSE}_n = \sum_{t \in T_n} (x_{t,n}^{calc} - x_{t,n}^{obs})^2 \tag{3.8}$$

An optimization model has been created with Python in Jupyter Notebook, Anaconda (Anaconda, 2020; Jupyter, 2020; Python, 2020). Using this script, individual optimal values for $a_{\max}$ and P_{used} have been found, resembling their actual vehicle acceleration trajectory. Using these results of a number of vehicles leads to a collection of P_{used}-values and $a_{\max}$-values.

3.4.3 Estimating the acceleration distribution

In order to determine the maximum acceleration distribution, the individual calculated results for $a_{\max}$ that are deemed to be valid are put in SPSS and a distribution will be fitted around this data (IBM, 2020). This will be done with the Kolmogorov-Smirnof test (SPSS, nd). This distribution for the $a_{\max}$ in turn, will be put into the simulation for the vehicle characteristics. The driver model present in the microscopic simulation model will make sure that the driver will have an acceleration somewhere between the maximum deceleration and the maximum acceleration that is drawn out of the provided distribution. The driver model that is present in the simulation tool is based on the Intelligent Driver Model (IDM).

3.5 COMPARING THE DIFFERENT CONTROL STRATEGIES

The effects of the proposed new RM control strategy, the existing control strategy and the no RM control at all, will be simulated. It is decided to test the extent to which a microscopic approach to RM is beneficial by means of a simulation. This is the best suited research method that still provides quantitative results, without having to perform a field experiment. The simulation outcomes will provide information about the performance of the different control strategies on the Key Performance Indicators (KPIs). In this section, first the simulation tool will be examined more thoroughly. After this, the comparing methods will be described.

3.5.1 Simulation tool

When considering the findings regarding the various simulation tools as outlined in Chapter 2, it seems that MOTUS, OTS and VISSIM are the preferred simulation tools. In order to come up with a single favoured simulation tool, additional advantages and disadvantages will be outlined in this section.

An additional advantage of MOTUS over VISSIM is that it is open source. Moreover, MOTUS enables researchers to build up a simulation model from top to bottom. Additionally, MOTUS was developed by employees of the Delft University of Technology, enabling researchers working for the Delft University of Technology to seek support when using MOTUS more easily.

However, when the various microscopic driving simulation models were compared in Van Beinum (2018), OTS was still under development. It was already

mentioned in Van Beinum (2018) that the developments regarding OTS were very interesting and that OTS could potentially provide solutions to existing limitations of MOTUS. Just like MOTUS, OTS was developed by researchers at the Delft University of Technology. OTS is also open-sourced, calibrated for driver behaviour in the Netherlands and researchers are able to build up the model from the bottom to the top. There is even an overlap in the developers of the two microscopic traffic simulation models. And according to one of these developers, OTS is indeed even better suited for the research described in this report than MOTUS. Therefore, OTS has been used as the microscopic simulation model in this research.

OTS is a Java-based coding program (Java, nd). The coding interface used in this research is Eclipse (Elipse, nd). Furthermore, OTS provides underlying standard scripts, developed mainly by researchers at the Delft University of Technology in the fields of simulation and traffic engineering. Some examples of what the underlying scripts in OTS determine, are:

- The driver behaviour;
- Vehicle characteristics per group (e.g. vehicle length);
- Standard loop detectors characteristics;
- Standard Traffic Light characteristics;
- Standard Rijkswaterstaat Ramp Metering case study.

These present scripts are left intact as much as possible. However, the road layout and the control structure of the RMI still have to be programmed. Furthermore, changes to some values and input variables in the standard OTS scripts will be made. Some input variables are properties of the proposed control structure, other input variables are more deterministic and data will be gathered in order to get an as accurate as possible value for these input variables. Some examples of these input variables are:

- Demand on the main lane;
- Demand for the on-ramp;
- Truck percentage;
- Minimum required gap time;
- Acceleration distribution of the (merging) vehicles.

A complete index of all the input variables will be provided in Chapter 6. In the same chapter all other settings, including the road layout, will be described as well.

3.5.2 Comparing the results

As stated previously, the outcomes of the OTS simulation tool will provide information regarding the performance of the multiple control alternatives on the performance on the various KPIs. The different control strategies that will be tested are:

1. No Ramp Metering Control;
2. The current Rijkswaterstaat Ramp Metering Control;
3. The newly developed Microscopic Ramp Metering Control.

Following the necessities and goals of RMIs as described in Section 2.4, KPIs can be drawn up. Summarising that section, the primary goal of installing an RMI is to reduce the total travel time losses for the system as a whole. Moreover, as stated in Section 2.4, the throughput from the on-ramp onto the main road should not be limited too much, since this would result in traffic congestion on the underlying road network. Additionally, preventing rat routing is one of the potential side-goals of RMIs. However, for the sake of simplicity, only one on-ramp will be simulated in this research and thus rat routing is not an option for vehicles in the simulation. Therefore, this will not be taken into account in this research.

OTS generated simulation results

Basically, the total travel time delays for the entire system is the main KPIs. Additionally, travel time delays for the various origin-destination (OD) pairs can be used as KPIs. The OD pairs that can be travelled in this research are gathered in set I.

$$I = \begin{bmatrix} \text{1: Origin at start of main lane with destination end at the of main lane} \\ \text{2: Origin at start of main lane with destination off-ramp upstream of the controlled on-ramp} \\ \text{3: Origin at the start of the controlled on-ramp with destination at the end of main lane} \end{bmatrix}$$

The KPIs can be identified in multiple ways. This could be done at the end of a simulation run with a single statistic, but speed contour plots or cumulative curves could also provide insight regarding the travel time delays. For this research, the single statistic at the end will be logged and the cumulative curves will be drawn up. Both will be computed for all OD pairs.

The first single statistic that will be computed at the end of the simulation is the free flow travel time. The free flow travel time for the routes in set I can be calculated by taking the distance and divide this by the maximum theoretical speed, which is equal to the speed limit.

$$FTT_i = \frac{s_i}{v_i^{\max}} \tag{3.9}$$

Furthermore, the actual total travel time for all vehicles combined travelling from their origin to their destination can be computed by taking the sum over all individual vehicle travel times for these origin destination pairs.

$$TTT_i = \sum_{n=1}^{N_i} TTT_i^n \tag{3.10}$$

Combining these two statistics, the total travel time delay for a single route in set I can be calculated by subtracting the total free flow travel times from the actually measured total travel times. Reducing these delays is the main purpose of implementing an RMI.

$$DTT_i = TTT_i - FTT_i \tag{3.11}$$

However, the average travel time delays per vehicles are better suited for comparisons between the various control alternatives than the total travel time delays, since the number of vehicles that originate at the origins for every route differ between these control alternatives. Therefore, the total travel time delays will differ for sure, but the travel times per vehicle might not. These average travel time delays for every OD pair can be determined by dividing the total travel time delay for the specific OD pair by the number of vehicles that have travelled that route at the end of the simulation.

$$DTT_i^n = \frac{DTT_i}{N_i} \tag{3.12}$$

When the travel time delays per OD pair are known, the total travel time delay of the entire system can be computed by taking the sum of travel time delays for all OD pairs. A reduction in the travel time delay for the entire system is what is aimed to be achieved by implementing an RMI.

$$DTT_{\text{system}} = \sum_{i \in I} DTT_i = \sum_{i \in I} TTT_i - \sum_{i \in I} FTT_i \tag{3.13}$$

Finally, following the same remarks about the variation in the number of vehicles originating for every route, the average travel time for the entire system is determined. This is the most important KPI when comparing the performance of the various alternatives. This average travel time delay for the entire system per vehicle can be calculated by dividing the sum of all OD route travel time delays by the sum of vehicles for all OD pairs.

$$DTT^n_{\text{system}} = \frac{\sum_{i \in I} DTT_i}{\sum_{i \in I} N_i} \tag{3.14}$$

Moreover, some other statistics will be computed on simulation end in order to compare different (microscopic) RMIs with each other include:

- The time the RMI was activated [s];
- The time the RMI was deactivated [s];
- The number of vehicles that got a green light while the RMI was activated [#];
- The percentage of controlled vehicles that had to wait too long in front of the RMI. A vehicle had to wait too long if it had to wait for more than 15 seconds while being at the front of the queue [%];
- The percentage of controlled successful mergers. A merger is considered to be successful if the merging vehicle merges onto the right lane behind the leader of the measured gap. So, the leading vehicle of the gap still has to be on the right lane as well [%].

Computing cumulative curves

Additionally, in order to gain insight at what happens during the simulation, cumulative curves for every OD pair and the entire system will be drawn up. Besides the static simulation results as described above, the OTS code also generates text files with the vehicle count on one side and its destination arrival time on the other side. This is logged for every OD pair, making it possible to compute the cumulative curves on a minute time-interval.

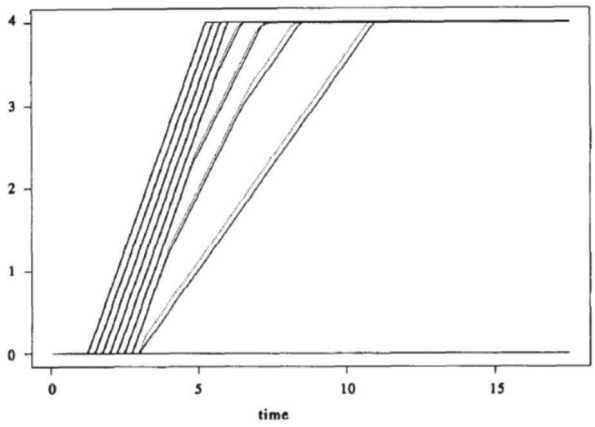

Figure 3.3: Example of cumulative curves (Daganzo et al., 1997)

Unfortunately, when comparing these free flow cumulative curves with the actual cumulative curves, the differences between the various control settings are so small that they are hard to notice by eye. Therefore, slanted cumulative curves are computed as well. These are basically regular cumulative curve minus a component that consists of a certain offset flow multiplied by the then passed time. The formula for computing slanted cumulative curves, is provided in Equation 3.15. The offset for regular cumulative curves is 0. Normally, for computing slanted cumulative curves, the chosen offset is equal to the road capacity. This way, a horizontal line is provided when the flow on the main road is equal to the capacity. The capacity is normally determined as the capacity on the road just after a traffic jam. This is the so called discharge rate. In this situation, drivers choose their desired headway between themselves and their predecessor, resulting in the road capacity. However, before congestion kicks in, an increasing line can be found most times, indicating that the capacity on the road before congestion is larger than after the vehicles have been congestion. This phenomenon is called the capacity drop.

$$N_{\tau}^{\text{Cumulative}} = N_{\tau} - q_o * \tau \tag{3.15}$$

However, showing a capacity drop is not the goal of this research. Thus, an offset which is not equal to the road capacity can be chosen. In this research, the used offset has been chosen in such a way that differences in performance between the various alternatives are limited below the horizontal axis, but the differences above the horizontal axis will be more easily visible. This is a result of the extreme values being substantially lower due to the with time increasing deduction of the number of (slanted) cumulative vehicles vehicles. The chosen offsets in this research are shown in Table 3.1.

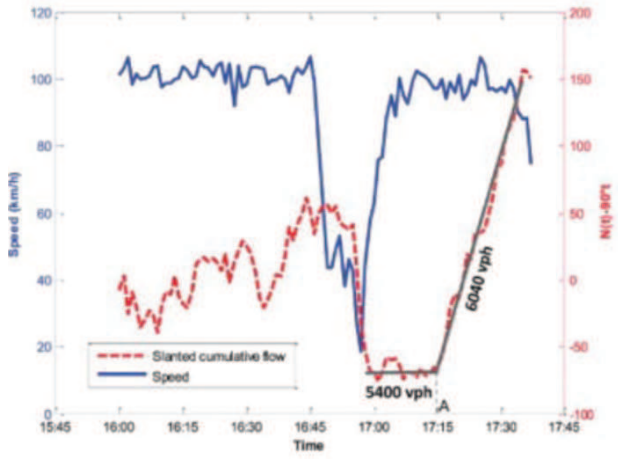

Figure 3.4: Example of a slanted cumulative curve (Yuan et al., 2017)

Table 3.1: Used offsets to compute the cumulative curves

	System	Main lane	On-ramp	Off-ramp
Chosen offset [$\frac{vehicles}{hour}$]	4500	4000	300	300

Comparing total travel time savings with cumulative curves

During the research, it was observed that the computed delays by OTS at the end of the simulation seem to be inaccurate. For instance, when comparing the delays from the vehicles that originate at the controlled on-ramp, it is very unlikely that the microscopic RM approach that requires larger gaps for the merging vehicles leads to less delay than a microscopic RM approach that requires smaller gaps. Especially, when the delay on the main lane is not significantly negatively influenced by this decrease in the required gap.

The hypothesis that the total travel time delay for vehicles originating at the on-ramp for a microscopic RM approach with a 2.0 seconds gap should be larger than the same settings, but with a required minimum gap of 1.8 seconds, was confirmed by looking at the (slanted) cumulative curves as shown in Chapter 7. Nonetheless, the average delays according to the OTS outputs indicate the opposite. Thus, it was concluded that OTS makes use of a vertical queuing model when there is no space on the road in the simulation to spawn the vehicles on. The start time that is given to the vehicles in OTS is only assigned when the considered vehicle is present on the road for the first time. Thus the waiting time in the vertical queue is accounted for. This leads to unregistered delays. Since a fair comparison between the total delays for the vehicles is required, another way of computing the total delays is recommended.

Fortunately, the total travel time delays can be computed by taking the area under the line without traffic jams (i.e. a theoretical situation) and subtracting the computed surface under the line of the considered actual cumulative curve therefrom (Knoop et al., 2018). The destination time for the uncontested situation is determined by calculating the free flow travel time and adding this to the start time of the vehicles when they enter the simulation. Then, by combining the cumulative total number of vehicles for every minute that would have reached their destination when there is no congestion, the uncontested cumulative curve is computed. Unfortunately though, due to the vertical queuing in OTS, determining the precise desired start times is impossible, since this could be in the invisible vertical queuing part of the simulation. This disables computing the cumulative curve without delays.

It is possible, however, to compare the cumulative curves of the different RM control strategies with each other. So, the area under the chart needs to be calculated. This can be done by determining the integral of the cumulative curve. For the total area underneath one function, the integral on the interval [0,∞] is calculated. Since the simulation time is only 130 minutes, the interval becomes [0,130].

One challenge with this approach is the fact that the observed cumulative curves do not follow an exact function. Therefore, a linear increase function between two logged adjacent time steps $[\tau, \tau + 1]$ is assumed. A function describing this linear increase on that specific interval is computed.

$$f(\tau) : N = u\tau + b \tag{3.16}$$

The time steps are chosen to be one minute in order to limit the computational effort a bit. In the example, the logged adjacent points are called K and L.

$$K\Big(\tau, N_\tau\Big) \wedge L\Big(\tau + 1, N_{\tau+1}\Big) \tag{3.17}$$

Additionally, for a simulation of 130 minutes, this already results in 130 areas under the graph. Smaller time steps might get a little bit more accurate results, but the differences in accuracy between 130 areas and 1300 areas are probably not very large. Furthermore, the data points in the cumulative curves are already averages over 30 different simulation runs for a single alternative, which will limit the fluctuations between time steps as well.

Computing the area under a linear line, is done by taking its integral.

$$\int f(\tau)d\tau = \frac{1}{2}u\tau^2 + b\tau \tag{3.18}$$

When the value for u and b are calculated (see Appendix C), the end result for the computation of the area under the line between points K and L is found.

$$\int_{\tau}^{\tau+1} f(\tau)d\tau = N_{\tau+1}(\tau+1) - N_{\tau}\tau + \frac{N_{\tau+1} - N_{\tau}}{2}\left(\tau^2 - (\tau+1)^2\right) \tag{3.19}$$

Then, the entire area under the line can be calculated by taking the sum of all adjacent time steps for the entire simulation.

$$\int_{0}^{130} f(\tau)d\tau = \sum_{0}^{130}\int_{\tau}^{\tau+1} f(\tau)d\tau \tag{3.20}$$

Thereafter, the travel time savings for control strategy k versus control strategy l can be calculated by subtracting one from the other.

$$TTD^{k,l}_{[0,130]} = \int_{0}^{130} f_k(\tau)d\tau - \int_{0}^{130} f_l(\tau)d\tau \tag{3.21}$$

Comparing average total travel time savings with fractional cumulative curves

Unfortunately however, this method faces a difficulty as well. As stated before, the average number of vehicles that pass through the entire simulation in the OTS simulations is not equal for the same random seed with different control strategies. This is still the case when considering the average number of vehicles that originate per OD pair over 30 different seeds. The differences do get smaller though when comparing these average number of vehicles.

Nonetheless, the differences result in an advantage for the control strategy that has accommodated the largest number of vehicles during the simulation. This is the case, since the cumulative number of vehicles will be higher when the traffic states are similar. However, not only during the simulation the cumulative number of vehicles could be higher, but also during the final tens of minutes when the simulation is still running, but there is no new traffic demand anymore. These final minutes without demand are implemented to accommodate all vehicles that originate during the simulation reaching their destination, ensuring that there is no delay still present in the system. Especially considering this final simulation stage, an unfair advantage for the control strategy with the largest number of vehicles that have passed through the system is gained.

To ascertain that there is no additional delay taken into account for the control strategy that was unfortunate to have the lower number of vehicles passing through the simulation, the fraction of arrived vehicles at a time step is taken instead of the actual number of passed vehicles. This way, the area under the graph for a single time step when all vehicles have reaches their destination equals one for all RM alternatives, regardless of the exact number of vehicles that have passed the system. Unfortunately, fluctuations in the arrival pattern during the simulation still remain and these are not resolved by using the fractional cumulative curves. Nevertheless, computing the travel time savings by means of the fractional cumulative curves is regarded to be the better alternative compared to the computations of the regular cumulative curves and the delays computed by OTS.

The fractional cumulative vehicles that have reached the considered position at a certain time step is computed by dividing the actual number of vehicles that have reached the considered position by the number of vehicles that have reached that position at the end of the simulation. This total number of vehicles that have reached their destination is always equal to the total number of vehicles that have originated for that OD pair, since the demand in the simulation for the final 40 minutes is kept

at 0. For an entire simulation length of 30 minutes and with a maximum distance to be travelled of 6 kilometers including regular highway speed limits, this is always enough to allow all vehicles reaching their destination.

$$F_{\tau}^{k} = \frac{N_{\tau}^{k}}{N_{130}^{k}} \tag{3.22}$$

Combining Equation 3.22 with the equations leading up to Equation 3.21, results in the equations that determine newly computed area under the graphs.

$$\int_{\tau}^{\tau+1} g(\tau)d\tau = F_{\tau+1}(\tau+1) - F_{\tau}\tau + \frac{F_{\tau+1} - F_{\tau}}{2}\left(\tau^2 - (\tau+1)^2\right) \tag{3.23}$$

Then, the fractional travel time savings between control strategy k versus control strategy l can be determined.

$$FTTD_{[0,130]}^{k,l} = \int_{0}^{130} g_k(\tau)d\tau - \int_{0}^{130} g_l(\tau)d\tau \tag{3.24}$$

This fractional travel time savings can in turn be used to calculate the total travel time delay, by multiplying this value by the (average) number of vehicles that have passed through the simulation.

Simulation runs

Since there are quite some stochastic variables involved in the simulation, all different control strategies will be run with 30 different random seeds (which are the same for the three different strategies) and the averages of these results will be compared. These runs will be performed in batches, meaning that multiple seeds will be simulated without having to hit 'run' for every single simulation run. On average, one simulation run with a single control alternative takes between 10 and 15 minutes. If it takes longer than 30 minutes, it is assumed that something went wrong and the output for that simulation run will write "ERROR" for the statistics that are computed on simulation end. The outputs that are only computed on the simulation end, are stored in Excel for every single simulation run (Microsoft, 2020).

The cumulative curves are only computed while taking the average data for all seeds for the specific setting. The same applies to the calculated differences in the delay by comparing the area underneath the cumulative curves. If a simulation error occurs, no cumulative vehicle data for that run will be stored in Excel, which means that the average cumulative curves will be determined for less than 30 simulations (Microsoft, 2020). If more than 5 errors occur, more seeds will be run in order to get closer to the desired 30 simulation runs. If 5 or less errors occurred, less than 30 simulation runs are considered when computing the averages over all simulation runs.

The code that enables this batch running is written for this specific research. The language of the batch running code is Python (version 3.7.2) and the coding interface that was used is SublimeText (Python, 2020; SublimeText, nd). The code will be called upon with the Windows Command Prompt.

Firstly, several microscopic RM settings with the control structure as proposed in Chapter 4 will be evaluated. The best performing microscopic control structure will be chosen as the microscopic RM control structure that will be compared to the Rijkswaterstaat control and to no control at all. This will be done for a base case scenario. Additionally, for some variables, a sensitivity analysis will be performed to come up with a recommendation for different conditions.

3.6 DEMAND DATA CHARACTERISTICS GATHERING

In an effort to get a realistic demand pattern and truck percentage for the simulation, data for the considered case study regarding demand patterns and truck percentages is gathered. This is done by means of the Dexter database (Dexter, nd). The Dexter database provides hourly flow data, which is regarded to be the minimum demand, since the demand can be higher than the measured flow, but not the other way around. Additionally, the percentages on heavy truck, small trucks and passenger cars are provided on an hourly basis. The outcomes for the case study will be used to derive the demand patterns and the truck percentages.

4 DEVELOPMENT MICROSCOPIC RAMP METERING STRATEGY

In order to get to a new Ramp Metering (RM) control structure, a design methodology has been chosen. This methodology was described in Section 3.3 and will be used in this chapter to get to the microscopic RM control structure.

4.1 CURRENTLY USED ALGORITHM

The algorithm that is currently in operation at multiple on-ramps in the Netherlands has already been mentioned in Section 2.3. As stated there, it uses a macroscopic approach. The algorithm gets input from loop detectors located 500 meters upstream of the merging point and 500 meters downstream of this point. The detectors measure individual vehicle speeds. Comparing these observations with predetermined threshold values, the control structure is either activated or deactivated. When the control structure is activated, the speed on the main lane 500 meters upstream of the start of the merging area determines the temporary fixed cycle time of traffic light. This is done by looking at the difference between the pre-determined desired flow on the main lane and the coupling of a current flow on the main lane to the measures speeds.

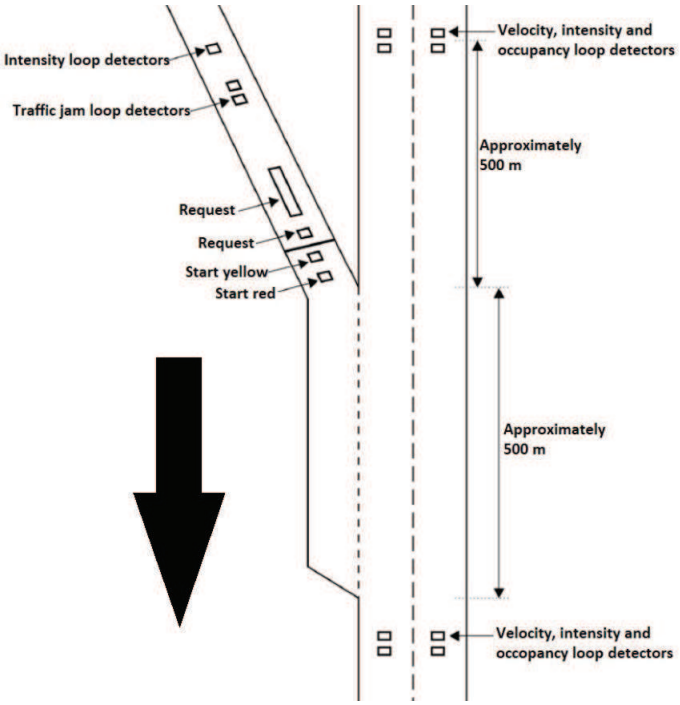

Figure 4.1: Currently used algorithm layout (Rijkswaterstaat, 2018)

Due to this macroscopic approach, it is still rather likely to encounter a fully occupied (right lane on the) main road when having to merge onto the highway. Therefore, stop-and-go jams can still originate at on-ramps, even with RM in place.

4.2 TRAFFIC FLOW IMPLICATIONS

Therefore, it is desired to fit merging vehicles in measured gaps in the flow instead of reducing the chance of (too many) vehicles having to merge while encountering insufficient space on the main lane. This method of using measured gaps in the flow on the main lane will be called the microscopic ramp metering approach. After all, when the merging vehicles always have a sufficient gap, drivers will not have to brake harshly when the merging vehicle forces itself on the main lane in front of the drivers. It is this harsh braking of main lane vehicles that cause stop-and-go jams when operating at (or near) road capacity. Therefore, preventing this action by vehicles will result in less traffic jams and thus in travel time gains compared to the existing situation.

Considering the currently available technologies, there are limitations to what is possible. For instance, currently it is not possible to control the acceleration behaviour of drivers. The same goes for the driving speeds and courtesy lane changes of vehicles on the main lane.

However, what is possible to control, is the moment of showing a green traffic light (and thus an estimated 'release' time of the vehicle in front of the traffic light). With this control and the estimation of the relative travelled distance of the main lane vehicle versus the merging vehicles, individual merging vehicles can be fitted in the measured gaps in the flow on the main lane.

Furthermore, the acceleration of the merging vehicles and the speed of the vehicles on the main lane could possibly be influenced by variable speed limits or colour-blimps (like the ones at airports) indicating if the current acceleration of the merging vehicles is in line with the desired acceleration. However, estimating (and simulating) the degree to which the drivers would follow these recommendations is very variable. An overestimation of this compliance rate could easily lead to an overestimation of the effects of implementing microscopic RM which include such advice-systems. Therefore, these systems are not taken into account in this research.

In order to get the biggest chance of success, the acceleration of the merging vehicles and the speeds of all involved vehicles have to be known as precisely as possible. This way, without communication between the vehicles, a coordinated merger in a measured gap would be possible. Moreover, the measured gaps on the main lane have to remain sufficient gaps as much as possible. Therefore, it is recommended to prohibit merging manoeuvres from the middle lane of the highway onto the right lane on the main road for at least the road between the gap measurement loop detectors and the end of the on-ramp merging area. Furthermore, preferably, the deviation between the acceleration profiles of the merging vehicles has to be as small as possible. This is, however, not controllable without giving acceleration recommendations to the drivers. Finally, all vehicles should fall within a chosen group. In this research these groups are limited to personal vehicles and trucks only.

4.3 CONTROL SCHEME

As stated in Chapter 2, there are basically three different control schemes: feed-back, feed-forward and a combination of the two. Since the merging vehicles will be fitted in measured gaps, the control concept in this research is primarily a feed-forward control scheme. Nonetheless, there is also some feed-back control, as can be seen in the eventual control scheme provided in the final section of this chapter (Figure 4.6).

4.4 CONTROL ENGINEERING IMPLICATIONS

This section will provide the microscopic control structure that has been developed in this research. This will be done step by step by taking a closer look into the different possible control situations. Firstly, the activation and deactivation conditions of the microscopic control approach will be outlined. Secondly, the process of identifying the waiting vehicle and when the traffic light should turn green will be elaborated upon. Finally, the control sequence to turn the traffic light back to red via yellow, is explained. In the next section, all these components will be put together and lead to the entire control concept as shown in Figure 4.6. The control concepts start at the top of the figure. In all shown control concepts, the green lines indicate what the next step in the control structure is when the answer to the considered question is 'yes'. A red line indicates the next step when the answer to the considered question is 'no'. Black lines indicate a follow-up step regardless of the considered action. Furthermore, in these control schemes, rectangles are actions and diamond-shaped blocks indicate yes/no questions. An approximation of the location of all loop detectors is provided in the next section in Figure 4.8.

4.4.1 Activation and deactivation

The control structure will be activated when the measured flow on the main lane is higher than a certain threshold value. Additionally, the control structure can be activated when the speed drops below a speed threshold value. On activation, the traffic light will show red to prevent the first car from accelerating towards the merging area when there is no gap measured yet. Deactivation of the microscopic RM control approach is subject to multiple conditions. For instance, when the speed has dropped below a certain value (i.e. a traffic jam is present), the speed on the main road is not predictable anymore, making it (nearly) impossible to show green to the merging vehicles at the right time. In other words, it is very hard to ensure that the merging vehicles actually have the measured gap available next to them when they want to merge on the main road.

Furthermore, the control structure could be deactivated when the on-ramp is full of waiting vehicles. This is done in order to limit spillback on the underlying road network. Finally, the control structure will be deactivated when the traffic conditions on the main lane are not of a near capacity nature anymore. This way, merging vehicles are not held up unnecessarily. These different conditions are shown in Figure 4.2 and are summarised below:

- The speed gets above a certain value and the flow simultaneously drops below a threshold value, meaning the traffic has returned to free flow from a (near) capacity state;
- The speed on the main lane drops below a critical value. This means a traffic jam has emerged on the main lane, compromising the measured gaps. Therefore, it is irrational to continue with the microscopic control structure;
- A vehicle is stationary at the loop detector at the beginning of the on-ramp. In other words, the on-ramp is full of vehicles, which may lead spillback on the underlying road network.

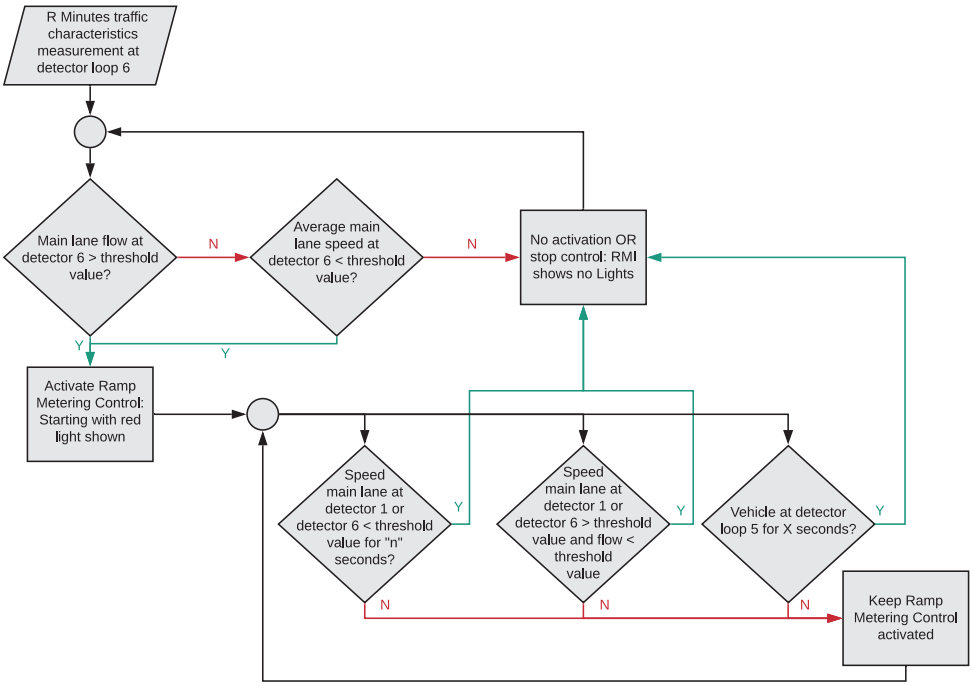

Figure 4.2: Control concept activation/deactivation

4.4.2 Turning the traffic light green

When the control structure is activated, the first indicator that has to be checked is whether a vehicle is waiting in front of the traffic light. If this is not the case, the traffic light can remain red. When a vehicle is indeed waiting in front of the RMI, the vehicle type has to be determined. If the waiting vehicle is a truck and the gap measurement detector loop for trucks (i.e. the detector that is located furthest upstream on the right lane of the main road) has not been triggered by a vehicle for s seconds, the traffic light will turn green and the truck will start accelerating. If the control algorithm works well, the truck will have reached the merging speed (or the end of the on-ramp) when the gap has also arrived there (see Figure 4.3).

When the waiting vehicle is a passenger car and the previous vehicle is not a truck, the principle is the same as control theorem for trucks as described in the previous sub-section, but the detector that measures the gap is located more closely to the on-ramp (i.e. the gap detector for passenger vehicles). This is the case, since passenger cars accelerate more quickly than trucks (Fitzpatrick and Zimmerman, 2007; Yang et al., 2016b). If the previous vehicle is a truck however, a longer red light period will be scheduled due to the risk of measuring the same gap twice and only having space for one vehicle. Additionally, in the considered scenario, the passenger car is not able to overtake the truck. This means that if a new gap has emerged and is measured, the passenger car is not able to merge into that gap if its acceleration is hindered by a truck. This results in a minimum waiting time the first w seconds. Effectively, this means that a measured gap for passenger vehicles will not trigger a green phase and the traffic light will remain red for at least this duration. After this w seconds, a measured gap at detector seven will initiate a green phase. This process is shown in Figure 4.4.

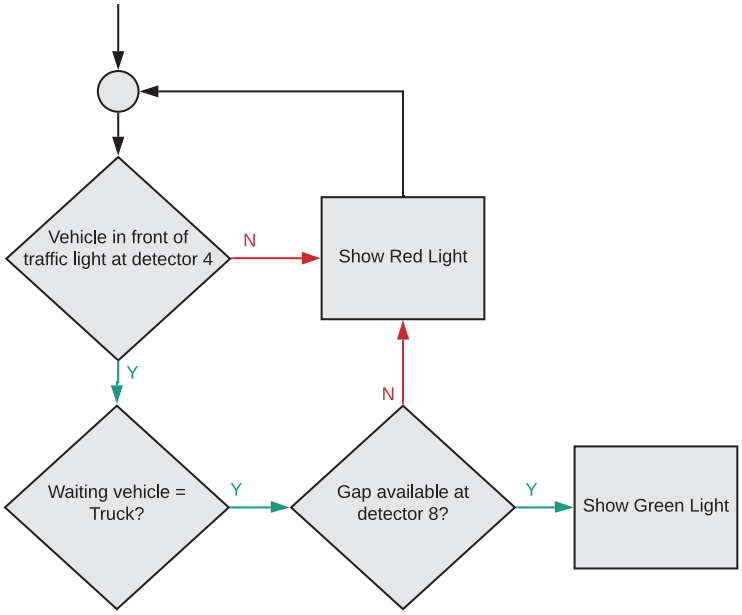

Figure 4.3: Control concept when waiting vehicle is a truck

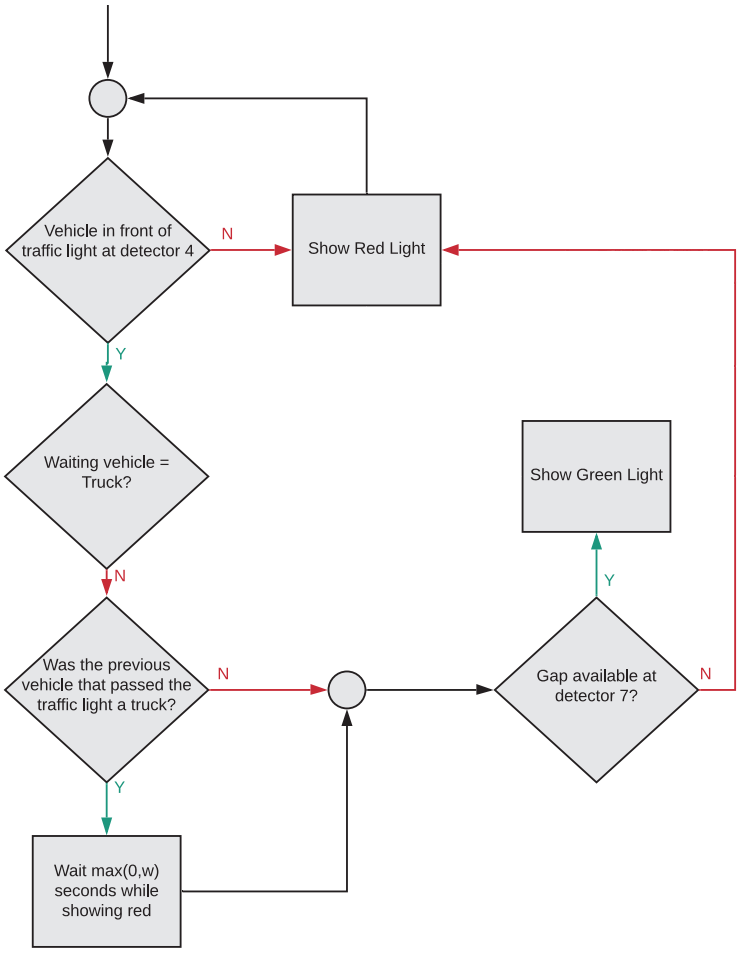

Figure 4.4: Control concept when waiting vehicle is a passenger car

4.4.3 Turning the traffic light red

After a green phase has been activated, detector loops on the on-ramp will check if the vehicle has passed the traffic light. When that is the case, firstly a detector initiating a yellow phase will be triggered, after which triggering of a second detector will initiate a red phase (see Figure 4.5). By placing these close to the traffic light ascertains only one vehicle to be able to pass the traffic light per cycle. A sign saying it is prohibited to pass the traffic light with multiple cars per green phase could also be installed. These signs are present at numerous RMI sites already.

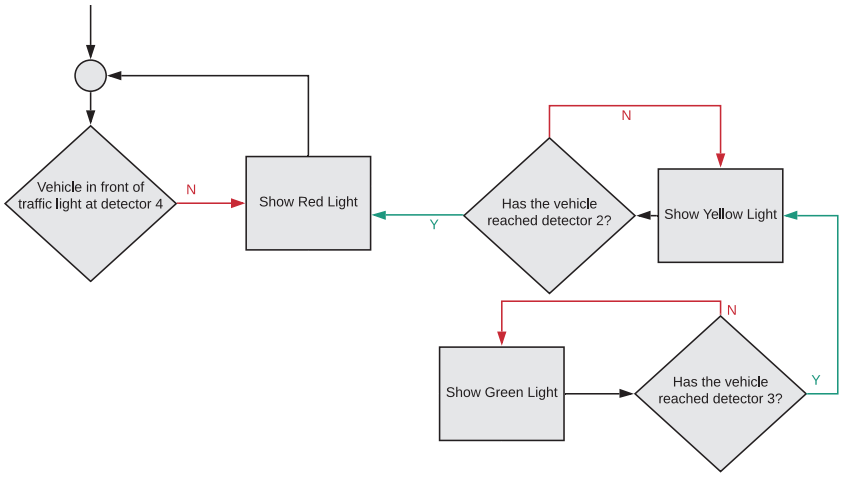

Figure 4.5: Turning the traffic light back to red

4.5 MICROSCOPIC RAMP METERING STRATEGY

To conclude this chapter, an overview of the control structure will be presented. Additionally, an overview of the assumptions that come along with proposed control scheme will be provided. Furthermore, an overview of the necessary equipment will be presented. Following this, the adjustments that have to be made in order to change the RM control from a macroscopic to a microscopic approach will be summarised.

4.5.1 Control structure

Summarising the steps explained in Section 4.4 results in the entire control structure, as shown in Figure 4.6. An approximation of the location of the gap measurement detectors can be found in Figure 4.8.

In Figure 4.6, as in all previously shown control schemes, the green lines indicate what the next step in the control structure is when the answer to the considered question is 'yes'. A red line indicates the next step when the answer to the considered question is 'no'. Black lines indicate a follow-up step regardless of the considered action. Furthermore, rectangles are actions and diamond-shaped blocks indicate yes/or questions. The control schema starts at the top.

Additionally, it can be seen in Figure 4.6 that there are several variables that have yet to be determined. The calculations for determining the location of the gap measurement detectors will be provided in the sub-section called "Gap detector location". The formulae for calculating the minimum waiting time for passenger cars when following up a truck, will be provided in the sub-section called "Minimum waiting time". The actual values of the remaining yet to be established variables, will be be outlined in Chapter 6.

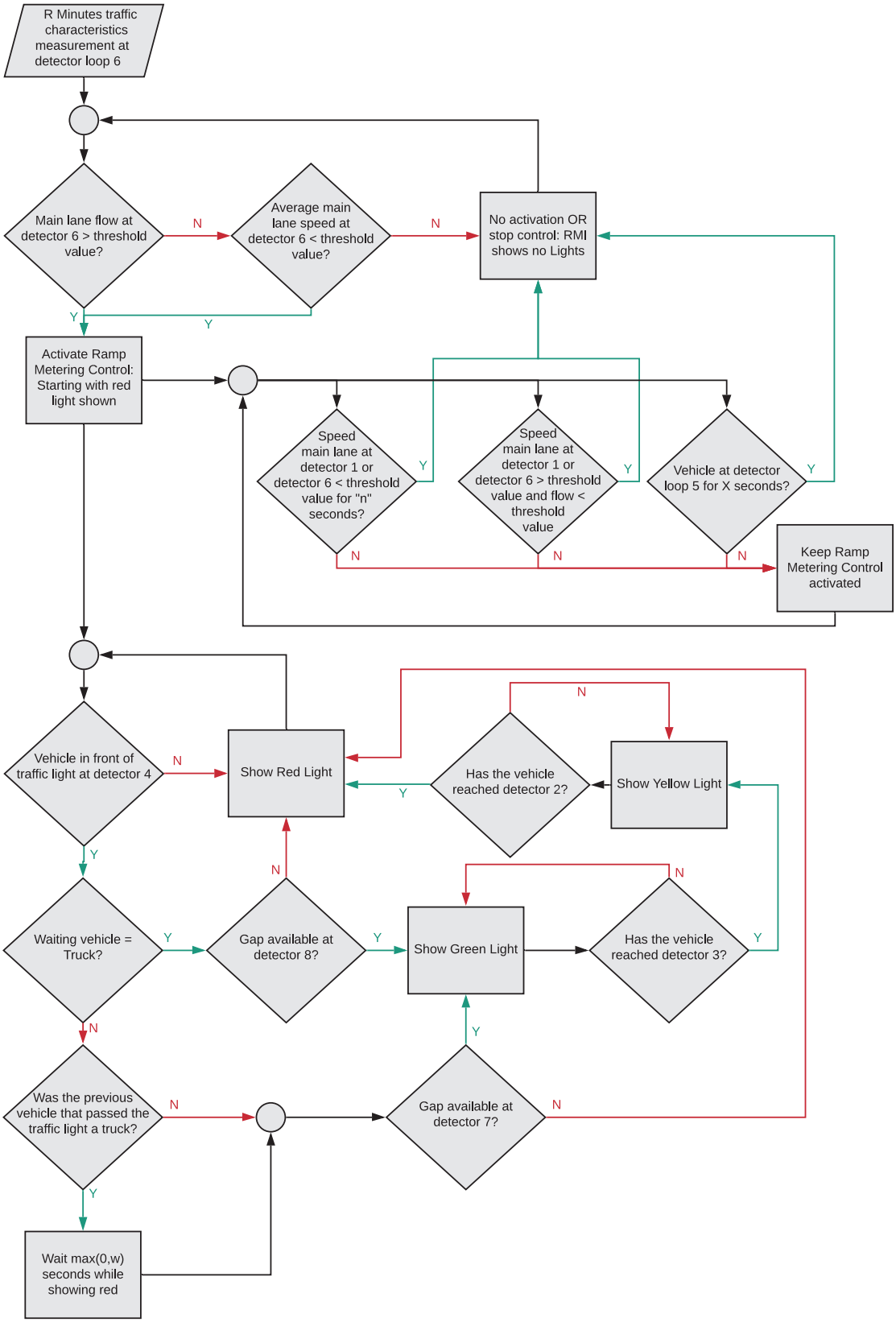

Figure 4.6: Control concept

4.5.2 Road layout

As stated in Section 4.4, a single lane on-ramp for the main part of the on-ramp is assumed. Furthermore, interviews with multiple Rijkswaterstaat employees led to the conclusion that most RMIs in the Netherlands have a three lane highway. Having a multiple lane main road leads to a lower density on the right lane, since rabbits can overtake slugs (Daganzo, 2002). Accordingly, a single lane on-ramp with a three lane main road is studied.

Furthermore, it is important that measured gaps are still sufficient gaps when the merging vehicles has caught up with the gap. Without connectivity between the vehicles or without an advice for the following vehicle of the gap, it is not possible to ensure this completely. Nevertheless, what can be done, is to prohibit vehicles from the middle lane to fill up the gaps on the right lane. To accomplish this, a semi-permeable lane demarcation is put in place. In other words, a continuous line to prevent vehicle movement from the middle lane to the right lane and a normal demarcation to enable lane switches from the right lane to the middle lane. An example of this in the Netherlands is shown in Figure 4.7. This semi-permeable lane demarcation should start at least several meters upstream of the most upstream gap detector on the main road and continue to at least the end of the merging area in an effort to preserve the measured gaps until the merging manoeuvre.

Figure 4.7: semi-permeable lane on the A20, the Netherlands (Google, 2020a)

Finally, in order to increase the chance of having a gap on the right lane of the main road available, the presence of an off-ramp upstream of the controlled on-ramp is useful. In order to create even more gaps in the traffic flow on the right lane, the semi-permeable lane demarcation could be extended all the way up to this off-ramp.

A road layout as described in this sub-section is shown in Figure 4.8. It is assumed that passenger cars accelerate more quickly than trucks. This leads to the gap detector for trucks being located more upstream of the RMI than the gap detector for passenger cars. The locations of the loop detectors are approximated in this figure. The actual locations for the loop detectors that are also already present in the currently used macroscopic Rijkswaterstaat RM algorithm will be discussed in Chapter 6. The calculations to determine the location of the gap measurement detectors are provided in the next section.

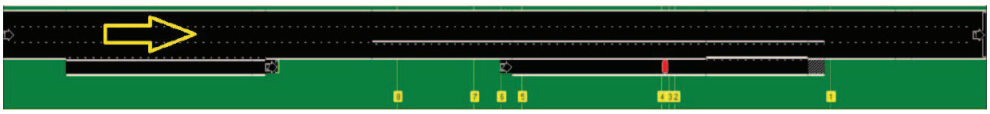

Figure 4.8: Road layout example, including the approximate loop detector locations

4.5.3 Gap detector location

A fundamental control idea behind the microscopic RM control structure is that the merging vehicle has the measured gap at its disposal when it actually wants to merge. Therefore, determining the correct location of the gap detector locations is of the utmost importance. These gap detectors are also present in the control scheme developed in this research, as shown in Section 4.4.

By reverse engineering, the location of the gap measurement detectors can be determined. This location, in meters upstream of the traffic light is the travelled distance of the main lane gap minus the travelled distance of the merging vehicle.

$$x_{\text{loop}} = s_{\text{main}} - s_{\text{eff}} \tag{4.1}$$

The acceleration distance of the merging vehicle can be calculated with some assumptions. The first assumption is that the speed of the merging vehicles is $0\frac{km}{h}$ at the beginning of the acceleration. Additionally, the acceleration is assumed to be constant. This is of course not true, but by implementing an average acceleration the calculations get a lot less complicated. Additionally, the results do not differ greatly. With these assumptions, the travelled acceleration distance can be calculated by dividing the speed squared by two times the average acceleration.

$$s = \frac{v^2}{2a} \tag{4.2}$$

Obviously, this acceleration distance has a minimum value (i.e. the vehicle can not merge before the start of the merging area) and a maximum value (i.e. the vehicle has to merge before the end of the merging area). Therefore, the actual merging acceleration has a certain maximum and minimum, which depend on the infrastructure. If the calculated desired acceleration distance does not fall within these system boundaries, the speed of the merging is not equal to the desired merging speed. This means that the speed of the vehicle when merging has to be computed. This can be done by taking the square root of the boundary acceleration distance times the average acceleration times two.

$$v = \sqrt{2sa} \tag{4.3}$$

The time it takes the merging vehicle to start the merging manoeuvre can now be determined by dividing the acceleration distance by the average speed during the acceleration distance. The average speed can be calculated by dividing the merging speed by two, assuming the vehicle starts off at standstill.

$$t_{\text{acc}} = \frac{s_{\text{eff}}}{\frac{1}{2}v_{\text{merg}}} \tag{4.4}$$

This acceleration time can in turn be used to compute the travelled distance of the measured gap. The main lane speed is multiplied by the this acceleration time to get to the travelled distance of the measured gap. It is assumed that the speed of the gap is constant.

$$s = vt \tag{4.5}$$

Subtracting the effective acceleration distance from this travelled distance leads to the location of the gap measurement detector location upstream of the traffic light.

As can be derived from looking at the aforementioned equations, the exact location of the gap measuring loop detectors depends on a lot of variables. The values of these variables, just like the other values stated in Figure 4.6 that are yet to be determined, will be established in Chapter 6. Additionally, a more in depth determination of the various calculations in this chapter is provided in Appendix D. Furthermore, an overview of the variables is presented in Appendix A.

4.5.4 Minimum waiting time

Besides the exact location of the loop detector, the minimum waiting time for passenger cars when they follow up upon a truck, has to be calculated. This has to be done because the locations of the gap detector loops are different, enabling the both detectors to measure the same gap with a time interval in between the measurements. To ascertain that the same gap for a single vehicle is not used for both a truck and a passenger vehicle, the minimum waiting time is put in place. This minimum waiting time can be computed by dividing the difference in the location of the gap measurement loop detectors by the travelling speed of the measured gap, added to the required minimum gap time.

$$t_{\text{wait}} = \frac{x_{\text{loop}}^{truck} - x_{\text{loop}}^{car}}{v_{\text{main}}} + t_{\text{gap}}^{truck} \tag{4.6}$$

This should also prevent the need for a passenger vehicle to overtake a truck to reach the measured gap on time. However, to make sure these situations do not occur, an additional minimum waiting time can be computed. This minimum waiting time to ensure that a passenger car does not have to overtake a truck on the on-ramp is equal to the acceleration distance of the passenger car divided by the average speed for the truck over the acceleration distance for the passenger car. This average speed is equal to halve the speed of the truck at the end of the acceleration distance of the passenger car, assuming the trucks has an initial speed of $0\frac{km}{h}$. These equations are provided in Appendix D. The eventually used minimum waiting time for a passenger car with a truck as predecessor should be the maximum between the two calculations, which is always equal to Equation 4.6 when the equations are correctly executed.

4.5.5 Assumptions

Considering all previous statements in this chapter, several assumptions have been made in order to get the the control structure as presented in Figure 4.6. Firstly, it is assumed that there are no defect loop detectors or errors with either the loop detectors or control algorithm during the time the microscopic RM control structure is activated.

Secondly, it is speculated that there are no traffic offenders, such as red light running or unlawfully crossing semi-permeable lane demarcation. Thirdly, it is assumed that there are two types of vehicles (ie. trucks and passenger cars) and that all vehicles can be categorised as one of these two. Fourthly, it is estimated that all drivers have the same reaction time.

Fifthly, as stated in the road layout sub-section, a single lane on-ramp for the main part of the on-ramp is assumed. Additionally, a multiple lane main road is considered. Furthermore, with regards to the road layout, it is assumed that the on-ramp downstream of the RMI and the main road are (more or less) parallel to each other and that the waiting vehicles stop a negligible distance in front of the traffic light. Moreover, it is assumed that the merging vehicles have an initial speed of 0 $\frac{km}{hour}$ when they start to accelerate and their acceleration is assumed to be constant.

Lastly, it is assumed that passenger cars accelerate more quickly than trucks (or at least not so much slower that trucks want to overtake passenger cars when being released t_{gap} seconds later). Therefore, the extended minimum waiting time only applies for situations when a passenger car follows up upon a truck. Additionally, this assumption leads to the gap detector for trucks being located more upstream of the RMI than the gap detector for passenger cars.

4.5.6 Equipment and adjustments

As can be seen in Figure 4.6, not much equipment nor high-tech equipment is needed. According to the control scheme, there are at least twelve loop detectors in total at eight different locations (the flow detector loops need to be present at all lanes on the main road), a traffic light and one semi-permeable lane demarcation between the middle lane and right-hand lane necessary. When comparing this to the current control structure, there are basically just two loop detectors added in total. These are located on the right-hand lane on the main road in order to measure gaps in the main lane flow.

Besides these changes in hardware, the algorithm for the proposed microscopic RM control structure is different than the current macroscopic RM control structure. For instance, gaps will be measured by keeping track of the time since the last trigger at the specific loop detector. Furthermore, the loop detector in front of the traffic light on the on-ramp is the only loop detector that has to be able to determine if the waiting vehicle is either a passenger car or a truck. The microscopic RM control structure in turn needs to be able to combine the waiting vehicle type to the right gap detector. Moreover, the algorithm has to be able to store the previous released vehicle and some time data in order to check the minimum waiting time of the vehicles in front of the traffic light.

Thus, the necessary changes to adjust the RM approach to a microscopic nature are minimal, which increases the chance of implementation.

5 ACCELERATION DISTRIBUTION AT RAMP METERING INSTALLATIONS

As mentioned in Chapter 3, an experiment in order to get acceleration data at RMIs in the Netherlands has been performed. This way, a distribution for the acceleration which mimics the actual behaviour can be put in the OTS simulation software. This chapter will give insights in the setup and outcomes of the acceleration experiment. How this was implemented in OTS will be explained in Chapter 6.

5.1 DATA GATHERING AND PREPARING

As described in Section 3.4, firstly, data had to be gathered in order to get an acceleration distribution for vehicles in the Netherlands. This was done by filming the vehicles on the on-ramp A13 Delft-North in the direction of Rotterdam for nearly two and a half hours during the evening peak on Tuesday the 5th of November 2019 (see Figure 5.1). The result is five videos with a duration of just under 30 minutes.

Figure 5.1: Example single video frame

Then, the videos were split into individual frames. This was done by means of a program called **ffmpeg** (FFmpeg, nd). The code that has been run to obtain the individual frames of the first 30 minute video of the conducted experiment, came down to ***ffmpeg.exe -i VIDEO_00022.mts -r 25.000 image%05d.jpg***.

Next, these frames will be combined into vehicles trajectories with a MATLAB-code, provided by Victor Knoop (MathWorks, 2020). A few of the vehicle trajectories for the first 30 minutes video is shown in Figure 5.2.

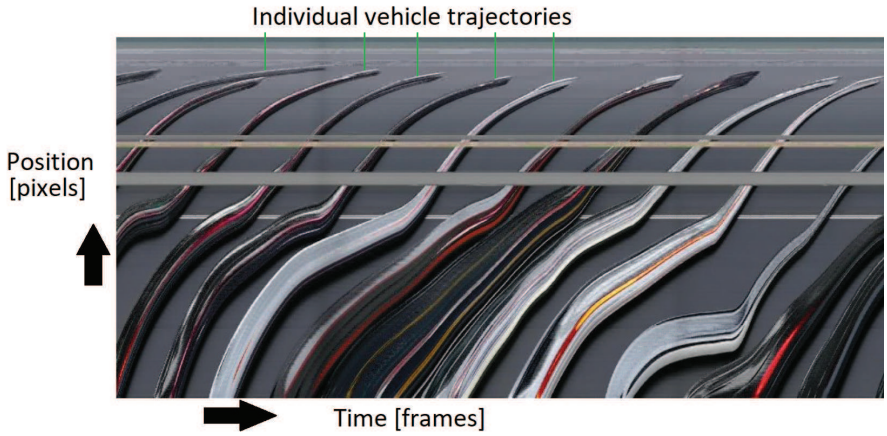

Figure 5.2: Example of vehicle trajectories

Of the drawn up trajectories, only the acceleration part is interesting for this experiment. Therefore, only vehicles with a low speed (i.e. a more or less horizontal trajectory near the stop-line of the RMI) are taken into account. The pixel data of the trajectories is determined by hand, by looking at the border between the coloured trajectory and the shadow of the vehicle in GIMP 2.10.14 (GIMP, 2019). The videos had a total of 25 frames per second. Therefore, one pixel in time is known to be equivalent to 0.04 seconds. Additionally, as explained in Section 3.4, one of the first vehicles was driven by a fellow student (William van Lindonk). This vehicle was driving a constant speed of 66$\frac{km}{hour}$ for the entirety of the on-ramp. With this knowledge and the hand derived pixel data from GIMP 2.10.14, a conversion from pixel to meters has been configured in Excel (GIMP, 2019; Microsoft, 2020). The equations that result in the conversion, as shown in Table 5.1, are listed from Equation 5.1 to Equation 5.4. Moreover, the conversion graph is portrayed in Figure 5.3.

Firstly, the inverse distance (from low to high) in pixels at data point i is equal to the distance in pixels of that vehicle at the beginning of the considered acceleration trajectory minus the originally measured distance in pixels at data point i from high to low.

$$X_i^{'f} = X_0^f - X_i^f \tag{5.1}$$

The time at data point i is equal to the value of the data point in frames divided by 25.

$$T_i^s = \frac{T_i^f}{25} \tag{5.2}$$

Then, the position of the controlled vehicle in meters at data point i is equal to the difference in the position in pixel data of the current data point and the previous data point times the constant speed of the controlled vehicle, added to the position in meters in the previous data point.

$$X_i^m = (X_i^{'f} - X_{i-1}^{'f})V_c + X_{i-1}^m \tag{5.3}$$

Combining the distances in pixel and meter data enables the conversion of the position data in pixels to the position data in meters. The linear increase of meters over frames between data point i and data point $i-1$ is calculated by dividing the difference between the two data points in meters by the difference of the two data points in pixels.

$$\Delta\frac{X_i^m}{X_i^f} = \frac{X_i^m - X_{i-1}^m}{X_i^f - X_{i-1}^f} \tag{5.4}$$

Table 5.1: Conversion of pixel data into SI base units

Known vehicle trajectory					
T_i^f	X_i^f	$X_i^{'f}$	T_i^s	X_i^m	$\Delta \frac{X_i^m}{X_i^f}$
377.5	1080	0	15.10	0.00	0.00
380	1029	51	15.20	1.83	0.04
383	981	99	15.32	4.03	0.05
386	938	142	15.44	6.23	0.05
389	903	177	15.56	8.43	0.06
392	872	208	15.68	10.63	0.07
395	843	237	15.80	12.83	0.08
398	819	261	15.92	15.03	0.09
401	797	283	16.04	17.23	0.10
404	778	302	16.16	19.43	0.12
407	760	320	16.28	21.63	0.12
410	745	335	16.40	23.83	0.15
413	731	349	16.52	26.03	0.16
420	703	377	16.80	31.17	0.18
423	691	389	16.92	33.37	0.18
432	663	417	17.28	39.97	0.24
443	639	441	17.72	48.03	0.34
451	625	455	18.04	53.90	0.42
471	591	489	18.84	68.57	0.43
481	579	501	19.24	75.90	0.61
493	567	513	19.72	84.70	0.73
503	559	521	20.12	92.03	0.92
512	552	528	20.48	98.63	0.94
525	544	536	21.00	108.17	1.19
533	540	540	21.32	114.03	1.47
550	532	548	22.00	126.50	1.56
567	524	556	22.68	138.97	1.56
580	518	562	23.20	148.50	1.59
596	512	568	23.84	160.23	1.96
604	510	570	24.16	166.10	2.93
621	506	574	24.84	178.57	3.12
634	503	577	25.36	188.10	3.18
652	499	581	26.08	201.30	3.30
667	496	584	26.68	212.30	3.67
688	492	588	27.52	227.70	3.85
705	489	591	28.20	240.17	4.16
726	486	594	29.04	255.57	5.13
746	484	596	29.84	270.23	7.33
786	480	600	31.44	299.57	7.33
826	476	604	33.04	328.90	7.33
880	471	609	35.20	368.50	7.92
922	467	613	36.88	399.30	7.70
954	464	616	38.16	422.77	7.82

5.2 OBSERVED PASSENGER CAR TRAJECTORY DATA

For a total of 19 passenger cars, data points were obtained from all computed vehicle trajectories as a result of the data preparation. All 19 vehicles were at (or near) standstill conditions before they started to accelerate. The limitation to a total of 19 vehicles is primarily a result of research time constraints. Nonetheless, a distribution fitted to this 19 vehicles at least allows for randomness between the

maximum acceleration between the vehicles, which is the most important factor for this research.

For these 19 considered passenger vehicles, the pixel data was converted to time data in seconds and distance data in meters with the help of the conversion matrix shown in Table 5.1. Then, these data points (in meters and seconds) were used to fit the acceleration physics formulae as stated in Section 3.4 and Appendix B. An example regarding the first vehicle is shown in the this sub-section. This starts off with the raw data in pixels as visualised in Table 5.2.

Table 5.2: Example of obtained raw data points

Raw data points vehicle 1			
T (frame)	X (frame)	T (s)	X (m)
15602	764	624.08	21.14
15622	764	624.88	21.14
15633	759	625.32	21.78
15646	749	625.84	23.25
15662	731	626.48	26.03
15693	691	627.72	33.37
15718	661	628.72	40.64
15734	641	629.36	47.36
15752	620	630.08	56.06
15776	595	631.04	66.84
15792	582	631.68	74.07
15841	550	633.64	101.02
15879	531	635.16	128.06
15903	522	636.12	142.14
15928	514	637.12	156.32
15949	508	637.96	172.33
15970	503	638.80	188.10
16013	494	640.52	220.00

For this first vehicle, assuming the first data point starts at $(0,0)$, these data points are shown in Table 5.3. Furthermore, the observed data is rounded to the second decimal.

Table 5.3: Total absolute time and distance data

T abs [sec]	X abs [m]
0.00	0.00
0.80	0.00
1.24	0.64
1.76	2.10
2.40	4.89
3.64	12.22
4.64	19.49
5.28	26.22
6.00	34.91
6.96	45.70
7.60	52.92
9.56	79.87
11.08	106.91
12.04	121.00
13.04	135.18
13.88	151.19
14.72	166.96
16.44	198.86

Since it is assumed that the vehicles start accelerating from the beginning, the second data point is neither 0 for the time, nor 0 for the distance. That leads to the eventual used data point for the first vehicle as displayed in Table 5.4.

Table 5.4: Used absolute time and distance data

T abs [sec]	X abs [m]
0.00	0.00
0.44	0.64
0.96	2.10
1.60	4.89
2.84	12.22
3.84	19.49
4.48	26.22
5.20	34.91
6.16	45.70
6.80	52.92
8.76	79.87
10.28	106.91
11.24	121.00
12.24	135.18
13.08	151.19
13.92	166.96
15.64	198.86

5.3 FITTING VEHICLE TRAJECTORIES

Now that the measured data points are determined, an acceleration curve can be estimated. As explained in Section 3.4, this is done by means of Equation 3.1 to Equation 3.7. Considering these equations, assumptions on several variables need to be made. This includes the mass of the vehicles and the maximum delivered power of the engine for example.

The mass of the vehicles is assumed to be $1400kg$. An absolute top speed of $250\frac{km}{h}$ is assumed in this experiment. These statistics are in the common ranges of a top speed of $225\frac{km}{h}$ and $250\frac{km}{h}$ and an empty mass of between $1200kg$ and $1400kg$ (BWM, nd; Honda, nd). A speed of $250\frac{km}{h}$ is equivalent to $260bhp$. Furthermore, as can be derived from Equation 3.5, $F^r = F^e$ when the acceleration is 0. When operating at a top speed of $250\frac{km}{h}$, the engine delivers a force of $2477.65N$ (see Equation B.3). Then, the combined air resistance components that applies to the vehicle, without the speed (i.e. ϕ), is equal to $0.513765\frac{m}{s^2}$. The chosen time step dt is 0.01 seconds.

Now that the ϕ component is known, the $F_t^r, a_t^{eff}, v_{t+1}$ and x_{t+1} can be calculated when the p_{used} and a_{max} are estimated and the vehicle starts with a speed of $0\frac{m}{s}$ at location $0m$. Repeating this procedure for numerous values for p_{used} and a_{max}, minimising the MSE, results in an optimal value for the to be fitted variables. The then corresponding calculated times and positions of the vehicle are rounded to the second decimal.

For the first vehicle, the optimal values are:

- MSE: 17.1226 m^2;
- MSE_{average}: 1.0072 m^2;
- a_{max}: 3.1765 $\frac{m}{s^2}$;
- p_{used}: 19340 $Watt$.

This results in the effective acceleration of the vehicle per time t (Figure 5.4), the calculated speed of the vehicle per time t (Figure 5.5) and the calculated position of the vehicle per time t (Figure 5.6). Additionally, the observed data points can now be compared with the calculated position of the vehicle, as shown in Table 5.5. This way, the differences and the squared differences can be calculated as well.

Table 5.5: Observed and calculated data points vehicle 1

Observed and calculated data points vehicle 1				
T observed	X observed	X calculated	Xobs - Xcalc	(Xobs - Xcalc)^2
0.00	0.00	0.00	0.00	0.00
0.44	0.64	0.31	0.33	0.11
0.96	2.10	1.46	0.64	0.40
1.60	4.89	4.06	0.83	0.69
2.84	12.22	12.08	0.14	0.02
3.84	19.49	20.61	-1.12	1.25
4.48	26.22	26.85	-0.63	0.39
5.20	34.91	34.52	0.39	0.16
6.16	45.70	45.7	0.00	0.00
6.80	52.92	53.71	-0.79	0.63
8.76	79.87	80.75	-0.88	0.78
10.28	106.91	104.03	2.88	8.27
11.24	121.00	119.67	1.33	1.76
12.24	135.18	136.68	-1.50	2.24
13.08	151.19	151.49	-0.30	0.09
13.92	166.96	166.77	0.19	0.04
15.64	198.86	199.40	-0.54	0.29

Taking the sum of the squared differences and dividing this by the total number of observations, results in the average MSE (MSE_{average}) per observation. Taking the square-root of the MSE_{average} results in the average absolute deviation between the calculated position and the observed position. The results for all considered vehicles for a_{max}, p_{used}, MSE_{average} and this absolute deviation are displayed in Table 5.6.

Table 5.6: Fitting results of the 19 considered vehicles

Vehicle	a_{max}	p_{used}	MSE_{average}	deviation
1	3.1765	19340	1.0072	1.0036
2	1.5412	30331	3.3517	1.8308
3	1.3481	51661	4.0164	2.0041
4	2.1223	13821	1.1714	1.0823
5	1.7017	29332	1.9376	1.392
6	1.5265	23160	0.9287	0.9637
7	2.5977	16954	3.3461	1.8292
8	1.6429	20447	0.6225	0.789
9	1.3817	17237	1.6542	1.2862
10	2.8791	11247	0.4046	0.6361
11	1.6414	9367	0.5043	0.7101
12	2.6248	14269	0.3862	0.6214
13	2.0635	63227	16.3741	4.0465
14	3.8414	38307	2.6412	1.6252
15	1.5065	18335	0.9995	0.9997
16	2.8139	21681	1.7681	1.3297
17	2.1074	99999	24.7351	4.9734
18	1.9534	26045	0.551	0.7423
19	1.9136	31462	0.8183	0.9046

5.4 STATISTICAL TESTS

When considering the results shown in Table 5.6, a correlation check between a_{max} and p_{used} can be performed with SPSS. Additionally, a distribution can be fitted to the data with the Kolmogorov-Smirnof test in SPSS (IBM, 2020; SPSS, nd). However, when performing these statistical tests, vehicles 13 and 17 are not considered, since the MSE_{average} value is a lot higher than for the other vehicles. In other words, the calculated trajectory deviates a lot from the observed trajectory and these calculated trajectories are thus deemed to be outliers. This could for instance be due to measurement errors. Moreover, vehicle 14 is not taken into consideration, because the value for a_{max} is a lot higher than for the other vehicles. Therefore, this vehicle is treated as an outlier as well.

As shown in Table 5.7, there is no significant correlation between the a_{max} and the p_{used} of the vehicles. Additionally, having a normal distribution for the maximum acceleration of the drivers seems logical. There is a mean maximum acceleration for the population; some people will accelerate faster, some will accelerate more slowly. The Kolmogorov-Smirnof test indicates that there is no evidence to reject the null-hypothesis, resulting in keeping the normal distribution for both the a_{max} and the p_{used} variables (see Table 5.8).

Table 5.7: Correlation test between a_{max} and p_{used}

Correlation			
		a_{max}	p_{used}
a_{max}	Pearson Correlation	1	-0.419
	Sig. (2-tailed)		0.106
	N	16	16
p_{used}	Pearson Correlation	-0.419	1
	Sig. (2-tailed)	0.106	
	N	16	16

Table 5.8: Kolmogorov-Smirnof test for normality

One-Sample Kolmogorov-Smirnov Test			
		amax	pused
N		16	16
Normal Parameters	Mean	2.023206	22168.06
	Std. Deviation	0.6007555	10272.220
Most Extreme differences	Absolute	0.204	0.149
	Positive	0.204	0.149
	Negative	-0.143	-0.106
Test Statistic		0.204	0.149
Asymp. Sig (2-tailed)		0.075	0.200

5.5 TRUCK ACCELERATION

Unfortunately, just one truck was filmed that was close to a standstill at the traffic light before accelerating. Therefore, the same method could not be used to obtain a distribution of truck accelerations in the Netherlands. In order to get a distribution anyway, the same standard deviation as for the passenger cars is considered, but a lower mean maximum acceleration for trucks is estimated. This mean is taken from Rakha et al. (2001). In Rakha et al. (2001), the maximum acceleration for heavy trucks was found to be $1.64\frac{m}{s^2}$. This is lower than the found average for passenger cars, which is in line with expectations, thus this value is regarded as the mean maximum acceleration for trucks in this research.

5.6 CONCLUSION

The conclusion of this chapter is that the maximum acceleration that drivers have in the beginning of their acceleration curve is not correlated with their used power, which limits their acceleration later on in the curve. Furthermore, both their maximum acceleration and used power are fit to be normally distributed over the population. For the a_{max}, this comes down to a mean of $2.023\frac{m}{s^2}$ and a standard deviation of $0.600\frac{m}{s^2}$. For the used power (p_{used}) the characteristics of the normal distribution are estimated to include a mean of $22168 Watt$ and a standard deviation of $10272 Watt$. These distributions will be used as input in the actual simulations.

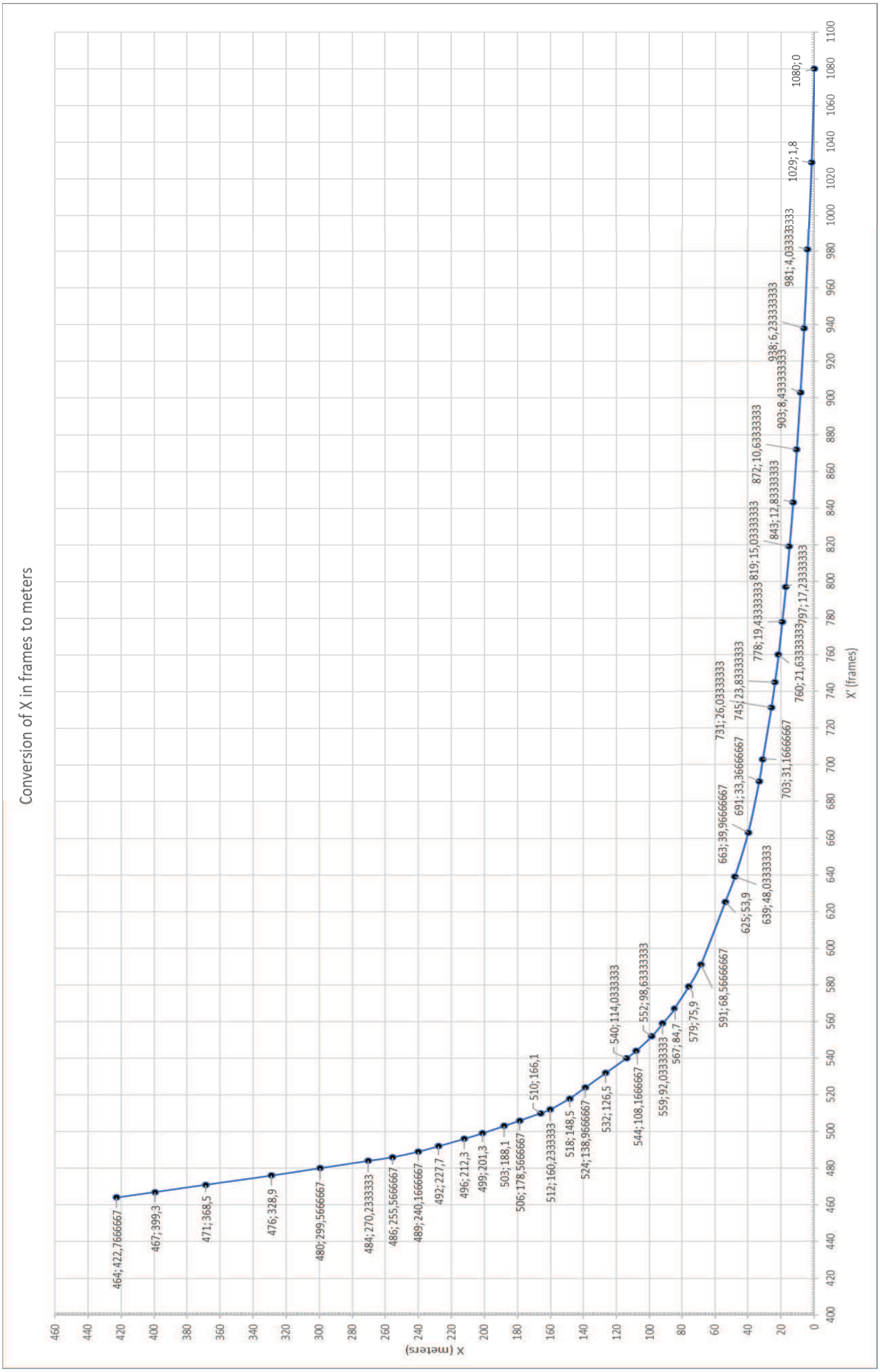
Conversion of X in frames to meters
X (meters)
X' (frames)
464; 422,7666667
467; 399,3
471; 368,5
476; 328,9
480; 299,5666667
484; 270,2333333
486; 255,5666667
489; 240,1666667
492; 227,7
496; 212,3
499; 201,3
503; 188,1
506; 178,5666667
510; 166,1
512; 160,2333333
518; 148,5
524; 138,9666667
532; 126,5
540; 114,0333333
544; 108,1666667
552; 98,63333333
559; 92,03333333
567; 84,7
579; 75,9
591; 68,56666667
625; 53,9
639; 48,03333333
663; 39,96666667
691; 33,36666667
703; 31,16666667
731; 26,03333333
745; 23,83333333
760; 21,63333333
778; 19,43333333
797; 17,23333333
819; 15,03333333
843; 12,83333333
872; 10,63333333
903; 8,433333333
938; 6,233333333
981; 4,033333333
1029; 1,8
1080; 0

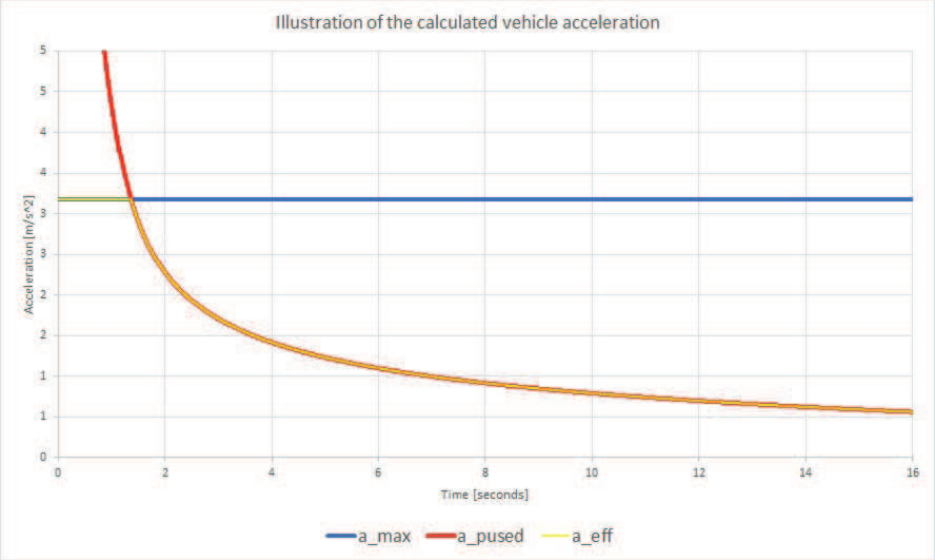

Figure 5.4: Effective acceleration of vehicle 1

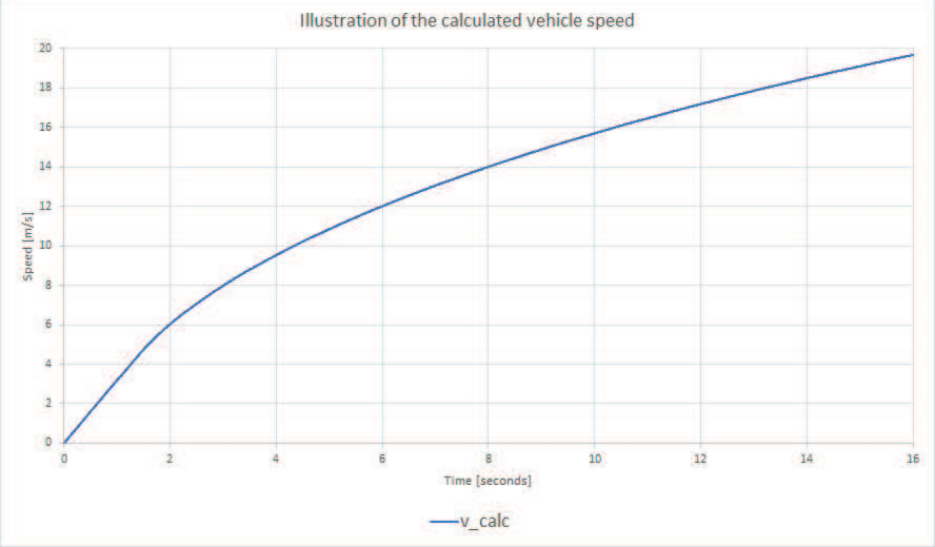

Figure 5.5: Speed of vehicle 1

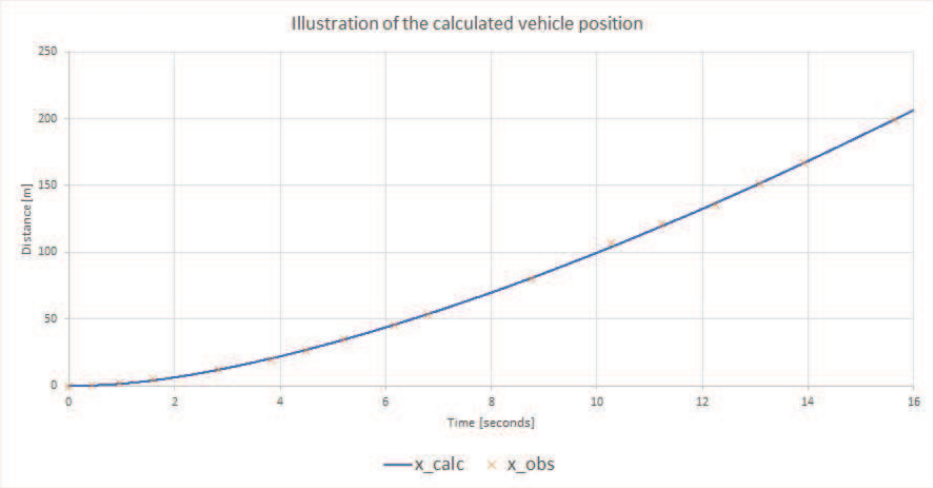

Figure 5.6: Calculated position and observed position of vehicle 1

6 SIMULATION

This chapter will outline the simulation characteristics used in this research. Firstly, the network layout will be described. Secondly, all simulations will be shortly outlined, including a summary of the outputs as stated in Chapter 3. Thirdly, the input for the different simulations will be specified.

6.1 NETWORK LAYOUT

As mentioned in Chapter 4, a single lane part of the on-ramp from the Ramp Metering Installation (RMI) to the end merging area, using only one traffic light, is preferred. Thus, a single lane on-ramp with a three lane main road is chosen. Furthermore, three lane highways are very common in the Netherlands, especially regarding sites with an RMI. However, most location with an RMI have two traffic lights the the on-ramp. Therefore, the combination of a single RM traffic light with a three lane main road does not occur frequently in the Netherlands. Nonetheless, the site used for fitting the acceleration behaviour of the merging vehicles is a location with a three lane main road and a single lane on-ramp. Therefore, this site is also used as a blueprint for the road layout in OTS. This site is the A13 Delft-North on-ramp in the direction of Rotterdam. This location is shown in Figure 6.1 and the off-ramp upstream of this on-ramp is shown in Figure 6.2.

The characteristics related to the length of the on-ramp, length of the merging area, location of the RMI and distance between the off-ramp upstream of the on-ramp and the considered on-ramp, are measured with the distance measuring tool in Google Maps. The findings are used in OTS. Additionally, as can be seen from Figure 6.2, the off-ramp shared a merging area with the on-ramp upstream of the off-ramp. However, this led to some complications in OTS and since this extra on-ramp is not relevant for simulating the considered on-ramp, it is left out in the network layout. Moreover, as described in Chapter 4, a semi-permeable lane demarcation is recommended, but this is currently not present at the considered site. Therefore, this semi-permeable lane demarcation is added in the simulation road layout. This results in the network layout in OTS, displayed in Table 6.1 and in Figure 6.3.

It should be noted that the existing semi-permeable lane demarcation to prevent going back from the off-ramp to the main road is not put in place in the OTS road layout. This is, because this caused crashes in the simulation as a results of drivers staying right and then realising that they had to continue straight too late. Strangely enough, the drivers do not go back and forth to the off-ramp without this semi-permeable lane demarcation. However, in congestion conditions, drivers sometimes go to the off-ramp lane when they assume that saves them travel time. This can lead to traffic jams originating next to the off-ramp.

Figure 6.1: Considered on-ramp, A13 Delft-North in the direction of Rotterdam (Google, 2020b)

Figure 6.2: Off-ramp upstream of the considered on-ramp (Google, 2020b)

Table 6.1: Simulation road layout characteristics

Simulation road layout characteristics		
Description	X-coordinate in meters	Y-coordinate in meters
Start location	0	0
Begin off-ramp merging area	2050	-3.5
End off-ramp merging area	2239	-3.5
Off-ramp destination sink	2450	-27
On-ramp spawn point	2629	-28.5
On-ramp traffic light	2864.6	-13.5
Begin on-ramp merging area	3000	-3.5
End on-ramp merging area	3310	-3.5
Final destination sink	5950	0
Main flow loop detectors	2800	0
First traffic light demand detector	2853	-13.7
Second traffic light demand detector	2859	-13.7
Traffic light yellow detector	2866.5	-13.7
Traffic light red detector	2868.8	-13.7

Figure 6.3: Zoomed in OTS simulation road layout

6.2 OUTPUTS AND SIMULATIONS

Section 3.5.2 mentions the various generated outputs and grazed the surface of the simulation runs. The outputs and the numerous simulations will be described in more detail in this section.

6.2.1 Simulations

As mentioned in Section 3.5.2, the three different control structures that have been simulated are:

- No Ramp Metering (RM) control;
- Current Rijkswaterstaat Ramp Metering (RM) control approach;
- Microscopic Ramp Metering (RM) control approach.

For the no control alternative, no variables, besides the traffic flow input, need to be determined. This is not the case for the other control approaches. Considering Section 4.5, there are several variables in the microscopic Ramp Metering (RM) control approach that need to be resolved. These include:

- Activation flow;
- Deactivation flow;
- Necessary gap time;
- Maximum free flow speed (i.e. with a lower speed, the RMI is always activated);
- Minimum required speed to have an activated RMI;
- Passenger vehicle gap detector location;
- Truck gap detector location;
- Minimum waiting time passenger vehicle behind truck;
- Placement of the other detectors (i.e. flow on the main road, at the beginning of the on-ramp, just in front of the RMI, yellow detector, red detector);
- Aggregation level (i.e. the time the measured flow and speed are determined).

Similarly, the current Rijkswaterstaat algorithm has numerous comparable variables. Basically, the same variables apply to Rijkswaterstaat, apart from the gap measurement detectors, the minimum required speed to have an activated RMI and the minimum waiting time for a passenger vehicle at the on-ramp when they succeed a truck (see Figure 6.4).

In addition to these overlapping variables, the Rijkswaterstaat control structure includes some supplementary variables. These consist of a maximum waiting time for the front waiting vehicle and a maximum cycle flow (i.e. the flow when this maximum waiting time is put in place). For the simulated Rijkswaterstaat control structure, the values of all variables are chosen to be as closely to the actual values as possible. Since traffic jams will not originate downstream of the on-ramp in the considered research scope, which could have caused a spillback congestion at the considered site, the flow detectors downstream of the merging areas are left out to prevent the simulation from being unnecessarily complicated. Furthermore, the detector at the beginning of the on-ramp is left out for a similar reason. The underlying road network is also not simulated, so spillback congestion on the underlying road network will not be simulated, preventing the need to actively check the length of the queue at t he on-ramp.

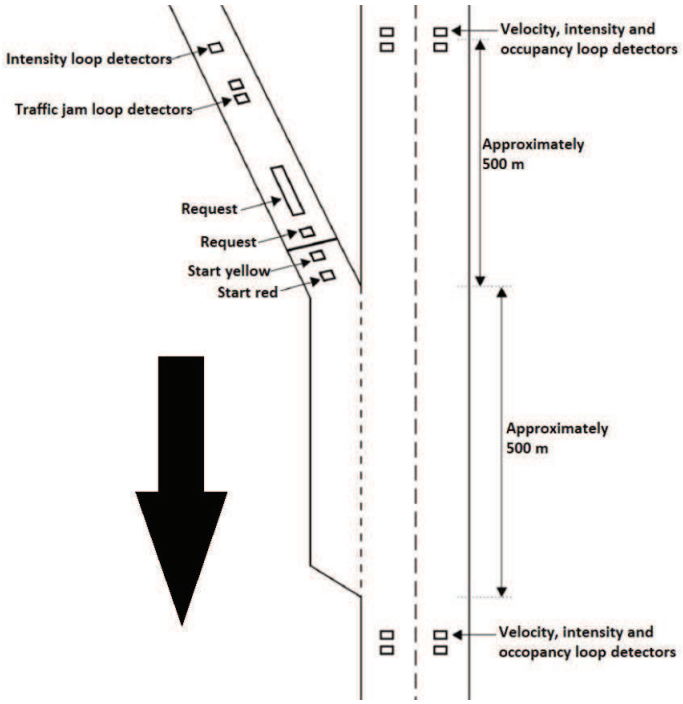

Figure 6.4: Layout of the current Rijkswaterstaat algorithm (Rijkswaterstaat, 2013)

To determine the location of the flow detector loops, mostly Rijkswaterstaat (2013) is consulted. Nonetheless, the loop detectors upstream of the RMI on the main lane are measured with the distance measuring in Google Maps. This is done by measuring the distance from the loop detectors shown in Figure 6.5 to the start of the merging area. This comes down to approximately 200 meters.

Figure 6.5: Picture of the loop detectors upstream of the on-ramp (Google, 2020b)

Considering all this, the values for the variables are summarised in Table 6.2. The cycle time for a measured flow between $1500 * \text{number of lanes}$ and $2000 * \text{number of lanes}$ is equal to the minimum of the calculated cycle flow and the maximum red time. When the measured flow is above the maximum cycle flow, the cycle time is equal to the maximum red time.

Table 6.2: Rijkswaterstaat algorithm settings

Variable	Value
Main road detector location	$200m$
Activation flow	$1500\frac{veh*lanes}{h}$
Maximum cycle flow	$2000\frac{veh*lanes}{h}$
Calculated cycle time	$\frac{3600}{2000*\text{lanes}-\text{flow}}sec$
Maximum red time	$15sec$
Minimum speed to be inactive	$70\frac{km}{h}$
Aggregation level	$60sec$

Regarding the variables for the Microscopic RM approach, some values are varied for the first simulations regarding the relative performance of various microscopic RM control parameter settings. Nevertheless, the variables that have a similar counterpart in the Rijkswaterstaat algorithm, are chosen to be the same as the current approach. An overview is shown in Table 6.3.

Table 6.3: Overview microscopic algorithm settings

Variable	Value
Main road detector location	$200m$
Activation flow	Varies
Maximum cycle flow	not applicable in the microscopic approach
Maximum red time	not applicable in the microscopic approach
Minimum speed to be inactive	$70\frac{km}{h}$
Minimum speed while activated	$0\frac{km}{h}$
Aggregation level	$60sec$
Passenger car gap detector	Varies
Truck gap detector	Varies
Minimum gap time	Varies
Minimum gap passenger car behind truck	Varies

Scenarios

Firstly, various combinations of microscopic RM settings are tested on the base case scenario. Comparing these results in one or two preferred microscopic RM combinations of parameters. The preferred settings will thereafter be tested against the results of the no control alternative and the current macroscopic RM approach. Lastly, several sensitivity analyses will be performed in order to gain insight on the robustness of the different control structures.

As explained in Section 4.5, the location of the gap detectors depends on several variables. These can be varied as well. This applies, for instance, to the maximum acceleration of the vehicle groups. The average can be used as well as a value that corresponds with a larger percentage of drivers. An advantage of this lower maximum acceleration value is that the chance that the merging vehicle has to merge behind the measured gap, is decreased. However, a side effect is that the probability of the merging vehicles merging in front of the gap increases. Nevertheless, merging vehicles that accelerate in front of the gap might be able to fit themselves in the gap more easily by lowering their acceleration than that the vehicles that travel behind the gap will be able to fit in the measured gap by accelerating at an increased rate. Furthermore, the vehicle on the main lane that is the leading vehicle of the gap could theoretically give room to the merging vehicle more easily by filling the gap himself.

All possible combinations between the various microscopic RM settings will be tested in the base case scenario in order to get to the preferred ones. The variables and their values are displayed in Table 6.4.

Table 6.4: Variable microscopic algorithm settings

Variable	Value
Activation flow [vehicles per hour per lane]	1500 ; 1650 ; 1800
Passenger car gap detector location [meters]	to be calculated
Truck gap detector location [meters]	to be calculated
Minimum gap time [seconds]	2.0 ; 1.8 ; 1.6
Minimum gap passenger car behind truck	37.5% car versus 62.5% truck
Acceleration percentage	50 ; 62.5

Regarding Table 6.4, these values are chosen in order to ensure there will be differences between the multiple results. The activation flow starts with $1500 \frac{veh*\text{lanes}}{h}$, since this is the same as the value for the current RM control approach. The minimum gap time of 2.0 seconds is chosen, because this is the time between two vehicles that is recommended by the Dutch authorities to keep to let a vehicle fit in between. Then, a decrease of 10% of this value is taken for every step since actual critical gaps (i.e. the smallest gaps that are accepted to merge into) are smaller (Knoop et al., 2018). A gap smaller than 1.5 seconds is basically always present between two vehicles considering the OTS driver model, so smaller gaps than 1.6 seconds are not considered.

The acceleration percentage of 50% is chosen to fit the merging vehicles as precisely as possible in the measured gaps. Additionally, 62.5% is chosen since this is halfway between the lower maximum acceleration quarter and the average maximum acceleration. This seemed to be a fair trade-off between trying to fit the vehicles in the measured gaps as precisely as possible while giving the somewhat slower accelerating vehicles a bit more time. For the minimum waiting time of a passenger vehicle behind a truck, the same deviation of 12.5% was chosen. In an effort to reduce the probability of a passenger car trying to overtake a truck, a faster than average acceleration for the passenger vehicles was considered and a slower than average acceleration was considered for the trucks.

Besides these microscopic analyses and a base case analysis, sensitivity analyses are performed. The first sensitivity analysis revolves around examining the effects of the alternatives on the current road layout (i.e. without the semi-permeable lane demarcation). Additionally, sensitivity analyses were conducted for various input variables. The simulations are always as much the same as the base case, in order to isolate the checked variable as much as possible. The different scenarios are shows in Table 6.5.

Table 6.5: Overview sensitivity analyses settings

Variable	Value
Speed limit [$\frac{km}{hour}$	80 ; 100 ; 120
Demand main lane	-10% ; 0% ; +10%
Demand on-ramp	-10% ; 0% ; +10%
Demand off-ramp	-10% ; 0% ; +10%
Truck percentage on-ramp	0 ; 5 ; 10

The speed limits apply to all road segments in the simulation and are therefore equal for all road segments. The listed speed limits are chosen, since all roads in the Netherlands have a speed limit of $100 \frac{km}{h}$ or $80 \frac{km}{h}$ during peak hours as of March 2020 (NOS, 2020a). Nevertheless, it is also scientifically useful to gain insight in the robustness when the maximum speed is higher. For the demands, a common sensitivity analysis of -10% and $+10\%$ is used. Finally, it was found that during rush hours, a regular truck percentage is 5% (Dexter, nd). This was chosen as the standard for all routes. The effects on the KPIs of adjusting the truck percentage on the main road route and the route to the off-ramp are not analysed. However, gaining insights in what happens when the truck percentage is actually higher

or lower for the on-ramp vehicles could be very interesting when making a first assessment whether the microscopic RM approach would be beneficial at a site with a different truck percentage for the demand at the on-ramp. In order to ascertain the changes are significant enough to get different outcomes, truck percentages of 0% and of 10% are analysed.

6.2.2 Outputs

As briefly mentioned in Section 3.5.2, the travel time delays of the different control strategies computed by OTS did not give accurate enough results due to the vertical queuing problem. Therefore, the travel time savings computed by means of the fractional cumulative curves were used as the leading outputs. The OTS outputs that are considered, are:

- Number of vehicles originated (and reached their destination) per OD pair [#];
- Number of vehicles that got a green traffic light while the RMI was activated [#];
- Percentage of vehicles that had to wait too long [%];
- Percentage of vehicles that merged in the measured gap [%];
- The simulation time the RMI was activated [seconds];
- The simulation time the RMI was deactivated [seconds].

Additionally, conclusions can be drawn up by considering the computed cumulative curves.

6.3 INPUT

Since differences in the simulation settings are now known, a base case has to be created. To examine the effectiveness of RMIs, it is important that a traffic jam occurs due to merging manoeuvres and not due to other reasons. Furthermore, a traffic jam has to occur at some point in time. Thus, the traffic demands need to be sufficient.

Originally, the demand pattern data and heavy truck percentages for the base case study are acquired by consulting the Dexter database (Dexter, nd). For the considered site, this resulted in an average minimum demand of 4700 vehicles per hour for the main lane in the evening peak, an average minimum demand of 1120 vehicles per hour for the off-ramp in the evening peak and an average minimum demand of 1170 vehicles per hour for the on-ramp in the evening peak. Furthermore, a heavy truck percentage of 5% seems realistic during the evening peak for the main lane. Statistics on truck percentages for the on-ramp and off-ramp are not provided logged in the database. Therefore, this 5% is used for all origin-destination (OD) pairs.

These traffic demand numbers do not provide a distribution. The desired demand pattern however, does consist of a distribution in order to mimic the distribution of real-life demand leading up to the highest demand and dropping back from the highest demand in rush hour. Additionally, the demand for the last 40 minutes of the simulation is kept at 0 to make sure that all vehicles can reach their destination before the simulation ends. After performing some test runs with the highest demand values in OTS, considering a truck percentage of 5% for all OD pairs, a demand pattern was composed that was as close as possible to the found demand statistics by consulting Dexter (nd) database, but that did provide the desired traffic behaviour.

To get the desired traffic behaviour, an off-ramp demand that is lower than the observed demand for the specific off-ramp is used. This had to be done in order to limit the probability of a traffic jam occurring as a result of abrupt lane changing behaviour as a result of getting to the off-ramp. This in turn led to a bit lower on-ramp demand as well, since the flow for the off-ramp greatly determines the number of gaps on the right lane of the main road. Additionally, the flows for the on-ramp are found to be very similar to those of the off-ramp. To ascertain traffic jams to originate in the simulation runs, the main lane demand is increased compared to the investigated main lane demand for the A13 Delft-North statistics. The changes to the found demands should be kept in mind when analysing the results in the next chapter. Graphical representations of the demand patterns are shown in Figure 6.6 and in Figure 6.7. In these figures, a negative demand should be interpreted as a demand of 0 vehicles per hour for that time. It should be noted that in Figure 6.7 at some points the off-ramp demand is higher than the on-ramp demand and 15 minutes later, the reverse is true. This is done in an effort to mitigate the effects of having one of these demand higher for the entire simulation, all the while the demands are not equal for the entire simulation. Having the exact same demand might benefit the microscopic RM alternative too much, since there would on average always be a gap for every merging vehicle. Nonetheless, the off-ramp demand and the on-ramp demand are similar for the considered site (Dexter, nd).

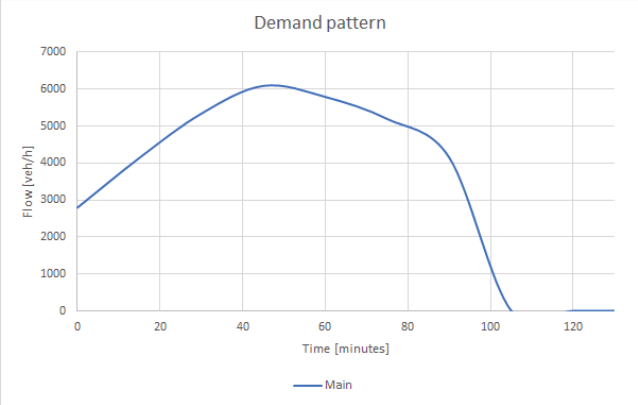

Figure 6.6: Base case demand patterns

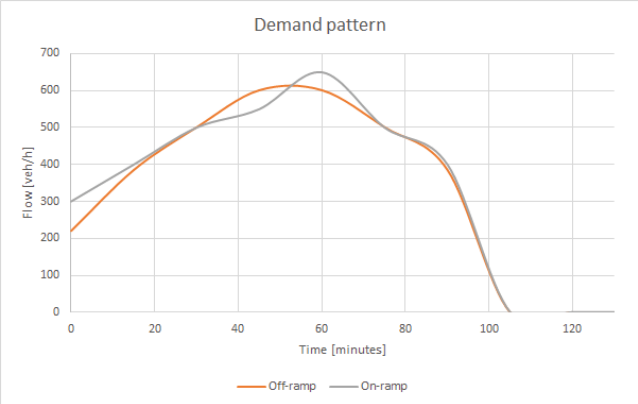

Figure 6.7: Base case ramp demand patterns

Furthermore, it was noticed during the testing phase in OTS that deactivating the RMI, for both the current Rijkswaterstaat control concept as well as for the microscopic control concept, led to traffic jams on the main lane. This is a consequence of all waiting vehicles on the on-ramp being flushed onto the main road when a slightly lower main road flow is measured, even though the flow is

not so much lower that there is enough space to fit all these vehicles in a short time-span. Consequently, it was chosen to only deactivate the RM control structure when the flow on the main road has reduced to below 500 vehicles per lane.

Additionally, the road layout is maintained the same for all RM control approaches. This way, the role a different road layout can play is prevented. However, this means that both the no control and the Rijkswaterstaat alternative make use of a semi-permeable lane demarcation from the end of the off-ramp until the end of the merging area of the considered on-ramp as well (see Figure 6.3). The effect of this semi-permeable lane demarcation is checked for the base case. That analysis is considered as the first sensitivity analysis.

Table 6.6: Overview of base case settings

Variable	Value
Speed limit [$\frac{km}{hour}$]	100
Simulation time [minutes]	130
Acceleration distribution	true
Demand time [minutes]	0; 15; 30; 45; 60; 75; 90; 105; 120
Main demand [vehicles per hour]	2800; 4150; 5350; 6100; 5800; 5200; 4150; 0; 0
Off-ramp demand [vehicles per hour]	220; 385; 500; 600; 600; 500; 385; 0; 0
On-ramp demand [vehicles per hour]	300,400,500,550,650,500,400,0,0
All truck percentages	5

In this base case scenario, all time instances are stated in minutes and the demands are in total $\frac{\text{vehicles}}{\text{hour}}$. The acceleration distribution is computed as a result of the experiment described in Chapter 5. Only the maximum acceleration is considered and used as input in OTS to keep the driver model in OTS intact. In order to make sure the vehicles do not get a negative maximum acceleration or a very unlikely high maximum acceleration, a maximum and a minimum is used for the maximum acceleration. This is done for the extreme 2.5% surface under the graph for both sides of the distribution, resulting in a total of 5.0% being adjusted. In order to prevent a random drawn value which is outside of the minimum and maximum boundaries, the normal distribution is factored and scaled in such a way that a normal distribution remains that meets the requirements. The values for this so called truncated normal distribution used as input OTS are shown in Table 6.7.

Table 6.7: Acceleration distribution settings

	Passenger car	Truck
Mean	2.02	1.64
Standard deviation	0.60	0.60
Maximum	3.20	2.80
Minimum	0.85	0.45

The last few variables that have to be known in order to calculate all variables for all simulation scenarios are some values for determining the gap detector loop locations. These are shown in Table 6.8. The average speed on the main lane corresponds with the speed limit. These values are obtained by analysing the simulation runs in OTS and checking the approximate average speed on the right lane in the first 10 minutes the RMI is activated. A similar method is used for determining the average acceleration of the merging vehicles. This came down to approximately 0.9 times the maximum acceleration speed. It has to be noted that this is too high in comparison with the results in Chapter 5. However, this is let intact to prevent fondling with the driver behaviour script in OTS. The minimum acceleration length is obtained by measuring the distance between the RMI and the beginning of the merging area by means of Google Maps. The same goes for the maximum accelerating distance, where the distance to the end of the merging area

from the RMI is measured. However, 30 meters is subtracted from this distance, since both OTS and the video-footage of the acceleration experiment showed that vehicles prefer to not use this last 30 meters. Lastly, the merging vehicles are fitted more closely to the leading vehicle than to the trailing vehicle of the gap in an effort to try to smoothen the merging manoeuvre. Drivers tend to find it easier to merge in a gap when they are a bit ahead of the middle of the gap and then slowly decelerate into the gap than having to aggressively accelerate at the end to fit into the gap.

Table 6.8: Remaining variables values

Variable	Value
Average speed main lane [$\frac{km}{hour}$]	80 ; 90 ; 100
Average acceleration [%]	0.9
Maximum acceleration length [meters]	300
Minimum acceleration length [meters]	140
Distance (in seconds) to leading gap vehicle	$\frac{\text{gap time}}{3}$

Considering all this information, all variables can be determined. The mentioned detector locations are distances upstream of the beginning of the merging area. An example of simulation settings regarding an analysis revolving around the performance of various microscopic RM controls using different combinations of parameter settings for the base case scenario is shown in Table 6.9.

Table 6.9: Microscopic 50% and 1.8sec settings

	Microscopic 1	Microscopic 2	Microscopic 3
Aggregate level [seconds]	60	60	60
Activation flow [vehicles per hour per lane]	1500	1650	1800
Minimum speed to be inactive [$\frac{km}{hour}$]	70	70	70
Minimum speed while activated [$\frac{km}{hour}$]	0	0	0
Acceleration percentage	50	50	50
Passenger car gap detector [meters]	334.46	334.46	334.46
Truck gap detector [meters]	374.19	374.19	374.19
Minimum gap time [seconds]	1.8	1.8	1.8
Minimum gap passenger car behind truck [seconds]	3.39	3.39	3.39

7 RESULTS

Since all prerequisites have now been discussed, the results of the simulations that were performed to answer the research (sub-)questions can be outlined. This will be done in this chapter. Firstly, the various different microscopic settings will be compared to each other. Next, the best microscopic control strategy will be examined against the current Rijkswaterstaat Ramp Metering (RM) control and no control at all in the base case scenario. Thereafter, various sensitivity analyses to the base case will be described. Finally, a summary of the verification and validation will be provided.

7.1 MICROSCOPIC APPROACHES

For the comparison between the numerous possible microscopic RM control settings, the effects of various combinations of settings are simulated for the base case scenario. These outcomes are also used to be able to easily compare all various microscopic combinations for the base case scenario analysis with the no control alternative and with the currently used macroscopic Rijkswaterstaat RM alternative.

7.1.1 Microscopic approaches simulation software outputs

As mentioned in Chapter 6, several simulations regarding various settings for the microscopic RM control approach will be compared to each other. The OTS outputs that are computed on simulation end are displayed in the next three tables. In Table 7.1, the mean OTS outputs values for all tested settings are outlined. In Table 7.2, the standard deviations are displayed and in Table 7.3, the number of successful simulation seeds for the various settings and the average number of vehicles that went through the simulation per OD pair are summarised.

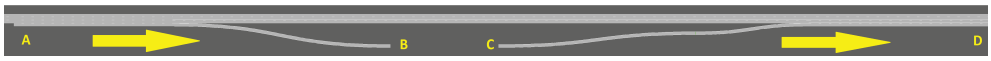

Figure 7.1: The origin-destination (OD) nodes in the simulation

For these three tables, the abbreviation of the outputs represent the following:

- AvDSys: Average computed delay (compared to total free flow conditions, where all vehicles drive the speed limit for the entire route) for the entire system [$\frac{\text{seconds}}{\text{vehicle}}$];
- AvDMain: Average computed delay for the main road flow (A to D) [$\frac{\text{seconds}}{\text{vehicle}}$];
- AvDOn: Average computed delay for the on-ramp flow (C to D) [$\frac{\text{seconds}}{\text{vehicle}}$];
- AvDOff: Average computed delay for the off-ramp flow (A to B) [$\frac{\text{seconds}}{\text{vehicle}}$];
- GotGreen: Number of vehicles at the on-ramp that received a green light at the RMI, while it was activated [#];
- WaitLong: Percentage of vehicles that had to wait longer than 15 seconds, while being first in line, against all vehicles that passed the RMI during its activated period [%];

- Success: Percentage of vehicles that merged in the measured gap divided by the total number of vehicles that passed the RMI during its activated period [%];
- Activation: The time in the simulation when the RMI was activated [seconds];
- Deactivation: The time in the simulation when the RMI was deactivated [seconds];
- 50% ; 1.6s ; 1500f: A microscopic RM control approach with an assumed acceleration that is chosen is such a way that 50% of all drivers have an acceleration that is equal or higher than that, with a minimum required gap time of 1.6 seconds and with an activation flow of 1500 vehicles per lane per hour.

Table 7.1: Mean OTS output values of all simulated microscopic settings

Microscopic comparison Mean Settings	AvDSys	AvDMain	AvDOn	AvDOff	GotGreen	WaitLong	Success	Activation	Deactivation
50% ; 1.6s ; 1500f	71	59	216	48	673	8	30	658	6166
50% ; 1.6s ; 1650f	64	52	209	42	659	8	32	794	6162
50% ; 1.6s ; 1800f	61	49	208	40	636	7	31	722	6102
50% ; 1.8s ; 1500f	51	39	194	32	545	12	41	397	6054
50% ; 1.8s ; 1650f	47	35	186	30	537	12	42	536	6070
50% ; 1.8s ; 1800f	48	36	189	31	523	12	40	722	6072
50% ; 2.0s ; 1500f	51	38	201	33	459	18	46	658	6070
50% ; 2.0s ; 1650f	49	36	197	30	448	19	47	526	6094
50% ; 2.0s ; 1800f	48	35	195	30	435	18	46	722	6094
62% ; 1.6s ; 1500f	63	50	214	40	674	7	25	712	6096
62% ; 1.6s ; 1650f	61	48	217	37	655	7	25	830	6118
62% ; 1.6s ; 1800f	57	45	203	35	635	7	27	1026	6114
62% ; 1.8s ; 1500f	50	38	194	31	556	11	34	540	6088
62% ; 1.8s ; 1650f	50	38	194	31	545	11	33	676	6074
62% ; 1.8s ; 1800f	48	36	189	29	526	12	33	722	6070
62% ; 2.0s ; 1500f	49	36	199	31	465	18	38	392	6072
62% ; 2.0s ; 1650f	46	33	195	28	451	18	39	526	6078
62% ; 2.0s ; 1800f	47	34	194	29	434	18	38	722	6072
Total	53	41	200	34	548	12	36	661	6093

Following Table 7.1, it is observed that the higher the activation flow, the later the RMI is activated most of the time. There are some exceptions however, which is strange, but could be due to the sharp increase in demand the beginning of the simulation, leading to effectively having a similar activation time. Moreover, fluctuations between the different random seeds could be a reason for the exceptions. Additionally, the larger the required gap time for vehicles waiting at the on-ramp in order to receive a green light, the lower the delay for the vehicles on the main lane. This can be expected, since the flow from the on-ramp is delayed in favor of the flow of the main road. Furthermore, the successful merger percentage is also dependent on the assumed acceleration of the vehicles on the on-ramp. When the assumed acceleration is equal to the mean of the distribution, the successful merger percentage is higher than when the assumed acceleration is chosen in such a way that 62.5% of the drivers will accelerate at that rate or faster.

Besides the aforementioned outcomes that are in line with what logically is to be expected, the following was observed as well. When considering the average delay for the vehicles that enter the system from the on-ramp, it should decrease with the decrease in the required gap time. This is in line with the number of vehicles

that have received a green traffic light, as stated above. However, when looking at the results in Table 7.1, this is not necessarily the case. For example, considering the average delay from the on-ramp when a gap time of 1.8 seconds is required, the average delay, regardless of the activation flow, is less than with a required gap time of 1.6 seconds. This is counter-intuitive and not in line with the other outcomes. Furthermore, as shown later in this analysis, it is not in line with the computed slanted cumulative curves (see Figure 7.5 and Figure 7.6).

This resulted in the conclusion that something goes wrong regarding the in OTS computed delays. Looking at the OTS code in more detail, this is probably due to the fact that when the on-ramp is full of vehicles and new vehicles have to arrive at the beginning of the on-ramp, they wait in a vertical queue. Waiting in this vertical queue is apparently not considered as waiting time in OTS, since it is outside of the drawn network layout. However, these vehicles are in fact actually already waiting, which shows up in the cumulative curve, but not in these OTS delay outputs. The reason why these vehicles do encounter less delay on average, is because the final number of vehicles do not suffer delay at all, since they come onto the on-ramp from the vertical queue when the RMI has been deactivated, due to the main road flow being lose to zero. Thus, these 'delay-free' vehicles decreases the average delay drastically computed by OTS, but in practice they actually suffered delay as well.

As referred to already in Section 3.5.2, this led to another way of comparing the delays between the different control strategies, namely by calculating difference in the area underneath the cumulative line between two cumulative curves.

Table 7.2: Standard deviation of OTS output variables for all simulated microscopic settings

Microscopic comparison Standard Deviation									
Settings	AvDSys	AvDMain	AvDOn	AvDOff	GotGreen	WaitLong	Success	Activation	Deactivation
50% ; 1.6s ; 1500f	33	32	56	27	43	4	10	989	202
50% ; 1.6s ; 1650f	32	31	52	27	32	4	9	960	177
50% ; 1.6s ; 1800f	21	20	43	18	47	3	9	236	116
50% ; 1.8s ; 1500f	14	14	20	12	33	2	6	174	71
50% ; 1.8s ; 1650f	9	10	6	11	32	2	2	176	68
50% ; 1.8s ; 1800f	10	11	19	11	36	2	7	236	78
50% ; 2.0s ; 1500f	12	13	9	12	25	2	5	994	65
50% ; 2.0s ; 1650f	12	13	9	12	23	1	4	182	73
50% ; 2.0s ; 1800f	8	9	8	9	22	2	4	236	70
62% ; 1.6s ; 1500f	25	24	52	19	35	3	8	1238	102
62% ; 1.6s ; 1650f	26	25	60	20	39	3	9	1191	118
62% ; 1.6s ; 1800f	23	22	51	18	36	2	8	1148	78
62% ; 1.8s ; 1500f	16	16	24	14	27	1	5	800	72
62% ; 1.8s ; 1650f	15	15	23	12	22	1	5	787	60
62% ; 1.8s ; 1800f	11	11	18	10	26	1	5	236	61
62% ; 2.0s ; 1500f	9	9	11	9	25	2	3	174	55
62% ; 2.0s ; 1650f	8	9	9	9	23	1	2	182	57
62% ; 2.0s ; 1800f	9	10	10	10	24	1	2	236	51
Total	19	19	34	16	91	5	9	708	100

When looking at the standard deviations of the OTS outputs in Table 7.2, some additional conclusions are found. The first conclusion regarding the standard deviations of the statistics is that the standard error for the delay on the main lane is higher for a 1.6 seconds gap time than for a 1.8 seconds gap time and for a 2.0 seconds gap time. This means that there is more fluctuation in the travel time delay for the vehicles on the main lane when using this smaller required gap time. This makes sense, because the probability of a merging vehicle not having a large enough gap when merging is desired increases, which leads to a traffic jam on the main lane. This same phenomenon also applies to the average delay the merging vehicles

and the system as a whole. Additionally, this is the case for the average delay for the off-ramp vehicles, when the traffic jam reaches all the way back, delaying the vehicles with a destination at the off-ramp.

However, there is a notable difference, namely that the standard deviation for the average delay for the vehicles originating at the on-ramp does increase substantially for the two larger activation flows, but not for the main lane, off-ramp and the entire system. When using a gap time of just 1.6 seconds, the standard deviations regarding the delays of all OD pairs increases substantially. This leads to the belief that even though using a gap time of 1.8 seconds might not be large enough for more merging vehicles than using a gap time of 2.0 seconds, thus resulting in an increase of their travel time, this usually does not lead to a congestion on the main road. In contrary to using a 1.6 seconds gap time, where the standard deviations for the delays for all OD pairs are substantial. Resulting in the conclusion that using a 1.6 seconds gap time does increase the chance of a congestion emerging at the main lane, consequently delaying the off-ramp vehicles and all vehicles in the system. The differences in the standard deviation for the other OTS outputs dare not large enough or consistent enough for such concluding remarks.

Table 7.3: Number of simulation runs and passed vehicles with different seeds of all simulated microscopic settings

Microscopic comparison					
Number of cases and vehicle numbers					
Settings	Number of cases	VehSys	VehMain	VehOn	VehOff
50% ; 1.6s ; 1500f	30	9596	8043	784	768
50% ; 1.6s ; 1650f	30	9617	8059	786	772
50% ; 1.6s ; 1800f	30	9611	8058	785	767
50% ; 1.8s ; 1500f	29	9597	8046	777	774
50% ; 1.8s ; 1650f	29	9572	8018	781	773
50% ; 1.8s ; 1800f	30	9595	8038	782	774
50% ; 2.0s ; 1500f	30	9584	8031	787	766
50% ; 2.0s ; 1650f	30	9581	8025	788	768
50% ; 2.0s ; 1800f	30	9580	8024	786	770
62% ; 1.6s ; 1500f	30	9592	8040	785	767
62% ; 1.6s ; 1650f	30	9595	8042	787	766
62% ; 1.6s ; 1800f	30	9598	8056	783	760
62% ; 1.8s ; 1500f	30	9587	8037	783	767
62% ; 1.8s ; 1650f	30	9584	8034	785	765
62% ; 1.8s ; 1800f	30	9615	8057	790	768
62% ; 2.0s ; 1500f	30	9600	8040	784	776
62% ; 2.0s ; 1650f	30	9579	8015	790	773
62% ; 2.0s ; 1800f	30	9597	8031	789	777

First and foremost, Table 7.3 shows that the average number of the total passed vehicles in the system with a certain OD combination is not equal for all alternatives. Due to the nature of the simulation setup, all vehicles that originate during the simulation have reached their destination at the end of the simulation. This is ascertained by letting the simulation run for an additional 40 minutes without having a demand. So, not having the same average number of vehicles reaching their destination means that not alternatives had the same number of vehicles originating during the simulation time. Not having the same number of vehicles originating for the various alternatives is not desirable and complicates the performance comparisons a bit. To limit the negative consequence of not having the exact same number of vehicles that originating for the various alternatives, the average delay per vehicle is compared instead of the total system travel time delay. Fortunately, the variations in the number of vehicles per OD pair that have reached their destination are relatively small. Combining this fact with the use of the average

delay per vehicle statistics, the differences in the number of vehicles originating for the various alternatives are neglected while interpreting the results as much as possible.

Moreover, Table 7.3 shows that not all simulation settings have successfully executed the desired number of cases, which is 30. Mostly, this is due to a vehicle that has to take the off-ramp not being able to actually take it, resulting in a simulation crash. Fortunately, this did not happen too often, resulting in the exclusion of the cases where it did.

Furthermore, it has to be noted that some of the successfully executed simulation runs posed unexpected results regarding the activation time of the settings. Sometimes (for approximately between 0% and 5% of all cases per setting) the activation time was far beyond an hour in the simulation. This indicates that the traffic on the main road did not reach the activation flow for the first hour, which should not be the case considering the demand patterns. Looking into the simulation runs in more detail, it was concluded that in those cases a traffic jam near the off-ramp upstream of the on-ramp originated due to drivers having to switch multiple lanes in order to take the off-ramp in a short distance. Forcefully doing so leads to wide-moving jams, since all drivers have to abruptly brake harshly, which is undesirable. This forcefully switching of multiple lanes in a short distance does not happen as often in reality as in the used simulation setup in OTS.

Additionally, it was observed that these high activation times were not necessarily found for all alternatives for the same random seeds with the same demand patterns. Hence, tracing back which random seeds should be removed is impossible. This is especially true for the no control alternative, which does not even compute the activation time of the RMI, since it does not consist of an RMI. Luckily, the late activation times did occur at most twice per 30 random seeds for all simulation runs in all analyses. Mostly, such an activation time was reported only once or even not at all for 30 simulation runs of a single alternative. Therefore, these results are just kept in the averages. This includes the cumulative curves and the calculated delays, since these are computed on the averages over the 30 simulation runs. Another argument for not removing the individual simulation runs with reported late activation times is that they will average out (which in the bigger picture at least they do, as can be concluded from the remarks to follow). The observation that traffic jams can occur at the off-ramp and the fact that the simulation will crash if vehicles are unable to reach their destination however, led to reducing the demand for the outflow in the simulations, as previously mentioned in Chapter 6.

Despite these unfavorable factors, a few conclusions can be summarised considering the results shown in these first three tables. Firstly, lowering the necessary gap time results in more vehicles getting a green traffic light while the RMI is activated. Secondly, the percentage of vehicles that had to wait for too long, decreases if a smaller gap is accepted. However, the percentage of vehicles that successfully merge in the measured gap decreases with the minimum accepted gap time as well. These conclusions are all in line with what can logically be expected.

7.1.2 Cumulative curves

An example of a set of cumulative curves is shown in Figure 7.2. Herein, the cumulative curves for the different origin-destination (OD) pairs are shown for the microscopic settings with an activation flow of 1650 vehicles per lane, a required gap time of 1.6 seconds and an assumed acceleration of the mean of the distribution. The cumulative curve describing the on-ramp can be used to determine the average flow from the on-ramp vehicles onto the main road while the RMI is activated. This can be done by taking two points on the curve that lie between the activation time and deactivation time, keeping in mind the travel time from the RMI to the destination node. Then, the difference in time in seconds divided by the difference in the number of cumulative vehicles that have passed between these two points results

in the average time between two vehicles reaching their destination. This time consists of the average red time between two green phases and the delay that can be encountered between the RMI and the destination. The delays suffered by the on-ramp vehicles are minimal, since they mostly merge downstream of the possible congestion location. Therefore, the average red time is equal to almost 11 seconds when a minimum required gap time of 1.8 seconds is used for the base case scenario. For a minimum gap time of 1.6 seconds this is even just 9 seconds. For a minimum gap time of 2.0 seconds, the average red time between two green phases is almost 14 seconds.

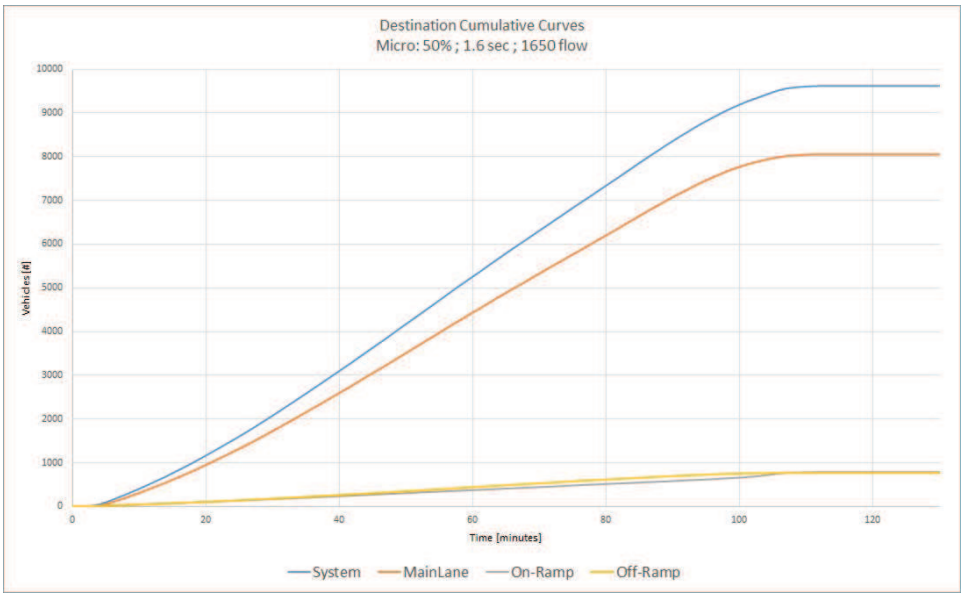

Figure 7.2: Cumulative Curves Microscopic: 50% ; 1.6s ; 1650f

The comparison of the cumulative curves for the entire system between the various activation flows for the microscopic RM control structure, with a minimum required gap of 1.6 seconds and an assumed acceleration which is equal to the provided mean acceleration, is displayed in Figure 7.3. In this graph, the blue line is the illustration of the settings with an activation flow of 1500 vehicles per lane per hour. The orange line represents an activation flow of 1650 vehicles per lane per hour and the grey line illustrates the results with an activation of 1800 vehicles per lane per hour.

Inconveniently enough, no real differences can be distinguished when considering Figure 7.3. Therefore, a slanted cumulative curve will be constructed, as stated in Section 3.5.2. The slanting is chosen in such a way that there are minimal differences between the various control strategies under the horizontal axis, but the maximum value is significantly lower than the approximately 10000 vehicles as is the case for Figure 7.3. The chosen offsets were already listed in Section 3.5.2, Table 3.1. The formula for computing the slanted cumulative curves is also shown in Section 3.5.2 by Equation 3.15. The offset for the normal cumulative curve is always 0 vehicles per hour.

Considering the slanted cumulative curves presented in Figure 7.4, the differences are much better visible. When an activation flow of 1800 vehicles per lane per hour is used, the microscopic RM approach performs better (i.e. the overall travel time savings are larger) than when an activation flow of 1500 vehicles per lane per hour is chosen. The differences between an activation flow of 1800 vehicles per lane per hour and 1650 vehicles per lane per hour are much less. However, this means that a

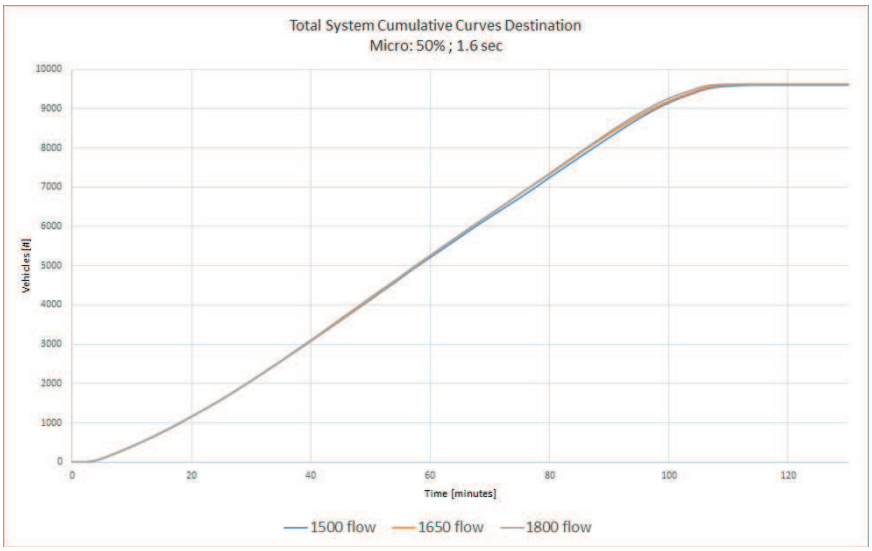

Figure 7.3: Total System Cumulative Curves Microscopic: 50% ; 1.6s

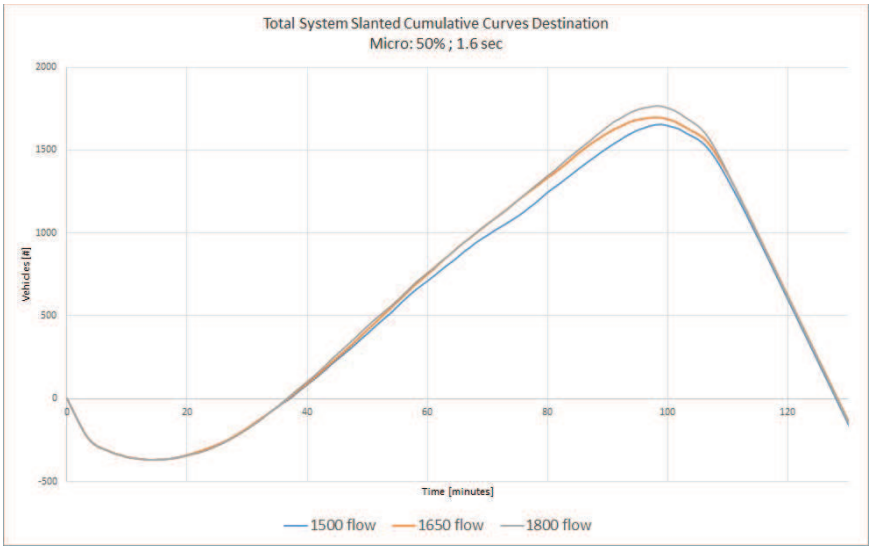

Figure 7.4: Slanted Total System Cumulative Curves Microscopic: 50% ; 1.6s

chosen activation flow of 1650 vehicles per lane per hour also outperforms the same settings with an activation flow of 1500 vehicles per lane per hour. Additionally, just as reported in Table 7.3, small differences at the end of the simulation in the total number of vehicles that have passed the system can be more easily found by examining the final 15 minutes in Figure 7.3.

Returning to the statement made in the previous sub-section about the incorrect information regarding the average delay for the on-ramp vehicles for a required gap time of 1.6 seconds versus one of 1.8 seconds, the considered slanted cumulative

curves are illustrated in Figure 7.5 and Figure 7.6. Following these figures, it is evident that the average delay for the vehicles originating at the on-ramp is less when using a gap time of 1.6 instead of a gap time of 1.8 seconds, since for most time steps, the slanted curves when using 1.6 seconds lays above the curve when using 1.8 seconds, regardless of the considered activation flow. This can easily be verified by the shorter steep increase at the end of the simulation as well.

However, this contradicts the results of Table 7.1. The average flow from vehicles on the on-ramp should be larger for a smaller required gap time, since the probability of measuring a valid gap increases when the required gap decreases. This is found in the (slanted) cumulative curves, but not in the delay statistics reported by OTS. Therefore, it is concluded that the (slanted) cumulative curves provide a better picture regarding the actual delay than the statistics computed by OTS.

Moreover, it can seen in both Figure 7.5 and in Figure 7.6 that after approximately 100 minutes, the curve suddenly increases. This is a result of the RMI deactivating a couple minutes before then, 'flushing' the vehicles waiting at the on-ramp. As a consequence, suddenly a lot of vehicles that originated at the on-ramp reach their destination at the end of the simulation, resulting in this sharp increase.

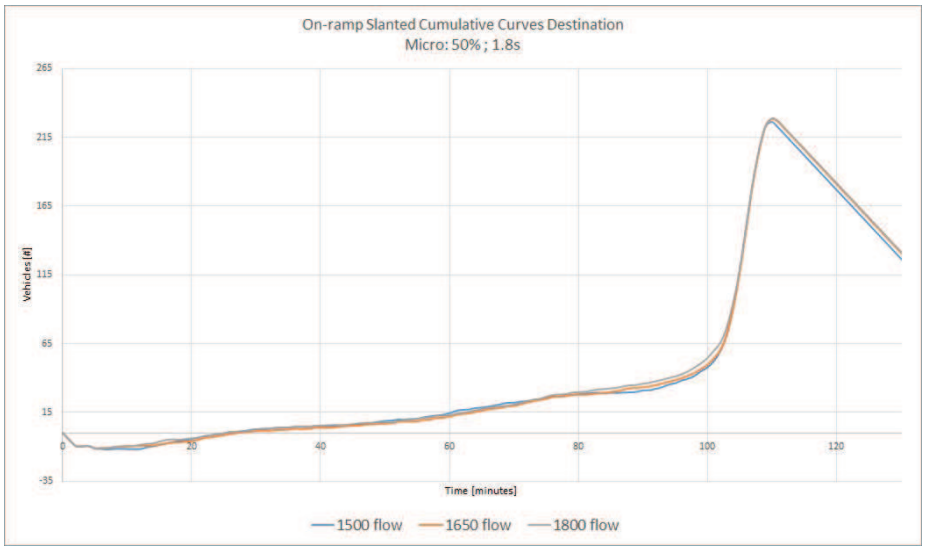

Figure 7.5: On-ramp Slanted Cumulative Curves Microscopic: 50% ; 1.8s

7.1.3 Computed travel time savings

As a result of the conclusion that the average delays outputs by OTS do not provide accurate results, the delays are also computed by means of calculating the area underneath the graphs, as explained in Section 3.5.2. In order to prevent an unfair advantage for a random RM control structure due to having randomly assigned and accommodated slightly more vehicles on simulation end, the cumulative fractions are used. This way, when all vehicles have arrived at their destination, regardless of the total number, the area under the graph is equal to one for adjacent time intervals of one minute. So, the unfair gain for either one of the RM control strategies for the final minutes when the simulation has accommodated all vehicles, is prevented. The fractional cumulative curves for the vehicles that started at the on-ramp for the microscopic RM approach with an assumed acceleration equal to the mean of

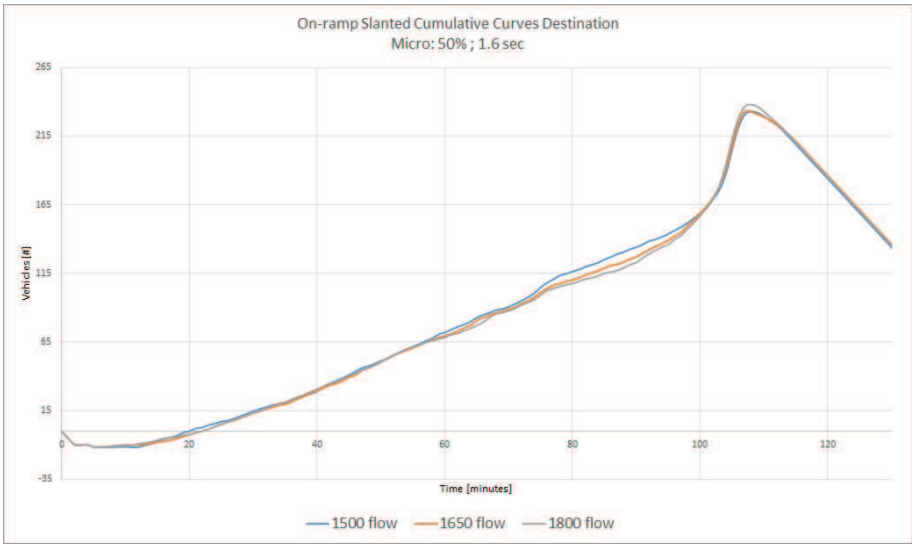

Figure 7.6: On-ramp Slanted Cumulative Curves Microscopic: 50% ; 1.6s

the distribution and a minimum required gap of 1.8 seconds are represented in Figure 7.7. The same fractional cumulative curves for the identical microscopic RM approach settings, but with a minimum required gap of 1.6 seconds, are illustrated in Figure 7.8.

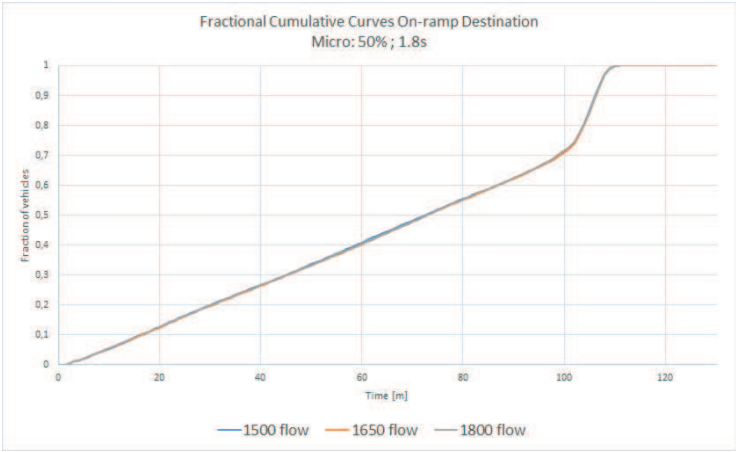

Figure 7.7: On-ramp Fractional Cumulative Curves Microscopic: 50% ; 1.8s

It can be concluded that Figure 7.7 and Figure 7.8 are almost identical to their regular cumulative counterparts, Figure 7.9 and Figure 7.10. Calculating the difference between the area under the different graphs leads to the results as summarised in Table 7.4.

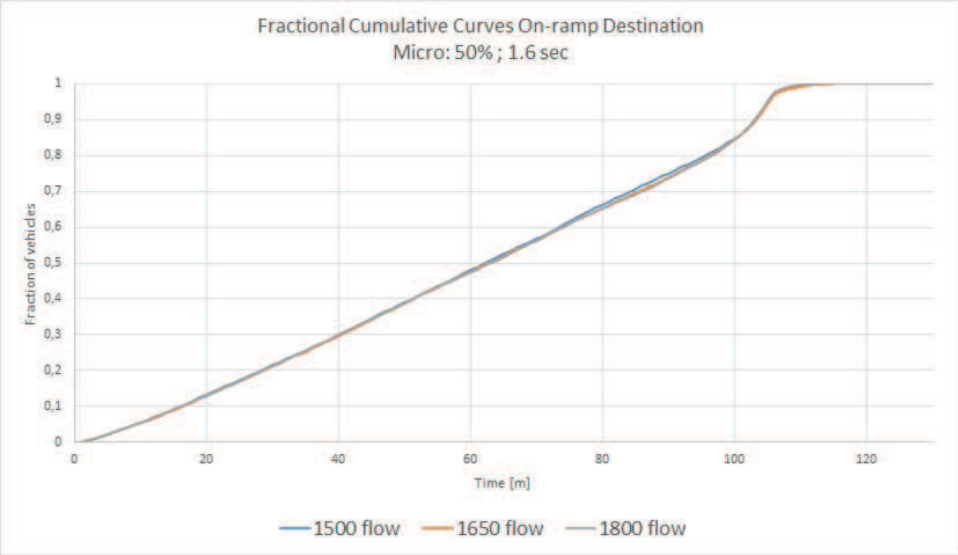

Figure 7.8: On-ramp Fractional Cumulative Curves Microscopic: 50% ; 1.6s

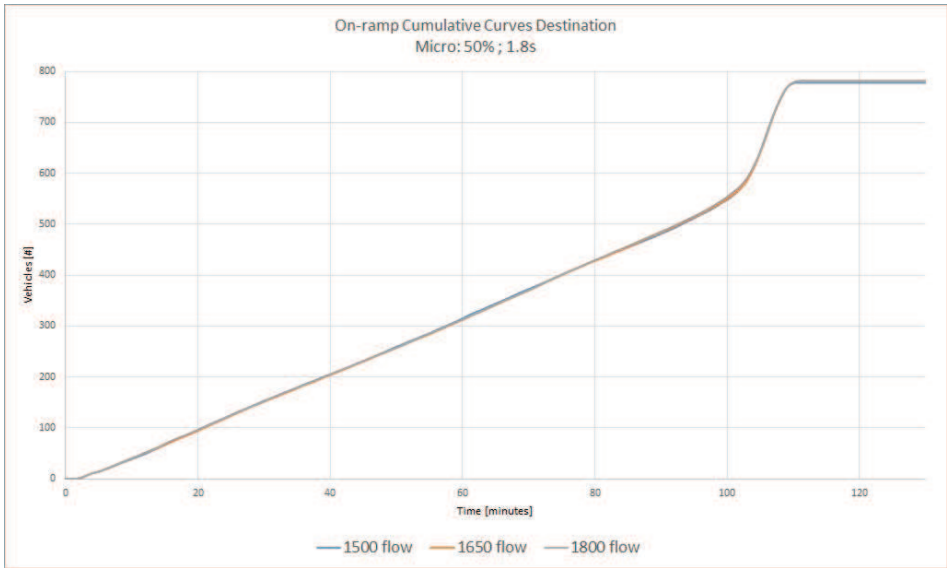

Figure 7.9: On-ramp Cumulative Curves Microscopic: 50% ; 1.8s

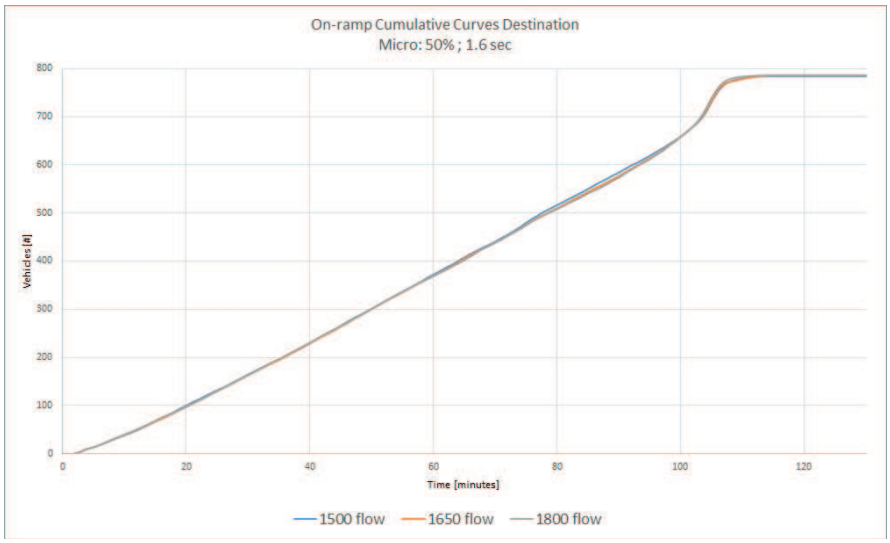

Figure 7.10: On-ramp Cumulative Curves Microscopic: 50% ; 1.6s

Table 7.4: Average on-ramp travel time savings in seconds per vehicle

On-ramp travel time savings			
Comparison activation flow	1650 vs 1500	1800 vs 1500	1800 vs 1650
50% ; 1.6 sec	-25	-23	1
50% ; 1.8 sec	-19	-8	11

Regarding Table 7.4, it is easily verified that the exact differences differ for both settings and the activation flows. For example, the travel time gains when using a minimum required gap time of 1.6 seconds, using an activation flow of 1650 versus using an activation flow of 1500, results in an average travel time gain per vehicle of approximately -25 seconds. In other words, the average travel time delay per vehicle for using an activation flow of 1500 vehicles per lane per hour with the considered settings is 25 seconds less than when using an activation flow of 1650 vehicles per lane per hour. Additionally, it can be easily verified that the difference between the travel time savings when using an activation flow of 1800 and 1650 vehicles per lane per hour can be calculated when the difference of the two with another alternative (1500 vehicles per lane per hour in this case) is known. Then, the difference between 1800 and 1650 is equal to the difference between 1800 and 1500 minus the difference of 1650 and 1500 vehicles per hour per lane (e.g. $-8-11=-19$). A difference of 1 second between the computed difference and the reported difference is due to rounding differences.

Considering the bigger picture of Table 7.4, it can be concluded that for both required gaps (i.e. 1.6 seconds and 1.8 seconds) an activation flow with 1500 leads to the best results. Furthermore, for both required gaps, an activation flow of 1800 performs slightly better than an activation flow of 1650. These conclusions are in line with the computed slanted curves as illustrated in Figure 7.5 and Figure 7.6. Therefore, it is reasoned that at least the sign of the travel time gains is correct.

Nevertheless, Table 7.4 is not a comparison of the differences of the average delays of the vehicles originating at the on-ramp between using a minimum required gap of 1.6 seconds and 1.8 seconds, but merely a comparison of the various activation flows within the considered minimum required gap time. This can be done as well,

but one combination of settings needs to be 'normalised' to no delay. Therefore, all further microscopic analyses will be compared to the microscopic RM that uses an assumed acceleration that is equal to the mean of the distribution, an activation flow of 1500 vehicles per hour per lane and a minimum required gap time of 2.0 seconds. This leads to the results outlined in Table 7.5.

Table 7.5: Average on-ramp travel time savings in seconds per vehicle, compared to 50% ; 2.0 sec ; 1500 activation flow

On-ramp travel time savings			
Assumed acceleration percentage	Minimum required gap	Activation flow	Travel time savings
50	1.6	1500	764
50	1.6	1650	739
50	1.6	1800	741
50	1.8	1500	380
50	1.8	1650	361
50	1.8	1800	372

Concerning the results as displayed in Table 7.5, it is concluded that the average travel time savings per vehicle for the vehicles originating at the on-ramp is greater with a required gap of 1.6 seconds compared to 1.8 seconds, since those savings are larger compared to the base case. This is in line with the computed cumulative curves (see Figure 7.5 and Figure 7.6), thus giving a more accurate result than the delay statistics computed by OTS (see Table 7.1).

Additionally, this can be done for all OD pairs and for all considered microscopic settings. Using the same microscopic RM settings as the norm, this leads to the actual travel time saving results, as outlined in Table 7.6.

Table 7.6: Average travel time savings in seconds per vehicle, compared to 50% ; 2.0 sec ; 1500 activation flow

Travel time savings						
Percentage	Gap time	Flow	System	Main	On-ramp	Off-ramp
50	1.6	1500	10	-60	764	-34
50	1.6	1650	26	-39	739	-18
50	1.6	1800	39	-26	741	-4
50	1.8	1500	27	-7	380	7
50	1.8	1650	35	4	361	16
50	1.8	1800	34	3	372	3
50	2.0	1500	0	0	0	0
50	2.0	1650	-5	-6	-12	10
50	2.0	1800	7	4	25	27
62.5	1.6	1500	49	-19	781	2
62.5	1.6	1650	49	-16	724	26
62.5	1.6	1800	57	-9	755	35
62.5	1.8	1500	27	-6	367	17
62.5	1.8	1650	33	1	363	28
62.5	1.8	1800	31	-1	361	22
62.5	2.0	1500	0	-4	31	3
62.5	2.0	1650	5	4	-2	29
62.5	2.0	1800	2	-2	36	10

In light of the results shown in Table 7.6, the computed main travel time savings can be compared with the differences in the delays calculated by OTS. Mostly the order is the same, but the actual travel time savings differ quite a bit for several comparisons. Since the computed delays as shown in Table 7.6 are more in line with the computed cumulative curves and the signs of the savings are more logical than the signs of

the delay differences as shown in Table 7.1 (for the average travel time savings for the on-ramp vehicles when using a gap of 1.8 and 1.6 seconds for example), the results of the computed travel time savings by means of the cumulative curves are considered to be more reliable.

From these travel time savings, it is concluded that the travel time savings for vehicles that originate at the on-ramp increase when the required gap decreases. This is in line with logical reasoning. Furthermore, there seems to be a trade-off between travel time savings on the main lane or travel time savings for the on-ramp. When vehicles originating at the on-ramp suffer more delays (i.e. less travel time savings), the vehicles that use the main lane all the way usually enjoy more travel time savings. In other words, the travel time savings for vehicles using the main lane increases with the minimum required gap time for the on-ramp vehicles. This makes sense as well.

Additionally, using a minimum required gap time of just 1.6 seconds causes a lot of traffic jams when the assumed acceleration is equal to the mean acceleration of the distribution. However, when the assumed acceleration is lower than that (i.e. is equal to the 37.5% fastest), the encountered delays on the main lane are less. This is probably due one of two reasons. The first explanation is the merging vehicles just barely fit in the measured gap with the lower assumed acceleration as opposed to the merging vehicles not being able accelerate fast enough to fit in the measured gap when using the standard assumed average acceleration which causes a new traffic jam. The other explanation is that the vehicles that barely fit in the measured gap when using the 50% acceleration, now merge just in front of the gap when using the lower assumed average acceleration, but the leader of the measured gap could decelerate into the measured gap, which prevents a congestion more often than merging behind the measured gap.

Lastly, the travel time savings for the entire system are at an optimum when the vehicles on the main road do not encounter too much delay (compared to the base case settings), but the on-ramp vehicles do save a lot of traffic time. Depending on the proportion of on-ramp vehicles versus main lane vehicles, the best performing combination of settings might differ.

7.1.4 Conclusion on the various microscopic settings

Considering all tables and cumulative curves, it is concluded that the microscopic settings where 62.5% of the vehicles accelerate at that rate or faster, with a required gap of 1.6 seconds and an activation flow of 1800 vehicles per lane per hour, performs the best in the base case scenario when the whole system is taken into account. However, this combination of settings has a relatively high standard deviation for the delays, meaning that there is quite some fluctuation between the performance for different seeds.

When disregarding the microscopic approaches that use a 1.6 seconds gap as the required minimum for that sole reason, three different combination of settings perform very similar for the spot of 'second best'. Of these three, all use a required minimum gap time of 1.8 seconds and two have an activation flow of 1650 vehicles per lane per hour. Furthermore, the successful merger percentage is higher for this combination of settings and the standard deviation for the travel time delays is lower (which is the case for most 50% settings when compared to their 62.5% counterpart). Therefore, this combination of settings is rules to be preferable over the other one when conducting the sensitivity analyses.

However, in order to prevent the possibility of disregarding the most beneficial microscopic settings combination, both are taken into consideration in the following analyses. This means that two microscopic RM approaches will be tested against no RM control at all and against the current Rijkswaterstaat RM control. Summarising, the following four RM control structures are considered in the base case scenario and the sensitivity analyses:

- No Ramp Metering (RM) control;
- Current Rijkswaterstaat Ramp Metering (RM) control;
- Microscopic Ramp Metering (RM) control 1: with an assumed acceleration of 50%, a required minimum gap time of 1.8 seconds and an activation flow of 1650 vehicles per lane per hour;
- Microscopic Ramp Metering (RM) control 2: with an assumed acceleration of 62.5%, a required minimum gap time of 1.6 seconds and an activation flow of 1800 vehicles per lane per hour.

Moreover, regarding the microscopic settings, the simulation seems to do what it is supposed to do. Namely, the activation time of the RMI increases with the activation flow. The number of vehicles that got a green traffic light decreases when the activation flow increases. Moreover, the successful merger percentage when using an assumed acceleration of 50% is higher than when an assumed acceleration of 62.5% is used. Additionally, when looking at the computed travel time savings by means of the cumulative curves, the delay for the on-ramp vehicles decreases when a smaller required gap time is being used. Also, the successful merger percentage drops with the required minimum gap time.

These are all logical consequences of the various settings. Thus, it is concluded that the simulation does what it is supposed to, at least in regards to the various microscopic RM settings. So, for this part at least, the simulation is verified.

7.2 BASE CASE RESULTS

This section will describe the comparison between the two chosen microscopic RM control approaches, no control and the current Rijkswaterstaat RM algorithm. This will be done by means of the same outputs as used in the previous section.

7.2.1 Base case simulation software outputs

Firstly, the mean and standard deviation of the OTS outputs are displayed. The mean can be found in Table 7.8 and the standard deviation table can be found in Table 7.9. The number of successful simulation runs per alternative and the average number of vehicles that originated per OD pair, which is equal to the number of vehicles that have reached their destination for these OD pairs, are displayed in Table 7.7.

Table 7.7: Number of simulation runs and passed vehicles with different seeds for the base case scenario

Base case scenario					
Number of cases and vehicle numbers					
Control settings	Nobs	VehSys	VehMain	VehOn	VehOff
No control	29	9599	8041	788	770
Rijkswaterstaat control	30	9623	8060	792	772
Microscopic 1	29	9572	8018	781	773
Microscopic 2	30	9598	8056	783	760

As can be seen in Table 7.7, the number of successfully executed simulation runs for the different RM control settings is either 29 or 30. Furthermore, just as in the microscopic RM settings comparison, not all OD pairs yield the same average number of passed vehicles over the 30 simulation runs. Again, the largest differences are in the range of just over one percent, which is not large. Therefore, these differences are neglected as much as possible.

Table 7.8: Mean OTS output values of the base case scenario

Base case scenario									
Mean									
Control settings	AvDSys	AvDMain	AvDOn	AvDOff	GotGreen	WaitLong	success	Activation	Deactivation
No control	88	75	254	58					
Rijkswaterstaat	48	37	176	31	558			650	6054
Microscopic 1	47	35	186	30	537	12	42	536	6070
Microscopic 2	57	45	203	35	635	7	27	1026	6114
Total	60	48	205	38	577	9	34	740	6080

Following the results shown in Table 7.8, it can be seen that the first indication is that the overall system average delays is less for all active RM control approaches compared to no control at all. Furthermore, the statistics for the two microscopic settings are equal to the outcomes shown in the previous section. This is due to the exact same settings and random seeds. However, as concluded in the previous section, these delays do not always tell the whole story. Additionally, the average activation time of the Rijkswaterstaat algorithm is later than for the chosen first microscopic RM control. This despite the fact that the activation flow of the Rijkswaterstaat control structure is 1500 vehicles per lane per hour in contrast to the 1650 vehicles per lane per hour activation flow for the chosen first microscopic RM control. This is unexpected, but could be due to the randomness factor due to the random seeds and the steep increase in the demand in the beginning of the simulation, leading to effectively having a similar activation time.

Moreover, it can be seen that the current Rijkswaterstaat RM control structure shows a green traffic light more frequently than the first microscopic RM approach. This seems counter-intuitive when keeping in mind the RMI is activated later in the simulation than this microscopic approach. Nevertheless it seems to be accurate, as can be seen in the slanted cumulative curve. This result is due to the use of varying brief fixed cycle times in the Rijkswaterstaat RM control structure. In the beginning and near the end of the activation period, the current Rijkswaterstaat control structure lets so many more vehicles pass that during the entire activation period the number of passed vehicles is just higher than with the first microscopic alternative. The second microscopic RM control structure, which uses a minimum required gap time of 1.6 seconds opposed to 1.8 seconds, does let more vehicles pass than the Rijkswaterstaat algorithm. This is due to this gap time resulting in lower average cycle times compared with the Rijkswaterstaat algorithm.

Lastly, the current Rijkswaterstaat RM control does neither report a percentage of vehicles that had to wait too long nor a successful merger percentage. A percentage of vehicles that had to wait for too long is absent, because the maximum red time in the current Rijkswaterstaat RM control structure is equal to 15 seconds. Since vehicles are only deemed to have waited for too long when their waiting time while being in front of the queue exceeds this 15 seconds waiting period, there are no vehicles that have to wait too long. There is no percentage of vehicles that merges successfully, since there is no measured gap in which the vehicles ought to merge. So, no successful or unsuccessful mergers are recorded.

Regarding the standard deviation of the outputs, it is observed that no control and the second microscopic RM control have the largest standard deviation for most all OD pair delays. The current Rijkswaterstaat RM control structure and the first microscopic RM approach follow at quite a large distance. Nonetheless, the first microscopic RM encounters a little lower standard deviation, meaning that there is less fluctuation in the calculated delays. However, it should be kept in mind that the calculated delays by OTS do not provide the real outcomes on which control structure performs best.

Table 7.9: Standard deviation of the OTS output variables for the base case scenario

Base case scenario Std. Deviation ControlSetting	AvDSys	AvDMain	AvDOn	AvDOff	GotGreen	WaitLong	success	Activation	Deactivation
No control	21	23	50	22					
Rijkswaterstaat	11	12	10	12	47			985	71
Microscopic 1	9	10	6	11	32	2	2	176	68
Microscopic 2	23	22	51	18	36	2	8	1148	78
Total	24	24	46	20	57	3	10	899	76

7.2.2 Cumulative curves

In order to provide an answer to the question which RM control approach works best, cumulative curves are computed. In order to limit the amount of graphs shown in the text however, only the slanted cumulative curves are illustrated in this sub-section, since they provide the most clear differences between the different RM control strategies. The same offsets as in the previous simulations have been used (see Table 3.1). Furthermore the average travel time savings compared to each other are determined by calculating the differences in the areas under the fractional cumulative curve graphs for the different control structures in the next sub-section.

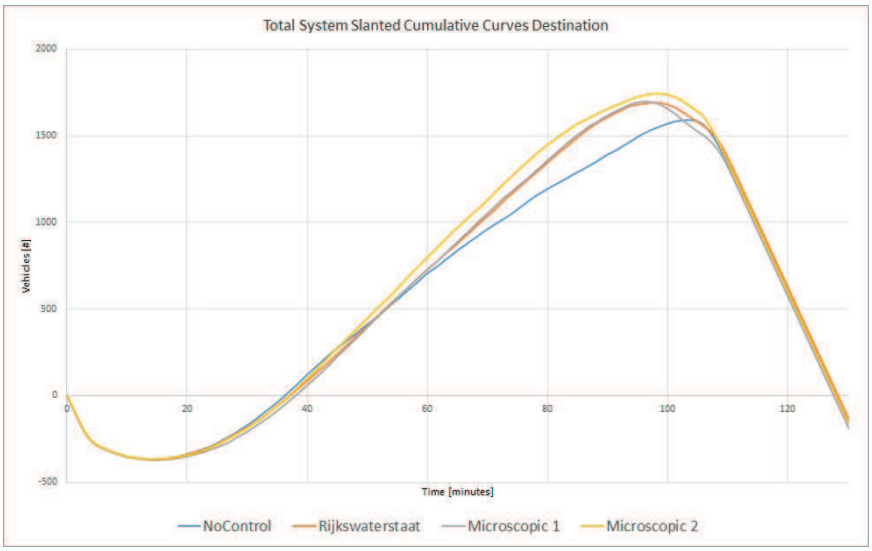

Figure 7.11: Base Case Total System Slanted Cumulative Curves

Considering the slanted cumulative curves for the entire system illustrated in Figure 7.11, several observations can be made. Firstly, it is evident that using no RMI control at all performs by far the worst. Especially, between the 60 and 100 minute mark of the simulation time the no control strategy performs considerably worse than the alternatives with an active RMI control approach. Additionally, it can be observed that the second microscopic RM approach performs the best. Moreover, the current Rijkswaterstaat algorithm seems to perform more or less on par with the first microscopic RM approach. Nevertheless, when looking at it more closely, it seems that the first microscopic control strategy lies just slightly above the current RM control strategy deployed in the Netherlands. Near the end of the simulation

however, the Rijkswaterstaat control lies above the first microscopic line, indicating that during the final stage of the simulation, the current RM control strategies outperforms this combination of settings for the microscopic RM approach. Finally, it is observed that all lines hold more or less the same value for the final 20 minutes of the simulation, meaning that approximately the same amount of vehicles have travelled through the system. Small differences can still be observed.

Furthermore, a closer look at the cumulative curves for the various OD pairs is presented. This will be done in a specific order. Firstly, the main lane vehicles (A to D) will be discussed. Secondly, the vehicles originating at the on-ramp will be regarded (C to D). And lastly, the vehicle taking the off-ramp upstream of the on-ramp will be examined (A to B).

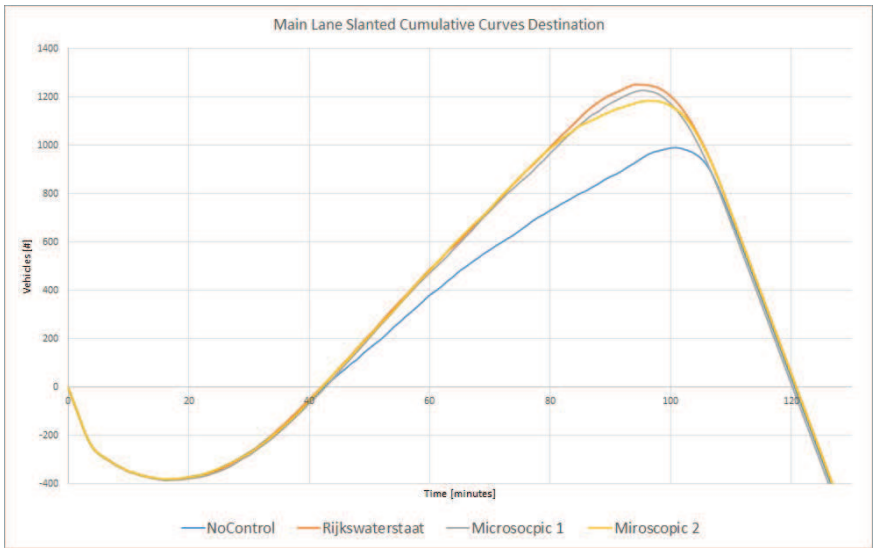

Figure 7.12: Base Case Main Lane Slanted Cumulative Curves

Looking at the vehicles on the main lane (Figure 7.12), slight changes compared to the total system are observed. First off all, the current macroscopic RM control strategy is the most beneficial for the main lane vehicles. Second best for the main lane vehicles is the first microscopic RM control settings and thereafter comes the second microscopic RM control. What has not changed, is that no control at all trails all the actively controlled RM alternatives at quite some distance.

How this change in the raking is possible, can be seen in the slanted cumulative curves for the vehicles originating at the on-ramp (Figure 7.13). Herein, the ranking seems to be the inverse of the main lane slanted cumulative curves. The best performer for the on-ramp vehicles is no RM control. A relatively close second is the second microscopic RM control settings. Slightly further down the standings, the first microscopic RM control is found. The worst performer for the on-ramp vehicles is the current Rijkswaterstaat algorithm. The change in the ranking is caused by the fact that the on-ramp vehicles in the no control alternative only suffer travel time delays when there is a traffic jam. The on-ramp vehicles already encounter additional travel time delays before traffic congestion emerges for the active RMIs alternatives.

However, the precise order of the RMIs in the performance for the on-ramp vehicles is not the same for the entire simulation time (see Figure 7.13. It is observed that at the beginning of the activated RMI, the currently used macroscopic RM control approach outperforms the first microscopic control structure and for a

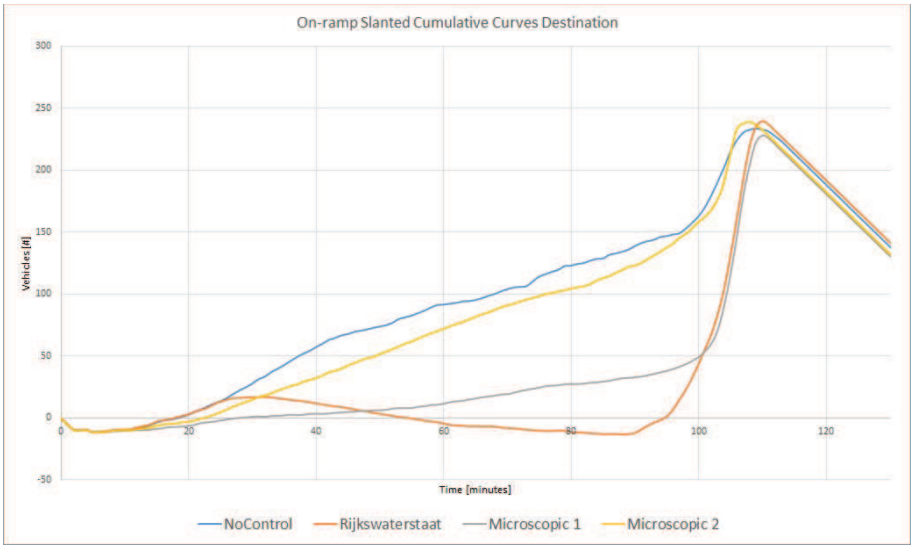

Figure 7.13: Base Case On-ramp Slanted Cumulative Curves

shorter period of time, the same can be said in regards to the considered microscopic RM control structure. Eventually though, both microscopic approaches overtake the Rijkswaterstaat RM control structure when looking at the on-ramp vehicles. This is due to the fact that the currently used algorithm uses varying short fixed red times, which are dependent on the measured main lane flow. In the beginning of the activated RMI, this flow is still relatively low, enabling short red times between two vehicles in the Rijkswaterstaat algorithm. However, when the flow intensifies during the middle section of the simulation, these red times get larger and at a certain point these cycle times are equal to the maximum red time of 15 seconds. The microscopic approaches do not use these temporarily fixed red times between two merging vehicles, but are dependent on measured gaps in the main lane flow. Apparently, the presence of gaps on the right lane of the main road is more or less stable regardless of the actual flow on the main lane when the RMI is activated (which is a flow of at least 1650 vehicles per lane per hour). Furthermore, a sufficient gap time occurs more frequently than every 15 seconds, namely nearly every 9 seconds, almost every 11 seconds and almost every 14 seconds, depending on the used minimum required gap time. Evidently, smaller gaps are measured more often, resulting in the difference between the two microscopic settings.

Regarding the slanted cumulative curves for the off-ramp vehicles (Figure 7.14), the order on which alternative performs the best is equal to the order of the main lane vehicles. This means that the probability of a traffic jam that originated at the on-ramp reaches all the way back to upstream of the off-ramp is more or less equal for all alternatives. The absolute differences between the different control strategies is smaller. This could be due to the fact that not all traffic jams will travel all the way back to upstream of the off-ramp and the demand for vehicles taking the off-ramp is less than for the main lane vehicles.

Considering all slanted cumulative curves (Figure 7.11 through Figure 7.14), it can be concluded that there is a trade-off between the travel time savings for the main lane vehicles and the additional delay for the on-ramp vehicles. The best performer for the entire system is the control strategy that manages to get as much travel time savings for the main lane vehicles, while minimising the incurred delays for these on-ramp vehicles at the same time. For the base case scenario, this seems to

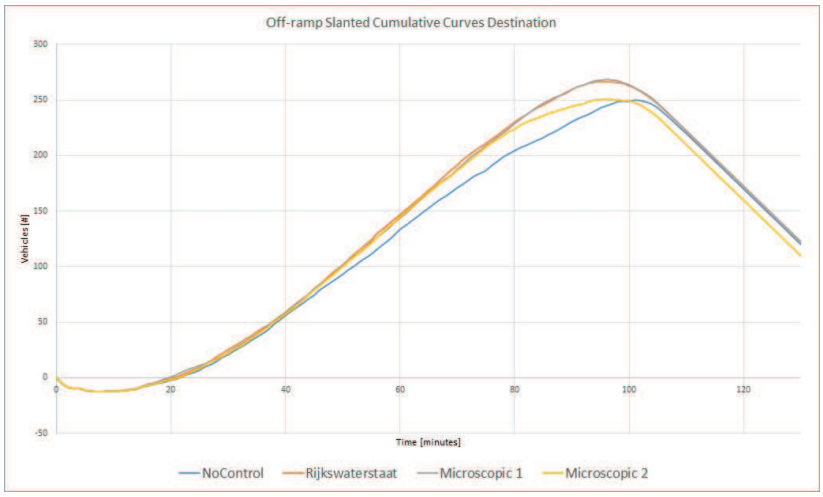

Figure 7.14: Base Case Off-ramp Slanted Cumulative Curves

be the second considered microscopic RM approach. By far the worst performer is the no control alternative. Additionally, following the slanted cumulative curves for the on-ramp vehicles, it is concluded that the currently used macroscopic Rijkswaterstaat RM control structure operates very differently compared to the microscopic approaches. There is more fluctuation in the red times between vehicles for the Rijkswaterstaat algorithm than for the microscopic approaches. Especially, the fluctuation for the Rijkswaterstaat control structure is in line with what can be expected, following the actual Rijkswaterstaat algorithm which adjusts their red times on the measured main lane flows (Rijkswaterstaat, 2013).

7.2.3 Computed travel time savings

The travel time savings are computed by means of the fractional cumulative curves. Showing these cumulative curves is not considered to be essential for the reader, since the differences in the cumulative curves can be much better observed by means of the slanted cumulative curves, as displayed in the previous sub-section. If desired, the data can be requested and the data will be provided. Regarding the base case travel time saving results shown in Table 7.10, the average travel time savings per vehicle are compared to the no control alternative. As explained in the same sub-section in the previous section, the difference between two other alternatives can be computed by calculating the difference of the newly considered two alternatives with the no control alternative.

Table 7.10: Average travel time savings in seconds per vehicle for the base case scenario, compared to the no RM control alternative

Base case scenario Travel time savings				
Control structure	System	Main	On-ramp	Off-ramp
No control	0	0	0	0
Rijkswaterstaat control	25	79	-583	87
Microscopic control 1	38	84	-476	78
Microscopic control 2	61	71	-82	98

Following Table 7.10, it is concluded that the rankings drawn up by looking at the slanted cumulative curves are the same as the rankings shown in this table for most OD pairs. This means that the signs of the computed travel time savings are correct. However, this is not the case for the main lane vehicles regarding the first microscopic RM control structure and the Rijkswaterstaat algorithm. By taking a closer look, it was found that this is due to the fact that the Rijkswaterstaat algorithm has almost 50 more vehicles travelling through the simulation. This gives an advantage in the total number of vehicles (as shown in the slanted cumulative curves). This advantage might not exist in reality. It can be stated with absolute certainty that the currently used RM control structure in the Netherlands is able to cope with this number of vehicles on the main lane, which might not be the case for the settings used for this microscopic control structure. Nevertheless, it can not be concluded that the microscopic control structure is certainly not able to cope with this number of vehicles. To combat this possibly unfair advantage, the fractional cumulative curves are used instead of the actual cumulative curves. When looking solely at the computed travel time savings by means of the fractional cumulative curves, the conclusion is that there is a very small advantage for the main lane vehicles with the first microscopic control structure compared to the Rijkswaterstaat algorithm. However, this advantage might not hold true when the extra 50 vehicles would have been present in the first considered microscopic simulation as well.

Looking at the actual numbers more closely, it can be seen that all controls gain somewhere between approximately 25 and 61 seconds per vehicle on average for the entire system. With the approximately 9600 vehicles passing the system in the simulation, this comes down to a total travel time savings of a range between 67.5 and 162.5 vehicle hours. This is for a simulated time of two hours during rush hour, basically one peak hour during one day for a single location. Additionally, the trade-off between the travel time savings for the main lane vehicles and the on-ramp vehicles is present in the overview as well.

7.2.4 Conclusion

Based on all results, it is concluded that the microscopic RM control approaches outperform both the currently used macroscopic control structure and the no control at all alternative for the base case scenario. This is the case for the first considered microscopic combination of settings, since the travel time savings for the main lane vehicles are more or less the same, but there is a gain of almost two minutes for the vehicles originating at the on-ramp. For the second microscopic control approach, there is a loss of 8 seconds for the main lane vehicles compared to the currently used Rijkswaterstaat algorithm, but this is more than compensated by the travel time savings of 501 seconds for the on-ramp vehicles. Therefore, the overall travel time savings for the whole system are the largest for the second microscopic control structure. The first microscopic control approach records the largest travel time savings thereafter. The no control alternative performs the worst for the base case scenario.

However, the standard deviation for the travel time delays of the second considered microscopic control structure is larger than for the other two control approaches. This means that this RM control structure is less robust. This should be taken into account. Additionally, the differences in approach for the Rijkswaterstaat algorithm and the microscopic control structures are certainly present in the simulation. The varying cycle times used in the Rijkswaterstaat algorithm change with the demand on the main lane, which it does in real life as well. This is not how the microscopic approach works however, which is why the cumulative curves for the on-ramp vehicles are more linear for these control approaches. Lastly, it has been observed that there is only a delay for the on-ramp vehicles when there is actually a traffic congestion with the no control alternative as opposed to the RMIs, which delay vehicles already before there is a congestion.

7.3 SENSITIVITY ANALYSES

To gain insights in what happens to the relative performance of the various different control strategy alternatives, several sensitivity analyses have been performed. The results shown in the text are limited to the tables of the computed travel time savings by means of the fractional cumulative curves, as a gesture to follow the arguments more easily. These travel time savings are the most Key Performance Indicator (KPI) for RMIs. In these tables, the travel time savings are compared to the no control alternative of the base case scenario, in order to see the differences of the considered sensitivity analysis to the base case scenario as well. Although, when making concluding remarks for the various sensitivity analyses, the OTS outputs and the slanted cumulative curves are consulted as well. If theses additional results are explicitly recalled in the concluding remarks regarding a sensitivity analysis, the specific additional results are provided in Appendix E. The remaining additional results can be requested.

Furthermore, the level of explanation for these sensitivity analyses will be reduced compared to the previously conducted scenarios. This is done to reduce the length of the report. The main findings will be posed before the tables. Below the tables, additional conclusions are presented.

7.3.1 Base case without semi-permeable lane demarcation

The first sensitivity analysis revolves around simulating the differences in the travel time savings without the implementation of the semi-permeable lane demarcation between the centre lane and the right lane. In the base case scenario, the semi-permeable lane demarcation is implemented but this is not currently the case in real life. Therefore, in this sensitivity analysis, the semi-permeable lane demarcation is removed. The results of this current situation and the results of the base case scenario are listed in the table. As explained previously, the difference between two alternatives can be computed by calculating the difference of these two alternatives normalised to the no control base case alternative.

Regarding the overall system results displayed in Table 7.11, it is concluded that all alternatives perform better with the semi-permeable lane demarcation in place than without it. Therefore, the semi-permeable lane demarcation is implemented in all remaining sensitivity analyses. Additionally, the differences in the performance between the two scenarios are the least for the first microscopic alternative ($35 - 38$) and the currently used Rijkswaterstaat alternative ($20 - 25$). The performance differences for the other two alternatives are significantly larger ($0 + 90$ & $61 + 48$). Lastly, the differences between the various alternatives for the scenario with the semi-permeable lane demarcation ($61 - 0$) are smaller than without it ($35 + 90$).

Table 7.11: Average travel time savings in seconds per vehicle for the sensitivity analysis without a semi-permeable lane demarcation, compared to the no RM control alternative in the base case scenario

Sensitivity analysis scenario 1 Travel time savings					
Control structure	Scenario	System	Main	On-ramp	Off-ramp
No control	Sensitivity analysis	-90	-86	-144	-78
Rijkswaterstaat control	Sensitivity analysis	20	71	-564	79
Microscopic control 1	Sensitivity analysis	35	86	-544	93
Microscopic control 2	Sensitivity analysis	-48	-35	-203	-33
No control	Base case	0	0	0	0
Rijkswaterstaat control	Base case	25	79	-583	87
Microscopic control 1	Base case	38	84	-476	78
Microscopic control 2	Base case	61	71	-82	98

Considering Table 7.11, several observations can be made. Firstly, all alternatives perform worse without the semi-permeable lane demarcation than their counterpart including the semi-permeable lane demarcation. Therefore, it is recommended to implement this demarcation, regardless of the preferred RM control strategy. Therefore, the semi-permeable lane demarcation is kept in place with the other sensitivity analyses, since all alternatives perform better with it than without it. Moreover, the Rijkswaterstaat RM control strategy and the first microscopic RM alternative perform better without the lane demarcation than the no control alternative including the semi-permeable lane demarcation (with an average of 20 and 35 seconds per vehicle respectively). These two are the best overall performers. The second microscopic alternative comes in third (-48) and the no control alternative holds the least travel time savings (-90).

Concerning the individual OD pairs, the vehicles originating at the on-ramp suffer more delays without the semi-permeable lane demarcation than when this lane demarcation is put in place for the microscopic RM approaches ($-544 \leq -476$ & $-203 \leq -82$). This could be explained by the fact that the probability of the merging vehicles not having their measured gap available any longer when they have to merge, is higher. This is supported by the lower successful merger percentage as well (see Appendix E, Table E.2). However, probably due to being able to use a higher percentage of the infrastructure for the main lane vehicles, the average travel time savings increases for the main lane vehicles and the off-ramp vehicles for the first microscopic RM alternative.

The inverse however, is the case for the current Rijkswaterstaat algorithm. An explanation for the inverse is not provided in this report. Nevertheless, it is logical that the unavailability of a measured gap is less of a problem for the current RM control structure, since this algorithm does not rely on the presence of such gaps in giving vehicles a green traffic light.

Summarising, having a semi-permeable lane demarcation is beneficial for all control strategies. However, the current Rijkswaterstaat algorithm and the first microscopic RM alternative are less affected by the absence of this lane demarcation than the other two alternatives. The interdependent differences between the various control strategies are larger in terms of travel time savings without the lane demarcation than when this lane demarcation is present.

7.3.2 Changes in the truck percentage at the on-ramp

The second sensitivity analysis is performed to check what happens when the truck percentage of vehicles originating from the on-ramp changes from 5% in the base case scenario to either 0% or 10%. This is especially useful when considering other possible sites which might yield different truck percentages at the on-ramp. Just like in the previous sensitivity analysis, the travel time savings are compared to the no RM control alternative in the base case scenario. These results are listed in the table. As explained previously, the difference between two alternatives can be computed by calculating the difference of these two alternatives normalised to the no control base case alternative.

One of the main conclusions that can be drawn from Table 7.12 is that having lower truck percentages benefits the no control alternative ($24 - 0$), but does not result in larger travel time savings for the RMI alternatives. The ranking remains the same as for the base case scenario. Encountering higher on-ramp truck percentages does change the ranking. In that scenario, the currently used Rijkswaterstaat RM alternative performs the best (4). Then, the second (-2) and first (-10) microscopic RM alternatives record the largest travel time savings. The no control alternative performs the worst (-59). The absolute differences for the two microscopic RM alternatives are substantially larger than the difference for the Rijkswaterstaat alternative between the base case scenario and the increased truck percentage analysis. It is concluded that there is still room for improvement for the microscopic

approach in regards to handling trucks at the on-ramp. To combat this, trucks might need larger gap times than the used 1.6 and 1.8 seconds. It is recommended for further research that this will be looked into.

Table 7.12: Average travel time savings in seconds per vehicle for the sensitivity analyses with variable truck percentages, compared to the no RM control alternative in the base case scenario

Sensitivity analysis alternating truck percentages Travel time savings					
Control structure	Scenario	System	Main	On-ramp	Off-ramp
No control	0% trucks	24	22	59	13
Rijkswaterstaat control	0% trucks	25	76	-532	64
Microscopic control 1	0% trucks	29	75	-467	60
Microscopic control 2	0% trucks	61	69	-35	74
No control	10% trucks	-59	-58	-76	-52
Rijkswaterstaat control	10% trucks	4	48	-520	71
Microscopic control 1	10% trucks	-10	32	-483	32
Microscopic control 2	10% trucks	-2	9	-132	13
No control	Base case	0	0	0	0
Rijkswaterstaat control	Base case	25	79	-583	87
Microscopic control 1	Base case	38	84	-476	78
Microscopic control 2	Base case	61	71	-82	98

Following Table 7.12, it is observed that the travel time savings realised by the current Rijkswaterstaat algorithm are the least dependent on the truck percentage (25, 4, 25). Having no RMI in place is the most dependent on the truck percentage (24, -59, 0). Encountering lower truck percentages on the on-ramp seems to have no to a little negative effect on the various active RMIs ($25-25$, $29-38$, $61-61$). However, it does have a positive effect on the travel time savings recorded by no RM control ($24-0$). This is probably due to the fact that passenger cars have less trouble merging, since they are smaller and thus can theoretically fit in smaller gaps. Therefore, controlling the on-ramp vehicles is less necessary when it they only consist of passenger cars. However, having to deal with higher truck percentages leads to worse performances for all alternatives, but the decline in the travel time savings is the worst for the second considered microscopic strategy and no RM control ($-2-61$). The Rijkswaterstaat algorithm is the least affected by the increase in the truck percentage ($4-25$).

The order for the no trucks scenario is the same as for the base case, which yields a truck percentage of 5%, but the differences in travel time savings between the various RMIs and the no control alternative are smaller ($61-41 \leq 61-0$). The order for the average travel time savings for the entire system does change however, when considering the 10% truck percentage. In this scenario, the currently used Rijkswaterstaat algorithm performs the best (4), closely followed by the second microscopic control approach (-2), which in turn is closely followed by the first considered microscopic approach (-10). The differences between the three RMIs are very small in this scenario, which can not be said about the differences between these RMIs and the no control alternative (-59).

Besides these changes in the travel time savings, the successful merger percentage fluctuates as well (see Appendix E). For the microscopic RM control settings, the successful merger percentage slightly increases when the truck percentage decreases and the successful merger percentage decreases when the truck percentage increases. Combining this observation with the losses in travel time savings (for the entire system, but especially for the on-ramp vehicles) leads to the conclusion that the currently used microscopic settings are better suited for passenger cars than for truck originating at the on-ramp. To combat this, trucks

might need larger gaps than the used 1.6 and 1.8 seconds. It is recommended for further research that this will be investigated.

7.3.3 Main lane demand changes

The third sensitivity analysis is performed to investigate what happens when the demand on the main lane changes from the base case with both -10% and $+10\%$. This is done in order to gain insights in what happens to the relative performance of the microscopic RM approach when the main lane demand is different than the used main lane demand. Just as in the previous sensitivity analyses, the travel time savings are compared to the no RM control alternative in the base case scenario. These results are listed in the table. As explained previously, the difference between two alternatives can be computed by calculating the difference of these two alternatives normalised to the no control base case alternative.

There are several main conclusions that can be drawn from Table 7.13. First of all, when the demand on the main lane is 10% less, the no control alternative (87) overtakes the Rijkswaterstaat alternative (71) and the first microscopic approach alternative (72) as the second best alternative. The second microscopic approach remains on top (89). When the main lane demand increases with 10% however, the first microscopic control alternative performs the best regarding the overall system (-55). This is closely followed by the currently used algorithm (-59). With a average travel time savings of 50 seconds per vehicle less, the second microscopic alternative comes in third (-109). In this scenario, the no control alternative performs the worst (-225). This leads to the overall conclusion that the controlled RMI alternatives require a sufficient main lane demand in order to gain travel time savings compared to the no control alternative.

Table 7.13: Average travel time savings in seconds per vehicle for the sensitivity analyses with adjusted main demand patterns, compared to the no RM control alternative in the base case scenario

Sensitivity analysis alternative main lane demand Travel time savings					
Control structure	Scenario	System	Main	On-ramp	Off-ramp
No control	-10% main demand	87	77	192	82
Rijkswaterstaat control	-10% main demand	71	105	-241	84
Microscopic control 1	-10% main demand	72	112	-327	120
Microscopic control 2	-10% main demand	89	91	85	91
No control	+10% main demand	-225	-233	-138	-229
Rijkswaterstaat control	+10% main demand	-59	-3	-754	-5
Microscopic control 1	+10% main demand	-55	-8	-642	-5
Microscopic control 2	+10% main demand	-109	-103	-193	-105
No control	Base case	0	0	0	0
Rijkswaterstaat control	Base case	25	79	-583	87
Microscopic control 1	Base case	38	84	-476	78
Microscopic control 2	Base case	61	71	-82	98

Regarding Table 7.13, it is easily verified that the demand for the main lane influences the travel time savings substantially compared to the base case scenario. When there is less traffic, all alternatives gain travel time savings compared to their base case counterpart. However, when the demand increases, all alternatives lose on average more than one minute per vehicle for the entire system than their base case counterpart.

Concerning the decrease in demand on the main lane, it is concluded that the RMIs still accomplish a gain in the travel time savings for the main lane vehicles compared to no control in this scenario (77, 105, 112, 91), but the losses for the

on-ramp vehicles do not outweigh the benefits of the main lane vehicles, following the system travel time savings (87, 71, 72, 89). Only for the second microscopic RM setting there is a minimal positive effect compared to no RM control (89 – 87). This is primarily caused by the later activation time and lower holding times for the on-ramp vehicles. Moreover, regarding the activation times, which are found in Appendix E (Table E.5), the considered first microscopic RM control does activate later than the currently used Rijkswaterstaat algorithm in the lower main demand scenario. The same is true for the scenario with the increased main lane demand. This later activation time is in contrast to the base case, but in line with expectations considering the activation flow for the Rijkswaterstaat algorithm is equal to 1500 vehicles per lane per hour, compared to the 1650 vehicles per lane per hour of the first considered microscopic RM approach.

For the higher demand scenario, the relative travel time savings for the overall system are larger for all RMI scenarios compared to the no control alternative than in the base case scenario (e.g. $25 - 0 \leq 225 - 59$). The number of successful mergers, which are found in Appendix E (Table E.6), decreases drastically when the demand on the main lane increases. This leads to the belief that a gap of 1.6 seconds is too small, if this is indeed the actual gap. In the base case scenario a gap time of at least 1.6 seconds can be measured, but the actual gap could be larger, benefiting this small required gap time microscopic approach. Furthermore, when the demand on the main lane increases, the microscopic approaches need to keep the on-ramp vehicles waiting too long more often, following the results in Appendix E (Table E.6). This is, because the probability of a large enough gap decreases when the flow on the main lane increases. This affects the microscopic RM control that uses a gap time 1.8 seconds more than the 1.6 seconds approach, resulting in a sharper increase in the percentage of vehicles that had to wait too long for the first considered microscopic setting. Since the influence of the main lane vehicles on the entire system is larger for the higher main lane demand scenario than in the base case scenario, the advantage of the first considered microscopic RM control is less compared to the Rijkswaterstaat algorithm in this scenario than for the base case. This is because the Rijkswaterstaat algorithm performs slightly better than first microscopic approach concerning the main lane vehicles and the inverse is true to a larger degree for the on-ramp vehicles. The differences for the two different OD pairs for the two scenarios between these two RMIs are similar.

The lower demand does not seem to influence the percentage of successful mergers for the microscopic RM approaches, following from the results shown in Appendix E (Table E.5). The same can not be said about the increased main lane demand scenario. The hypothesis is that this might be caused by the fact that when the speed on the main lane has dropped significantly, the gap will not have arrived at the merging spot yet when the on-ramp vehicles wants to merge. This will happen more often with higher demands on the main lane than with lower demands. The fact that there is little to no difference between the lower main lane demand scenario and the base case indicates that in both scenarios the average speed on the main lane is more or less equal for the different simulations. This is supported by Figure E.1 to Figure E.3, displayed in Appendix E. For the period between the 40 and 80 minute mark, the lowest main lane demand shows an increase in the number of passed slanted cumulative vehicles of 750 for the first microscopic alternative and the base case shows an increase of 1000 during the same time period for the first microscopic alternative. This means that for the highest main lane demand without extra traffic jams, the number of passed vehicles should be approximately 1250 vehicles during the same time period for the first microscopic alternative. However, this is only 1100 vehicles. This indicates that the traffic conditions for the higher demand scenario are indeed more congested on the main lane, resulting in a speed drop. This decreases the number of successful mergers due to a mismatch of the measured gap and the location of the merging vehicle.

7.3.4 On-ramp demand changes

The fourth sensitivity analysis is performed to investigate what happens when the demand on the on-ramp changes from the base case with both -10% and $+10\%$. This is especially useful for situations where an RMI is implemented that encounters a larger on-ramp demand. Just as in the previous sensitivity analyses, the travel time savings are compared to the no RM control alternative in the base case scenario. These results are listed in the table. As explained previously, the difference between two alternatives can be computed by calculating the difference of these two alternatives normalised to the no control base case alternative.

The main conclusion that can be drawn from Table 7.14 is that the performance of the various alternatives depends on the on-ramp demand, but there does not seem to be a clear direction. For example, the first microscopic alternative gains more ground on the currently used Rijkswaterstaat alternative when there is a decrease in the on-ramp demand ($38 - 25 \leq 46 - 27$) and loses some ground when the on-ramp demand increases ($0 - 7 \leq 38 - 25$). However, the second microscopic alternative loses a bit with the decreased on-ramp demand compared to the currently used algorithm ($60 - 27 \leq 61 - 25$). Just as for the first microscopic alternative, the increased on-ramp results yield a further decrease in relative travel time savings ($17 - 7 \leq 61 - 25$). However, the second microscopic alternative still results in more travel time savings than the Rijkswaterstaat alternative in all cases, which is not true for the first microscopic alternative. In the decreased on-ramp demand scenario, the no control alternative obtains better results than the Rijkswaterstaat alternative (26, 27). For the other cases, the no control alternative yields the worst overall performance.

Table 7.14: Average travel time savings in seconds per vehicle for the sensitivity analyses with adjusted on-ramp demand patterns, compared to the no RM control alternative in the base case scenario

Sensitivity analysis alternative on-ramp demand Travel time savings					
Control structure	Scenario	System	Main	On-ramp	Off-ramp
No control	-10% on-ramp demand	36	23	155	45
Rijkswaterstaat control	-10% on-ramp demand	27	59	-414	67
Microscopic control 1	-10% on-ramp demand	46	73	-299	70
Microscopic control 2	-10% on-ramp demand	60	53	115	58
No control	+10% on-ramp demand	-45	-32	-159	-27
Rijkswaterstaat control	+10% on-ramp demand	7	79	-678	69
Microscopic control 1	+10% on-ramp demand	0	65	-633	67
Microscopic control 2	+10% on-ramp demand	17	43	-240	52
No control	Base case	0	0	0	0
Rijkswaterstaat control	Base case	25	79	-583	87
Microscopic control 1	Base case	38	84	-476	78
Microscopic control 2	Base case	61	71	-82	98

With reference to Table 7.14, various conclusions can be drawn up. First of all, it is concluded that the microscopic RMIs outperform the no control alternative in both sensitivity scenarios (e.g. $36 \leq 46$ & $36 \leq 60$). However, of the two newly introduced scenarios, the Rijkswaterstaat RM algorithm only ensures average lower travel times for the entire system than the no control alternative, when the on-ramp demand is increased ($-45 \leq 7$). In the same scenario, the Rijkswaterstaat algorithm does also perform better than the considered first microscopic RM control structure ($0 \leq 7$). Regardless of which in this sub-section considered scenario is regarded, the chosen second RM alternative results in the largest average travel time savings for the entire system.

Considering the individual OD travel time savings, it is observed that the main lane vehicles benefit more from active RMIs when the on-ramp demand is higher compared to the no control alternative (e.q. $71 - 0 \leq 43 + 32$). This can easily be explained by the fact that when this demand is higher, the probability of multiple vehicles wanting to merge in a short time interval increases, which in turn increases the congestion probabilities for the no control alternative. Furthermore, when the on-ramp demand increases, the encountered average delay for the on-ramp vehicles for the Rijkswaterstaat control strategy decreases compared to the no control alternative, but it increases when the on-ramp demand is lower ($-583 + 0 \leq -678 + 159$). This can be explained by the fact that in the beginning and near the end of the activation period of the RMI the Rijkswaterstaat algorithm does not limit the on-ramp vehicles much and during these periods, more vehicle pass when the on-ramp demand is higher. The same goes for the number of vehicles that have passed after the RMI has been deactivated, lowering the average delay for the on-ramp vehicles when the on-ramp demand is higher. When the on-ramp demand is lower, the average delay for the on-ramp vehicles compared to the no control alternative is similar to the difference in the base case scenario.

However, the reverse is true for the microscopic approaches. These alternatives cause less delay for the on-ramp vehicles compared to the no control alternative when the on-ramp demand is lower than in the base case (e.q. $-299 - 155 \leq -476 - 0$) . For the higher on-ramp demand scenario, the encountered average delay for the on-ramp vehicles is similar. This can be clarified by the fact that these RM control structures do not let more vehicles pass in the beginning or near the end of the activation period. Therefore, only the vehicles that pass the system when the RMI is deactivated can lower the average delay for the on-ramp vehicles. However, since a lot of extra vehicles have already encountered extra delays, the extra number of vehicles reaching their destination does not make up for these extra travel time losses. When the on-ramp demand is lower, the queue on the on-ramp is shorter, which leads to less accumulated total delays and thus to shorter average delays.

Regarding the successful merger percentage of the two microscopic RMIs in Appendix E, Table E.7 and Table E.8, it is observed that the percentage for the increased on-ramp demand is slightly lower, approximately 4% for both settings. Additionally, this is also the case in the lower on-ramp demand scenario. The activation times, which are only dependent on the main lane flow, which is the same for all three scenarios, differ as well. They even differ to such a degree that the ranking fluctuates as well. For the base case scenario and the lower on-ramp demand scenario, the currently used Rijkswaterstaat algorithm activates later than the chosen first microscopic control settings, which is counter-intuitive when considering the higher activation flow for the microscopic approach. For the increased on-ramp demand, the Rijkswaterstaat RM control structure does activate later on average than the first considered microscopic approach. This leads to the conclusion that the operation of the seeds on the stochastic variables like the actual demand pattern depends on the combination of all settings and that the seeds does not individually have the same effect on a variable if that variable stays the same while others do change. Both the fluctuation in the activation time and the successful merger percentage are assumed to be the result of this randomness, caused by the simulation seeds. The concluding remark about these two factors is that they have not significantly changed, thus not individually impacted the travel time savings. This is in line with expectation, when considering that the probability of a single merging vehicle finding a gap is dependent on the main lane flow, which remains equal. The same reasoning applies to the activation flow.

7.3.5 Off-ramp demand changes

The fifth sensitivity analysis is performed to investigate what happens when the demand of the off-ramp upstream of the on-ramp changes is adjusted. This is done by changing this demand compared to the base case scenario with both −10% and +10%. This is especially useful for situations where an RMI is implemented that encounters a higher demand for the off-ramp just upstream of the considered on-ramp. Just as in the previous sensitivity analyses, the travel time savings are compared to the no RM control alternative in the base case scenario. These results are listed in the table. As explained previously, the difference between two alternatives can be computed by calculating the difference of these two alternatives normalised to the no control base case alternative.

The most important observation that can be made regarding Table 7.15 is that the on-ramp vehicles for the microscopic alternatives suffer less delay when the off-ramp demand increases (e.q. $-476\ leq - 372$) and that the on-ramp vehicles suffer more delay when the off-ramp demand decreases (e.q. $-543\ leq - 476$). These travel time savings directions are not found for the Rijkswaterstaat alternative. This is in line with expectations, since the microscopic alternative need gaps in order to show a green traffic light and the macroscopic Rijkswaterstaat alternative does not. When the off-ramp demand increases, the probability of a gap on the shoulder lane increases, especially when a semi-permeable lane demarcation is in place as is the case in these scenarios. Conclusions on the overall system performance are more difficult, since an increase in the off-ramp demand leads to congestion originating at the end of the on-ramp in the current layout in OTS. This limits the conclusions that can be made for the performance for the entire system for this specific scenario.

Table 7.15: Average travel time savings in seconds per vehicle for the sensitivity analyses with adjusted off-ramp demand patterns, compared to the no RM control alternative in the base case scenario

Sensitivity analysis alternative off-ramp demand Travel time savings					
Control structure	Scenario	System	Main	On-ramp	Off-ramp
No control	-10% off-ramp demand	-15	-13	-36	-3
Rijkswaterstaat control	-10% off-ramp demand	41	95	-542	93
Microscopic control 1	-10% off-ramp demand	29	83	-543	-4
Microscopic control 2	-10% off-ramp demand	67	87	-145	89
No control	+10% off-ramp demand	-57	-69	61	-62
Rijkswaterstaat control	+10% off-ramp demand	-8	35	-517	46
Microscopic control 1	+10% off-ramp demand	17	50	-372	54
Microscopic control 2	+10% off-ramp demand	9	11	-11	-6
No control	Base case	0	0	0	0
Rijkswaterstaat control	Base case	25	79	-583	87
Microscopic control 1	Base case	38	84	-476	78
Microscopic control 2	Base case	61	71	-82	98

Table 7.15 provides some interesting insights. First of all, when the off-ramp demand increases, the average delay encountered by the on-ramp vehicles decreases for the microscopic RMIs (e.q. $-476\ leq - 372$) and increases when the demand for the off-ramp vehicles decreases (e.q. $-543\ leq - 476$). This can be explained by the fact that these vehicles create gaps on the right lane of the main road (and these gaps are kept present due to the semi-permeable lane demarcation), which have to be present and measured for the microscopic control approach in order to let on-ramp vehicles pass the RMI. A lower off-ramp demand will create less gaps, thus increasing the average red time for the waiting vehicles, increasing the delays encountered by the on-ramp vehicles. This is supported by the percentage of vehicles that had to wait too long (see Appendix E, Table E.9), which increases by

0.5% to 1.5% (on a base case percentage of 7% and 11%) when the off-ramp demand is decreased by 10% and decreases by a similar amount when the off-ramp demand increases by 10% as can be found in Appendix E, Table E.10.

A similar reasoning applies to the no control alternative. When the off-ramp demand increases, merging vehicles will be able to find gaps more easily, since the probability of having one available in a close range is higher ($0 \leq 61$). However, this has not led to an increase in the travel time savings for the main lane vehicles ($-69 \leq 0$), hence not for the entire system either ($-57 \leq 0$). When the off-ramp demand decreases, the delay for the on-ramp vehicles increases compared to the base case scenario no control alternative ($-36 \leq 0$), also leading to more congestion for the main lane vehicles ($-13 \leq 0$), resulting in an overall worse performing system ($-15 \leq 0$).

For the Rijkswaterstaat algorithm, the increased off-ramp percentage also enables the merging vehicles to have an increased chance to merge in smoothly, reducing the average delay encountered by the on-ramp vehicles ($-583 \leq -517$). However, the opposite is not true for the decreased off-ramp demand scenario. There, the delay encountered by the on-ramp vehicles also decreases ($-583 \leq -542$).

When looking at the entire system performance, the order does change in both scenarios, but differently. Regarding the decreased off-ramp demand, the Rijkswaterstaat algorithm takes second place and the first considered microscopic approach comes in third. Concerning the increased off-ramp demand, Rijkswaterstaat remains third, but the second considered microscopic approach loses the top spot to the first considered microscopic RM control strategy. In all scenarios, the no control alternative performs the worst.

Furthermore, it should be noted that the increased off-ramp demand increases the average delays encountered by the main lane vehicles, but the decreased off-ramp demand does not lead to the inverse effect to the same proportions. This can be explained by the fact that the base case scenario yields a close to maximum off-ramp demand without causing (too many) traffic jams at the off-ramp, which happens with OTS, because drivers do not keep the right lane early enough. Then, increasing this off-ramp demand will lead to extra congestion near the off-ramp location, also delaying the main lane vehicles. The decrease in the off-ramp demand however, makes merging for the on-ramp vehicles more difficult, since there will be less gaps on the right lane. However, the quantitative results for this sensitivity analysis are mostly disregarded, because the traffic jams originating near the off-ramp interfere with the main lane delays and thus with the total system delays.

7.3.6 Speed limit changes

The sixth and final sensitivity analysis revolves around investigating what happens when the speed limit for the main lane, on-ramp and off-ramp is $80\frac{km}{h}$ and $120\frac{km}{h}$ compared to the base case scenario, which entails a speed limit of $100\frac{km}{h}$. This is interesting for scenarios where the maximum speed limit is different. Such sites are currently not common in the Netherlands, but they could be in different countries. Just as in the previous sensitivity analyses, the travel time savings are compared to the no RM control alternative in the base case scenario. These results are listed in the table. As explained previously, the difference between two alternatives can be computed by calculating the difference of these two alternatives normalised to the no control base case alternative.

The first main conclusion that can be drawn from looking at Table 7.16 is that higher maximum speeds yield more travel time savings and lower maximum speeds lead to more travel time delays. This is in line with what can logically be expected. However, it is observed that the currently used macroscopic Rijkswaterstaat alternative gains ground on the microscopic alternatives when the speed limit changes, regardless of the direction of the change. For the $80\frac{km}{h}$ scenario, the Rijkswaterstaat alternative performs better than both microscopic

alternatives $(-126, -171, -197)$. For the $120\frac{km}{h}$ scenario, the Rijkswaterstaat alternative performs similarly to (or slight better than) the microscopic approaches $(74, 67, 75)$. This, in combination with the successful merger percentage statistics displayed in Appendix E leads to the belief that the gap measurement detector locations are not placed entirely correct in the adjusted speed limit scenarios. This could be due to the fact that different speeds require different gap times (Van Beinum, 2018). Furthermore, the differences in the travelling speed of the measured gaps can differ more for the $120\frac{km}{h}$ scenario. This complicates the fitting of the merging vehicles with the measured gaps. Therefore, it is recommended to improve the proposed microscopic control approach with measuring the travelling speed of the gaps instead of assuming this travelling speed.

Table 7.16: Average travel time savings in seconds per vehicle for the sensitivity analyses with various speed limits, compared to the no RM control alternative in the base case scenario

Sensitivity analysis alternative speed limits Travel time savings					
Control structure	Scenario	System	Main	On-ramp	Off-ramp
No control	80 kmh scenario	-222	-222	-261	-180
Rijkswaterstaat control	80 kmh scenario	-126	-91	-539	-77
Microscopic control 1	80 kmh scenario	-171	-158	-342	-127
Microscopic control 2	80 kmh scenario	-197	-191	-296	-159
No control	120 kmh scenario	70	65	130	57
Rijkswaterstaat control	120 kmh scenario	74	124	-481	114
Microscopic control 1	120 kmh scenario	67	80	-65	64
Microscopic control 2	120 kmh scenario	75	71	124	71
No control	Base case	0	0	0	0
Rijkswaterstaat control	Base case	25	79	-583	87
Microscopic control 1	Base case	38	84	-476	78
Microscopic control 2	Base case	61	71	-82	98

Consulting Table 7.16, for the scenarios with all different speed limits for the main lane, on-ramp and off-ramp, the trade-off between the travel time savings for the main lane and for the on-ramp is present. In other words, the more an alternative delays the on-ramp vehicles, the more the main lane vehicles save travel time. This is in line with what can logically be expected. Additionally, it makes sense that when the speed limit goes up, the average travel time savings compared to the base case scenario are more, since the vehicles that do not encounter congestion can drive faster, reaching their destination quicker. It also makes perfect sense that the reverse is true for a decreased speed limit.

Nonetheless, differences can be found. For instance, the Rijkswaterstaat algorithm only encounters 170 more seconds of delays for the main lane vehicles when the speed limit is $80\frac{km}{h}$ compared to the Rijkswaterstaat algorithm with a speed limit of $100\frac{km}{h}$ $(79 + 91)$, whereas the no control alternative encounters 222 seconds more delay. The first considered microscopic control strategy encounters 242 additional seconds delay for the main lane vehicles $(84 + 158)$ and the second considered microscopic RM control approach faces an increase in the delay for the main lane vehicles of 453 seconds $(71 + 191)$. This indicates that the Rijkswaterstaat control structure suffers proportionally less congestion on the main lane when the speed limit goes down than the first microscopic approaches.

Furthermore, regarding the average on-ramp delays, the differences between the two considered microscopic RM control approaches is less for the newly tested speed limits compared to the base case speed limit (e.g. $124 + 65 \leq 476 - 82$). The difference for the on-ramp vehicles between the Rijkswaterstaat algorithm and the first considered microscopic algorithm increases in both newly tested speed limit

scenarios compared to the base case scenario (e.q. $583 - 476 \leq 539 - 342$). For the $120\frac{km}{h}$ scenario, this can be explained by the fact that drivers apparently leave larger gaps (both in space due to the increased speed, but also in time) when the drivers drive faster. This has been found in scientific research as well (Brackstone and McDonald, 2007). This increase in the desired time spacing between two vehicles causes more 1.8 seconds gaps to be measured, increasing the controlled flow from the on-ramp onto the main lane for the first considered microscopic settings combination. For the $80\frac{km}{h}$ this can be explained by the fact that there is more congestion on the main lane, leading to not measuring a vehicle on the gap measurement detector loop due to still standing traffic more often. These 'gaps' also increase the flow let through the RMI. The Rijkswaterstaat algorithm will measure a lower flow when the speed limit drops, also increasing the flow from the on-ramp onto the main lane, decreasing the relative delay for these vehicles. When the speed limit goes up to $120\frac{km}{h}$, higher main lane flows will be measured, resulting in a lower flow from the on-ramp onto the main lane. The reason the absolute average delay from the on-ramp is lower than in the base case scenario Rijkswaterstaat alternative is caused by the increased driving speed, decreasing the delays encountered by the on-ramp vehicles that can drive in free flow conditions. It is easily verified that the difference for the on-ramp vehicles for the Rijkswaterstaat alternative is less than the difference for the on-ramp vehicles in the no control alternative in both scenarios.

The increased desired distance in time between two vehicles probably also results in a larger desired gap to fit in. Additionally, gaps measured in congestion do not travel with the assumed main lane speed, causing the merging vehicles to miss their gap. Furthermore, the average acceleration percentage of the vehicles could be lower when the speed limit increases (and higher when the speed limit decreases). This is because drivers might accelerate to a lesser degree when driving faster, changing the average acceleration. Therefore, the successful merger percentage should be down in both alternative scenarios, which is indeed the case with approximately 20% for the first microscopic control approach and 10% for the second microscopic control approach as can be seen in Table E.11 and in Table E.12 in Appendix E. This comes down to more or less half of the in the base case scenario successful mergers now being unsuccessful in both cases. Summarising, when the speed limit changes, it is not enough to adjust the gap measurement locations by just changing the average speed on the main lane. Getting the exact location of the gap measurement detector right requires more adjustments in the calculations (see Appendix D).

Thus, the conclusion regarding the effectiveness of the microscopic RM control approaches is not final. However, if the microscopic RM control structures can not be improved for these speed limits, it is obvious that the Rijkswaterstaat algorithm should be preferred in a $80\frac{km}{h}$ scenario when considering the total system. Additionally, the first microscopic RM alternative outperforms the considered second microscopic RM alternative in such a scenario. The no control alternative performs the worst in such a scenario. When the speed limit is $120\frac{km}{h}$, there is almost no difference between the three considered alternatives regarding the total system travel time savings.

7.4 VERIFICATION AND VALIDATION

In order to conclude if the results are valid, this section will summarise the findings in regards to the verification and validation process. In order to provide insights regarding this matter, several important mechanics have been investigated. What should at least happen and be found in the results, is the following:

1. The Rijkswaterstaat RM algorithm should have variable average red times, based on the average flow on the main lane;
2. The Rijkswaterstaat RM algorithm should ensure travel time savings for the current road layout (without the semi-permeable lane demarcation), as found in (Rijkswaterstaat, 2019);
3. The average red time between two green phases for the Rijkswaterstaat algorithm should be equal to 15 seconds, when the flow on the main lane is very high (i.e. during the 40 and 60 minute mark in the simulation at least);
4. There should be a trade-off between the travel time savings for the main lane vehicles and the on-ramp vehicles;
5. When the required minimum gap time is lower, the average red time between two green phases should be lower;
6. When the required minimum gap time is lower, the average delay for the on-ramp vehicles should be lower;
7. When the off-ramp demand increases and the semi-permeable lane demarcation is in place, the number of measured gaps on the right line should increase, increasing the average flow from the on-ramp onto the main lane in the microscopic RM alternatives. The reverse should be true when the off-ramp demand decreases;
8. When a semi-permeable lane demarcation is in place, the percentage of successful mergers should be higher than without this lane demarcation;
9. When using the average maximum acceleration as the assumed acceleration, the percentage of successful mergers should be higher than when using a lower maximum acceleration than the assumed acceleration;
10. When the main lane demand increases, the activation times of the RMI alternatives should be earlier. The opposite should hold when the main lane demand decreases;
11. The higher the activation flow, the later the RMI should be activated on average;

In the previously mentioned simulation results all these conclusions have been found. Only the last one, regarding the activation flow, is not always the case when comparing two control structures with different activation flows. However, this is probably due to the steep increase in the activation flow in the beginning of the simulation and the stochastic nature of the demand patterns. Moreover, when taking the average of all control settings with a higher activation flow, it has been found to be true on average.

Additionally, the statistics computed by OTS do not support the fifth point. However, when looking at the cumulative curves and its travel time savings calculation, this is the case. Therefore, the computed travel time savings by means of the cumulative curves are deemed to be more accurate and are thus primarily used instead of the delays computed by OTS.

Moreover, the time gaps between two vehicles are larger when the speed limit is $120\frac{km}{h}$ compared to the time gaps when the speed limit is $100\frac{km}{h}$ or $80\frac{km}{h}$. This is in line with scientific research and therefore contributes to the reliability of the results.

8 CONCLUSION

Following Chapter 7, concluding remarks on the outcomes of the research can be provided. These will revolve around the research questions mentioned in Section 1.3 and the acceleration distribution results of Chapter 5. Additionally, a discussion points regarding this research will be added. Lastly, policy recommendations and further research recommendations will be presented.

8.1 RESULTS

The most important result of this research is the answer to the main research question. The main research question reads: **To what extent could a microscopic Ramp Metering (RM) control approach lead to less travel time delays compared to current alternatives?** In order to provide an answer to the main research question, several sub-questions have been defined. These sub-questions will be answered separately before the outcome of the main question will be summarised.

8.1.1 First sub-question

The first identified sub-question goes as follows: **What combination of characteristics of the microscopic Ramp Metering (RM) control approach attains the best travel time savings results?** The answer to this question can be provided with the findings in Section 7.1.

As stated in that particular section, evident differences between various best microscopic RM control settings can be found. First and foremost, the best results regarding the travel time savings are accomplished when there is a semi-permeable lane demarcation in place that prevents mergers from the middle lane onto the right hand lane of the main road. Additionally, the on-ramp flow should be hindered minimally all the while the travel time savings for the main lane vehicles is not limited too much.

Considering the current road layout with the semi-permeable lane demarcation in place, the best results are obtained by making use of a minimum required gap time of 1.6 seconds, an activation flow of 1800 vehicles per lane per hour and an assumed acceleration for the on-ramp vehicles that is chosen in such a way that 62.5% of all vehicles have an acceleration that is higher than or equal to this assumed acceleration. This combination of settings saves almost one minute per vehicle for the entire system compared to the worst combination of these settings when the semi-permeable lane demarcation is in place.

However, this combination of microscopic RM parameter settings is not a relatively robust alternative. In other words, the average travel time savings over the 30 random simulation seeds might be the highest, but the travel time savings between these seeds differ a lot. Another combination of parameter settings that records large travel time savings, but which is substantially more robust, is the alternative where the required minimum gap equals 1.8 seconds, the activation flow is 1650 vehicles per lane per hour and the assumed acceleration is equal to the mean of the distribution. Both alternatives have been taken into account for the sensitivity analyses. This secondly mentioned alternative will henceforth be called the first microscopic RM control alternative and the less robust alternative will be named

the second microscopic RM control alternative. Microscopic Ramp Metering (RM) control alternative 1 uses:

- A minimum activation flow of 1650 vehicles per lane per hour;
- A gap time of 1.8 seconds;
- An assumed acceleration which is chosen in such a way that 50% of drivers have an maximum acceleration that is equal or larger than the assumed acceleration.

Microscopic Ramp Metering (RM) control alternative 2 uses:

- A minimum activation flow of 1800 vehicles per lane per hour;
- A gap time of 1.6 seconds;
- An assumed acceleration which is chosen in such a way that 62.5% of drivers have an maximum acceleration that is equal or larger than the assumed acceleration.

Considering the various analyses, it was concluded that the second microscopic RM control alternative saves the most travel time on average per vehicle for the entire system for the current road layout including a semi-permeable lane demarcation. However, this alternative is not very robust. The first microscopic RM control alternative is less sensitive to variations than the second microscopic RM alternative. For example, regarding the current road layout (i.e. without the semi-permeable lane demarcation), the first microscopic alternative saves 83 seconds per vehicle on average compared to the second microscopic RM control alternative. The first microscopic alternative only loses a bit more than three seconds when the semi-permeable lane demarcation is removed. The second microscopic RM control alternative loses 109 seconds when the semi-permeable lane demarcation is removed. This is an evident example of the difference in the robustness between the two considered microscopic alternatives.

8.1.2 Second sub-question

The second sub-question reads: **How does the microscopic Ramp Metering (RM) control approach stack up against the no Ramp Metering Installation (RMI) control alternative?** In answering this question, both the first and the second microscopic RM control alternative will be examined.

For all scenarios, it was found that at least one of the two microscopic RM alternatives performs at least slightly better than the no control alternative, although the differences are negligibly small sometimes. For all tested scenarios, it only occurs twice that one of the microscopic RM alternatives does not perform better than the no control alternative and that the other one only performs slightly better. This is in the reduced main lane demand scenario and in the $120\frac{km}{h}$ speed limit scenario. In all other tested scenarios both microscopic RM control alternatives perform better than the no control alternative.

Considering these remarks, it is concluded that the microscopic RM control approach leads to less travel time delay for the entire system compared to the no control alternative. This is at least the case for the tested simulation settings.

8.1.3 Third sub-question

The third and final sub-question that has to be answered before the main research question can be answered, is: **How does the microscopic Ramp Metering (RM) control approach compare to the currently used macroscopic Rijkswaterstaat Ramp Metering (RM) control approach?** The answer to this question proves to be more nuanced.

For the base case scenario, both microscopic RM alternatives save more travel time than the currently used macroscopic Rijkswaterstaat RM control algorithm. For the first alternative, this is a gain of 13 seconds on average per vehicle for the entire system and for the second microscopic RM alternative, this is even 36 seconds. Without the semi-permeable lane demarcation, only the first microscopic RM alternative performs better. Then, the gain is 15 seconds per vehicle on average. The second microscopic RM alternative recorded an average extra travel time delay of almost 68 seconds per vehicle compared to the currently used macroscopic Rijkswaterstaat RM algorithm.

Without any trucks at the on-ramp, both microscopic RM control alternatives result in more travel time savings compared to the currently used algorithm. However, when 10% of the on-ramp vehicles is a truck, the currently used RM algorithm performs better than both microscopic alternatives. This leads to the conclusion that the current microscopic control structure obtains better results for passenger vehicles than for trucks. Thus, improvements can still be achieved when this weakness is improved.

Regardless of the direction of the main lane demand changes, the first microscopic RM control alternative performs slightly better than the Rijkswaterstaat control alternative, although the differences are negligibly small. Additionally, when the main lane demand decreases, the second microscopic RM control alternative records 18.5 seconds of travel time savings on average per vehicle for the entire system. However, when the main lane demand increases by 10%, this is completely turned around. This scenario results in a better performance of 49.5 seconds per vehicle for the currently used macroscopic Rijkswaterstaat alternative compared to the second microscopic alternative. So, the preferred microscopic RM alternative depends on the main lane demand. If this demand is relatively high, the first alternative is preferred. When the main demand is lower, the second microscopic alternative is preferred.

A similar conclusion can be drawn considering the sensitivity analyses regarding the on-ramp and off-ramp flow. For the reduced on-ramp flow and for the increased off-ramp flow, both microscopic alternatives obtain more travel time savings than the Rijkswaterstaat algorithm. For the increased on-ramp flow and the reduced off-ramp flow, the second microscopic RM alternative performs significantly better than the current algorithm. However, the Rijkswaterstaat alternative performs better than the first microscopic alternative in these scenarios. So the conclusion is similar to the conclusion for the main lane demand, namely that the preferred settings for the microscopic RM control alternative differ depending on the actual flows, but there is a combination of microscopic settings that result in a better performance than the currently used algorithm in all cases.

For the various speed limits, the result is that the microscopic alternatives perform similar or worse for the $80\frac{km}{h}$ and $120\frac{km}{h}$ analyses compared to the currently used RM algorithm. This might be (partially) due to the fact that the gap measurement detector locations of the microscopic RM control alternatives have not been determined properly for these speed limits. This conclusion is based on the low successful merger percentages for these speed limits compared to the base case scenario. The worse performance for different speed limits might be caused by drivers keeping a different time headway with different speeds (Van Beinum, 2018). This might require different minimum required gap times. Additionally, the assumed travelling speed of the measured gaps might be worse. Concluding, the

microscopic RM control structure needs additional adjustments when the speed limit is not equal to $100\frac{km}{h}$. If this is not performed, the currently used Rijkswaterstaat RM algorithm should be preferred.

8.1.4 Main research question findings

Combining the answers to all sub-questions results in the answer to the main question of this research. The main question reads: **To what extent could a microscopic Ramp Metering (RM) control approach lead to less travel time delays compared to current alternatives?** Since this is the main research goal, this sub-section describes the main findings.

Following the answer to the sub-questions, it is concluded that the microscopic RM approach could lead to an increase in the total travel time savings, not only compared to the no control alternative, but also to the currently used macroscopic Rijkswaterstaat RM control alternative. However, how much travel time can be saved, depends on several factors. These factors include:

- The presence of a semi-permeable lane demarcation preventing merging manoeuvres from the main road onto the right lane of the main road;
- The speed limit;
- Truck percentage on the on-ramp;
- The main lane, on-ramp and off-ramp demand.

Concerning some quantitative results regarding the average saved travel time per vehicle for the entire system, it was found that the microscopic ramp metering control approach could increase the average travel time savings for the entire system up to 36 seconds compared to the currently used Rijkswaterstaat algorithm. The exact value depends on the used combination of settings. When a more robust combination of microscopic settings is chosen, an average travel time savings of 13 seconds was recorded. The Rijkswaterstaat ramp metering algorithm already saves 25 seconds on average, making the proposed microscopic ramp metering approaches potentially save either 38 seconds or even 61 seconds compared to the no control alternative.

The advantage of the Rijkswaterstaat and microscopic RM control approaches compared to the no control alternative are mainly found in the main lane vehicles. The Rijkswaterstaat alternative gains 79 seconds on average for the main lane vehicles compared to the no control alternative. The microscopic settings obtain an average travel time saving compared to the no control option of between 71 and 84 seconds. So, the performance of the various RMIs for the main lane vehicles are similar and always better than the no control alternative.

However, the microscopic approach does limit the on-ramp vehicles less. The on-ramp vehicles during the Rijkswaterstaat option are delayed with an average of 583 seconds compared to the null alternative in the base case scenario. For the microscopic approach, this encountered average delay for the on-ramp vehicles compared to the no control alternative is in the range of 476 and only 82 seconds. This difference and the fact that the results for the main lane vehicles are similar leads to the overall better performance of the microscopic control approaches.

Nonetheless, differences in the recorded travel time savings are found for the various sensitivity analyses. For some scenarios, the first, more robust, microscopic alternatives performs better. This is the case for the current scenario (i.e. without the implementation of the semi-permeable lane demarcation), the increased main lane demand scenario and the increased off-ramp demand scenario. For other scenarios, the second alternative records the least travel time delays. Besides the base case scenario, this is the case for the 0% trucks at the on-ramp scenario, the decreased main lane demand scenario, the decreased and increased on-ramp

demand scenarios, the decreased off-ramp demand scenario and the 120 $\frac{km}{hour}$ speed limit scenario. Additionally, the Rijkswaterstaat RM control alternative occasionally performs better than one of the two considered microscopic RM approaches. However, in most cases, at least one of the two considered microscopic alternatives performs better than the Rijkswaterstaat and the no RM control alternative. The only two scenario where the Rijkswaterstaat alternative performs better than both microscopic alternatives are the scenario with the 10% truck percentage and the scenario with a speed limit of 80 $\frac{km}{hour}$. So, two remaining points of improvement for the microscopic RM control approach used in this research, are the performance for various speed limits and the performance of merging trucks.

8.2 DISCUSSION POINTS

Regarding the results, several assumptions and points of discussion should be kept in mind. The research makes use of quite some assumptions and simplifications. Some of these might have a greater impact than others. Comments on the assumptions and points of discussion of this research are listed in this section.

8.2.1 Vehicle acceleration

While determining the vehicle acceleration of the passenger vehicles, not all considered vehicles started at standstill, even though this was assumed. All observed vehicle trajectory points are determined by hand, which might have led to measurement errors. Especially near the end of the on-ramp, being one pixel off results in a big difference in distance in meters. Additionally, the importance of the conversion for the pixel data to distance in meters from the known vehicles trajectory can not be understated. If a slight measurement error is made in the measurement of the data points of this vehicle, all trajectories are incorrect. Nonetheless, the MSEs of the computed vehicles trajectories compared to the measured trajectories are not large, indicating that the method works and that the conversion was probably successful.

However, the acceleration distribution might still be improved. Besides the points mentioned in the previous paragraph, the assumed mass and top speed are equal for all vehicles, which in practice is not true. Using the actual individual mass and top speed characteristics might result in a bit different results regarding the perceived maximum acceleration statistics. Furthermore, the number of used vehicles to get to the acceleration distribution is limited. For trucks this is even 0. Therefore, the standard deviation for trucks is assumed to be equal to passenger vehicles in this research, even though in real life this does not have to be the case. Using more vehicles to fit a distribution might lead to a more accurate distribution. Concluding, the acceleration distribution used in this research is a decent representation of the deviation between the acceleration of various vehicles, but it could be improved even further.

Furthermore, the average acceleration for the whole acceleration trajectory in OTS is too high when compared to the measured trajectories. Nonetheless, the maximum acceleration can reach the used values. Therefore, the acceleration mechanics in OTS might need a revision for the acceleration of merging vehicles. Improving the maximum acceleration distribution and the OTS acceleration mechanics might result in more realistic acceleration patterns in the simulation, possibly influencing the results.

8.2.2 Driver behaviour

Besides the vehicle acceleration described in the previous sub-section, which is also partly subject to driver behaviour, there are other assumptions regarding the driver behaviour used in this research.

Firstly, there is no reaction time for the vehicles when they start to accelerate at the traffic light. This is not necessarily a problem, because if the reaction time in real life is equal for all drivers, this can just be added to the acceleration time when determining the gap detector loop locations. However, there might be differences between drivers in their acceleration time. Adding a reaction time distribution to the simulation could improve the resemblance of the real life situation.

Secondly, concluded from empirically investigating some simulation runs, it seems that the merging vehicles in OTS require quite large gaps to merge. This is concluded by observing the merging vehicles and noticing that these vehicles do drive parallel to the gap for quite a long time while they could have already fit in the gap.

In addition, possibly due to the need of these larger gaps, these merging vehicles sometimes get to a complete standstill on the on-ramp, even though there is no congestion at standstill on the main lane. This is unrealistic driver behaviour. This unrealistic driver behaviour however, is present in most, if not all, microscopic driver behaviour models. In fact, as stated in Section 2.5, OTS, the successor of MOTUS, even outperforms most, if not all, other microscopic vehicles simulation tools. Nevertheless, the fact that this sometimes happens during the simulation should be noted.

Furthermore, the traffic jams do originate at the merging area, whereas in real life the merging vehicles tend to accept smaller gaps when merging and then decelerate a couple hundred meters after the merging manoeuvre to obtaine the desired gap to the predecessor. Implementing this in OTS somehow could also improve the resemblance of the real life situation.

Moreover, drivers do not break the rules in this simulation tool. This means that there is no red running at the RMI, even though this was seen twice when filming the activated current RMI at the considered location, the A13 Delft-North on-ramp in the direction of Rotterdam. Additionally, there are no (major) speeding offences or drivers crossing the semi-permeable lane demarcation from the merging preventing side. Even though these offences might not occur to a high degree during peak hours, there will be drivers that do break the rules. Furthermore, a reaction time that is equal for all drivers is not likely. Adding a realistic distribution for the reaction time behind the active RMI and somehow some drivers breaking the traffic rules would improve the resemblance of the real life situation.

8.2.3 Simulation tool limitations

Apart from these points of improvement, there are limitations to the OTS simulation tool. This is not just the case for the average acceleration fraction for the acceleration manoeuvre.

First and foremost, the delay statistics computed by OTS did not provide the right picture regarding which alternative performs better. Thus, the travel time savings were computed by taking the area under the fractional cumulative curves of the various alternatives (see Section 3.5.2. This made sure the vertical waiting queue delays were taken into account in contrast to the OTS statistics. Additionally, by using the fractional cumulative curves as opposed to the regular cumulative curves, it was ensured that there was no unfair advantage allocated to the control alternative that had more vehicles being originated (and thus had more vehicles reaching their destination). Unfortunately, fluctuations in the arrival pattern during the simulation still remain and these are not resolved by using the fractional cumulative curves. Therefore, variations to the actual performance could still be found. Nevertheless,

computing the travel time savings by means of the fractional cumulative curves is regarded to be the better alternative compared to the computations of the regular cumulative curves and the delays computed by OTS.

Secondly, the off-ramp demand could not be set higher than 10% for the main lane vehicles, when the main lane demand reaches is equal to (or greater than) approximately 4500 vehicles per lane per hour. This disables using a realistic ratio of off-ramp vehicles compared to main lane vehicles, in turn limiting the on-ramp flow. This could interfere with the results of the RMIs, as can be seen in some late activation times. Therefore, the actual travel time savings might differ in a real life situation compared to the computed results. Moreover, investigating what would happen if the off-ramp demand increases was difficult in this research.

Finally, the vehicle distribution over the various lanes on the main road has not been investigated in detail. This distribution is important to investigate the number of gaps on the right lane. Empirically investigating some simulation runs led to the belief that not less than 30 to 35% of all main lane vehicles is at the right hand lane during the simulation, which is similar to the percentage of vehicles in the right hand lane for a regular three lane highway (Van Beinum, 2018). This means that the right hand lane on the main road in OTS does not seem to be underused, meaning the gaps measured on the right hand lane for the microscopic RMI are not overestimated, preventing an overestimation of the effectiveness of the microscopic RM approach. Nevertheless, investigating the lane distribution on the main road in more detail could provide valuable insights on the effectiveness of the microscopic RM control structures regarding the lane distribution.

8.2.4 Scope limitations

Due to the used research scope in terms of location, only a main road, controlled on-ramp and the first off-ramp upstream of the on-ramp have been considered. However, the network is larger in reality. In the larger real life network, traffic jams can spillback from downstream of the considered on-ramp to the on-ramp, hampering the movement of the gaps on the main lane, resulting in lower successful merger percentages. This is not simulated in this research.

Additionally, rat running by taking another on-ramp is also not possible in the conducted research. If the waiting times on the controlled on-ramp increase however, drivers might do this, limiting the effectiveness of the RM control approaches. This has not been taken into account.

Furthermore, due to research time limitations, a solution to combat traffic congestion originating as a result of deactivating an RMI has not been implemented in the algorithms. In order to prevent causing congestion in OTS by deactivating the RMIs, the RMIs are deactivated when the main lane is more or less empty already. This results in additional delays by the on-ramp vehicles in the alternatives with an activated RMI. In essence, regarding this assumption, the travel time savings as a result of using an activated RMI could be larger.

Finally, only a single lane on-ramp from at least the RMI location to the merging area has been considered. For multiple lanes on the on-ramp with multiple traffic lights, the microscopic RM control approach might not work as well if both traffic lights need to give green simultaneously, as is the case right now. Then, two gaps need to be measured. Changing one of these two lanes into a heavy truck lane only might increase the queue on the on-ramp lane for passenger vehicles drastically, limiting the activation time of the RMI. Hence, the conclusions provided in this research only apply to single lane on-ramp situations.

8.3 RECOMMENDATIONS

Following the concluding remarks on the results and the discussion, several recommendations in respect to scientists and policy makers are provided. Some of these recommendations are of a scientific nature, others are of policy nature. Firstly, the scientific recommendations for further research will be discussed. Thereafter, the recommendations for policy makers will be outlined.

8.3.1 Further research recommendations

The outcomes of this research are promising and there might still some room for improvement in the microscopic RM approach. First of all, researching if it is possible to measure the travelling speed of the measured gap on the main lane and then delaying the scheduled green phase for vehicles in front of the traffic light accordingly, might improve the successful merger percentage, improving the overall performance of the microscopic RM approach.

A similar reasoning applies to a method of being able to individually forecast the assumed acceleration of the waiting vehicle. This could be done, for example, by measuring the mass of the vehicle. Maybe the car could predict the probable acceleration characteristics of the driver. Additionally, somehow guiding the acceleration of the merging vehicles might be beneficial. This way, the successful merger percentage could be improved, improving the overall performance of the microscopic RM approach.

Furthermore, it could be worth investigating if the required minimum gaps for trucks and passenger vehicles are differentiated would improve the performance of the microscopic RM control approach. This might improve the situations with higher truck percentages, which is currently a weakness of the considered microscopic RMI alternatives.

Additionally, a measured gap time that is (at least) 1.5 times the size of a minimum required gap, but less than twice this gap, might be able to fit two merging vehicles, a small platoon if you will. If this is indeed the case and this would be added to the current control structure, this could lower the average red times between two vehicles, improving the average flow from the on-ramp vehicles onto the main lane. This might be worth exploring as well.

Another way to possibly decrease the average red time between two green phases might be implementing a dynamic required gap time in the algorithm. This means that in the beginning of the waiting period a larger gap is required in order to schedule a green phase for a waiting vehicle than later in the waiting period. It has been found in scientific research that vehicles accept smaller gap times when the waiting time increases. This finding combined with the percentage of vehicles that had to wait longer than 15 seconds led to this idea. Examining the effects of such a dynamic required gap time might be desirable.

Moreover, the effects of extending the semi-permeable lane demarcation to the beginning of the off-ramp should be investigated as well. This might lead to more gaps on the right hand lane, which could improve the microscopic RM approach. However, this can not be investigated in the current version of OTS. Nevertheless, it could be worth to be tested.

Finally, it was concluded that the Rijkswaterstaat algorithm works better with flows just higher than the activation flow. The microscopic RM control approach outperforms the currently used Rijkswaterstaat algorithm when the main lane flows increase above a certain value. Thus, combining these control structures might result in maximal travel time savings for the entire system. For example, the Rijkswaterstaat algorithm is used when the flow is between 1500 and 1867 vehicles per lane per hour, which yields a red time between two green phases of 2.4 seconds and 9.0 seconds for the Rijkswaterstaat algorithm, and the microscopic RM control approach (with a required minimum gap time of 1.8 seconds for example) when the

flow exceeds this 1867 vehicles per lane per hour. Researching the effects on traffic with a combination of the two control strategies is highly recommended.

8.3.2 Policy recommendations

Two policy changes are highly recommended. For instance, it was found that all alternatives benefit from implementing the semi-permeable lane demarcation that prevents mergers from the middle lane on the main road to the right lane. Since a similar lane demarcation is already present at different sites in the Netherlands and this is a low cost means, implementing this semi-permeable lane demarcation is highly recommended.

Furthermore, it has been concluded that the microscopic RM control approach can outperform the currently used Rijkswaterstaat algorithm. This is especially the case when the off-ramp and on-ramp flows are sufficient, which is true for the A13 Delft-North on-ramp in the direction of Rotterdam. Additionally, this is true when the main lane demand is high, resulting in the larger red times between two green phases in the currently used macroscopic Rijkswaterstaat algorithm. When the red times between two green phases are larger than 10 seconds, the microscopic RM control approach works better than the Rijkswaterstaat algorithm regarding the average travel time savings per vehicle for the entire system. Moreover, the microscopic RM control approach only needs an adjusted algorithm and some additional loop detectors. This is not very expensive and therefore it is certainly recommended to take further actions. The policy makers are advised to invest in exploring the effects of a combined macroscopic and microscopic control algorithm, as proposed in the final paragraph of the previous sub-section, since this could limit congestion and its duration, resulting in less social costs.

BIBLIOGRAPHY

Ahn, S., Laval, J., and Cassidy, M. J. (2010). Effects of merging and diverging on freeway traffic oscillations theory and observation. *Transportation Research Record*, 2188:1–8.

AIMSUN (2020). Your personal mobility modeling lab. Available at https://www.aimsun.com/aimsun-next/ (2020/01/17).

Anaconda (2020). Solutions for data science practitioners and enterprise machine learning. Available at https://www.anaconda.com/ (2020/01/13).

ANWB (2018). Anwb: 20 procent meer files op nederlandse wegen. Available at https://www.anwb.nl/verkeer/nieuws/nederland/2018/december/anwb-20-procent-meer-files-op-nederlandse-wegen (2019/06/17).

Barth, M. and Boriboonsomsin, K. (2009). Traffic congestion and greenhouse gases. *Access magazine*, 1.

Bergan, T. and Bushman, R. (2004). Variable speed limit system. US Patent 6,825,778.

Bertini, R. L., Boice, S., and Bogenberger, K. (2006). Dynamics of variable speed limit system surrounding bottleneck on german autobahn. *Transportation Research Record*, 1978(1):149–159.

Bonsall, P. W. and Joint, M. (1991). Driver compliance with route guidance advice: the evidence and its implications. In *Vehicle Navigation and Information Systems Conference, 1991*, volume 2, pages 47–59. IEEE.

Boyce, C. and Neale, P. (2006). *Conducting in-depth interviews: A guide for designing and conducting in-depth interviews for evaluation input*. Pathfinder International Watertown, MA.

Brackstone, M. and McDonald, M. (2007). Driver headway: How close is too close on a motorway? *Ergonomics*, 50(8):1183–1195.

BWM (n.d.). Kies uw bmw. Available at https://www.bmw.nl/nl/modellen.html (2020/01/16).

Calthrop, E. and Proost, S. (1998). Road transport externalities. *Environmental and Resource Economics*, 11:335–348.

Cameron, G., Wylie, B. J., and McArthur, D. (1994). Paramics: moving vehicles on the connection machine. In *Proceedings of the 1994 ACM/IEEE Conference on Supercomputing*, pages 291–300. IEEE Computer Society Press.

CBS (2019). Aantal wegvoertuigen blijft stijgen. Available at https://www.cbs.nl/nl-nl/nieuws/2019/14/aantal-wegvoertuigen-blijft-stijgen (2019/08/28).

Chaudhary, N. A. and Messer, C. J. (2000). *Ramp-metering technology and practice: Tasks 1 and 2 Summary*, volume 2121. Citeseer.

Chen, C., Li, L., Hu, J., and Geng, C. (2010). Calibration of mitsim and idm car-following model based on ngsim trajectory datasets. In *Proceedings of 2010 IEEE International Conference on Vehicular Electronics and Safety*, pages 48–53. IEEE.

Chin, H. C. and Quek, S. T. (1991). Traffic conflicts in expressway merging. *Journal of Transportation Engineering*, 117:633–643.

Chou, C.-S. and Nichols, A. P. (2014). Deriving a surrogate safety measure for freeway incidents based on predicted end-of-queue properties. *IET intelligent transport systems*, 9(1):22–29.

Daganzo, C. F. (2002). A behavioral theory of multi-lane traffic flow. part i: Long homogeneous freeway sections. *Transportation Research Part B: Methodological*, 36(2):131–158.

Daganzo, C. F., Lin, W.-H., and Del Castillo, J. M. (1997). A simple physical principle for the simulation of freeways with special lanes and priority vehicles. *Transportation Research Part B: Methodological*, 31(2):103–125.

Darbha, S., Konduri, S., and Pagilla, P. R. (2018). Benefits of v2v communication for autonomous and connected vehicles. *IEEE Transactions on Intelligent Transportation Systems*, 20(5):1954–1963.

Dexter (n.d.). Data exploration and exporter. Available at https://dexter.ndwcloud.nu/ (2020/01/20).

Dijkstra, A. (2011). *En route to safer roads: how road structure and road classification can affect road safety. Proefschrift Universiteit Twente, Enschede.* Leidschendam, Stichting Wetenschappelijk Onderzoek Verkeersveiligheid.

Eliasson, J. and Mattsson, L.-G. (2006). Equity effects of congestion pricing: Quantitative methodology and a case study for stockholm. *Transportation Research Part A: Policy and Practice*, 40:602–620.

Elipse (n.d.). The platform for open innovation and collaboration. Available at https://www.eclipse.org/ (2020/03/04).

FFmpeg (n.d.). A complete, cross-platform solution to record, convert and stream audio and video. Available at https://www.ffmpeg.org/ (2019/11/15).

Fitzpatrick, K. and Zimmerman, K. (2007). Potential updates to 2004 green book's acceleration lengths for entrance terminals. *Transportation Research Record*, 2023(1):130–139.

GIMP (2019). The free & open source image editor. Available at https://www.gimp.org/ (2019/11/18).

Giuliano, G. (1992). An assessment of the political acceptability of congestion pricing. *Transportation*, 19:335–358.

Goodwin, P. (2004). The economic costs of road traffic congestion.

Google (2020a). A20 near off-ramp crooswijk, rotterdam. Available at https://www.google.nl/maps/@51.940308,4.4696246,3a,75y,66.73h,62.74t/data=!3m6!1e1!3m4!1spzjg3opbbEKCoofHYQpR2w!2e0!7i16384!8i8192(2020/03/06).

Google (2020b). Maps. Available at https://www.google.nl/maps (2020/03/15).

Google (2020c). Sint jorispad, delft. Available at https://www.google.com/maps/@52.0260683,4.3608774,122m/data=!3m1!1e3 (2020/03/05).

Group, P. (2020). Vooruitdenken en zorgen door de mobiliteit van morgen. Available at https://www.ptvgroup.com/nl/innovatie-en-onderzoek/ (2020/01/17).

Guangchuan, Y., Zong, T., Hao, X., and Zhongren, W. (2016). Recommendations for acceleration lane length for metered on-ramps. *Transportation Research Record*, 2588(1):1–11.

Halati, A., Lieu, H., and Walker, S. (1997). Corsim-corridor traffic simulation model. In *Traffic Congestion and Traffic Safety in the 21st Century: Challenges, Innovations, and OpportunitiesUrban Transportation Division, ASCE; Highway Division, ASCE; Federal Highway Administration, USDOT; and National Highway Traffic Safety Administration, USDOT.*

Hellinga, B. and Mandelzys, M. (2011). Impact of driver compliance on the safety and operational impacts of freeway variable speed limit systems. *Journal of Transportation Engineering*, 137(4):260–268.

Hidas, P. (2005). A functional evaluation of the aimsun, paramics and vissim microsimulation models. *Road & Transport Research*, 14(4):45.

Honda (n.d.). Vraag een brochure aan. Available at https://www.honda.nl/cars/get-a-brochure/choose-brochure.html (2020/01/16).

Hoogendoorn, S. P. (1997). Optimal control of dynamic route information panels. *IFAC Proceedings Volumes*, 30(8):399–404.

IBM (2020). Ibm spss statistics. Available at https://www.ibm.com/nl-en/products/spss-statistics (2020/01/14).

Java (n.d.). Java powers our digital world. Available at https://go.java/?intcmp=gojava-banner-java-com (2020/03/04).

Jupyter (2020). Installing the jupyter software. Available at https://jupyter.org/install (2020/01/13).

Kang, K.-P., Chang, G.-L., and Zou, N. (2004). Optimal dynamic speed-limit control for highway work zone operations. *Transportation research record*, 1877(1):77–84.

Knoop, V., Hegyi, A., and Salomons, M. (2018). *Traffic Flow Modelling and Control (course material)*. Delft University of Technology, Delft, the Netherlands, 1 edition.

Kohler, W. J. and Colbert-Taylor, A. (2014). Current law and potential legal issues pertaining to automated, autonomous and connected vehicles. *Santa Clara Computer & High Tech. LJ*, 31:99.

Kotsialos, A., Papageorgiou, M., and Middelham, F. (2001). Optimal coordinated ramp metering with advanced motorway optimal control. *Transportation Research Record*, 1748(1):55–65.

Levy, J., Buonocore, J., and Von Stackelberg, K. (2010). Evaluation of the public health impacts of traffic congestion: a health risk assessment. *Environmental Health*, 9.

MathWorks (2020). Math. graphics. programming. Available at https://nl.mathworks.com/products/matlab.html (2019/11/15).

Microsoft (2020). Excel. Available at https://products.office.com/en-us/excel (2020/02/11).

Middelham, F. and Taale, H. (2006). Ramp metering in the netherlands: An overview. *IFAC Proceedings Volumes*, 39:267–272.

Neuman, W. (2014). *Social Research Methods: Qualitative and Quantitative Approaches*. Pearson Education Limited.

NOACA (2016). Ramp metering: Benefits, opportunities and key issues. Available at https://www.noaca.org/home/showdocument?id=15398 (2020/03/04).

NOS (2019a). Ns wil al jaren een minder drukke ochtendspits, waarom gaat dat zo moeilijk? Available at https://nos.nl/artikel/2300256-ns-wil-al-jaren-een-minder-drukke-ochtendspits-waarom-gaat-dat-zo-moeilijk.html (2019/09/04).

NOS (2019b). Veel meer treinreizigers dan verwacht, spoor in 2027 zo goed als vol. Available at https://nos.nl/artikel/2297754-veel-meer-treinreizigers-dan-verwacht-spoor-in-2027-zo-goed-als-vol.html (2019/09/03).

NOS (2020a). Op welke snelweg je ook rijdt: vanaf nu overal 100 kilometer per uur. Available at https://nos.nl/artikel/2327233-op-welke-snelweg-je-ook-rijdt-vanaf-nu-overal-100-kilometer-per-uur.html (2020/03/16).

NOS (2020b). Waarom je met een sluiproute geen meter opschiet. Available at https://www.youtube.com/watch?v=WZjXv6zeWUo (2020/03/04).

Panteia (2019). Fileschade vrachtverkeer stijgt naar 1,4 miljard euro. Available at https://www.panteia.nl/nieuws/fileschade-vrachtverkeer-stijgt-naar-1-4-miljard/ (2020/02/27).

Papageorgiou, M., Hadj-Salem, H., Blosseville, J.-M., et al. (1991). Alinea: A local feedback control law for on-ramp metering. *Transportation Research Record*, 1320(1):58–67.

Papageorgiou, M. and Kotsialos, A. (2002). Freeway ramp metering: An overview. *IEEE TRANSACTIONS ON INTELLIGENT TRANSPORTATION SYSTEMS*, 3:271–281.

Papgeorgiou, M. and Messmer, A. (1991). Dynamic network traffic assignment and route guidance via feedback regulation. *Transportation Research Record*, 1306:49–58.

Parkinson, S., Ward, P., Wilson, K., and Miller, J. (2017). Cyber threats facing autonomous and connected vehicles: Future challenges. *IEEE transactions on intelligent transportation systems*, 18(11):2898–2915.

Persaud, B., Yagar, S., Tsui, D., and Look, H. (2001). Breakdown-related capacity for freeway with ramp metering. *Transportation Research Record*, 1748:110–115.

Python (2020). Python is a programming language that lets you work quickly and integrate systems more effectively. Available at https://www.python.org/ (2019/12/24).

Rakha, H., Lucic, I., Demarchi, S. H., Setti, J. R., and Aerde, M. V. (2001). Vehicle dynamics model for predicting maximum truck acceleration levels. *Journal of transportation engineering*, 127(5):418–425.

Rijkswaterstaat (2013). *Verkeerstechnische specificatie van een applicatieprogramma voor toeritdosering*. Number 1.09. Rijkswaterstaat.

Rijkswaterstaat (2018). *Handleiding voorbereiding en uitvoering toeritdoseerinstallatie v1.40*. Rijkswaterstaat: Ministerie van Infrastructuur en Waterstaat.

Rijkswaterstaat (2019). *Periodieke monitoring TDI 708004 02-09-2019 t/m 20-09-2019*. Ministerie van Infrastrcutuur en Milieu, Rhoon, the Netherlands, 1 edition.

Rijkswaterstaat (n.d.). Treinen. Available at https://rwsduurzamemobiliteit.nl/praktijk-projecten/openbaar-vervoer/treinen/ (2019/09/03).

Schakel, W. J. (2015). *Development, simulation and evaluation of in-car advice on headway, speed and lane*. Technical University Delft, Delft.

Schefer, D. and Rietveld, P. (1997). Congestion and safety on highways: Towards an analytical model. *Urban Studies*, 34:679–692.

SPSS (n.d.). Spss kolmogorov-smirnov test for normality. Available at https://www.spss-tutorials.com/spss-kolmogorov-smirnov-test-for-normality/ (2020/01/14).

SublimeText (n.d.). A sophisticated text editor for code, markup and prose. Available at https://www.sublimetext.com/ (2019/12/24).

Sun, D. and Elefteriadou, L. (2010). Research and implementation of lane-changing model based on driver behavior. *Transportation Research Record*, 2161(1):1–10.

Sun, D. J. and Kondyli, A. (2010). Modeling vehicle interactions during lane-changing behavior on arterial streets. *Computer-Aided Civil and Infrastructure Engineering*, 25(8):557–571.

Talebpour, A. and Mahmassani, H. S. (2015). Influence of autonomous and connected vehicles on stability of traffic flow. Technical report.

Theofilatos, A. and Yannis, G. (2014). A review of the effect of traffic and weather characteristics on road safety. *Accident Analysis & Prevention*, 72:244–256.

Van Beinum, A. (2018). Turbulence in traffic at motorway ramps and its impact on traffic operations and safety.

Van der Berg, F. (2017). Alleen vvd wil meer asfalt tegen files. Available at https://m.leidschdagblad.nl/cnt/dmf20180926_28972387/alleen-vvd-wil-meer-asfalt-tegen-files?utm_source=google&utm_medium=organic (2019/09/02).

Van Lint, H., Calvert, S., Schakel, W., Wang, M., and Verbraeck, A. (2017). Exploring the effects of perception errors and anticipation strategies on traffic accidents-a simulation study. In *International Conference on Applied Human Factors and Ergonomics*, pages 249–261. Springer.

Van Lint, H., Verbraeck, A., Knoppers, P., Schakel, W., Tamminga, G., and Yuan, Y. (2020). The opentrafficsim project. Available at https://opentrafficsim.org/old/index.php (2020/01/17).

Vereniging Zakelijke Rijders (2017). Politieke partijen versus rekeningrijden. Available at https://www.vzr.nl/nieuws/details/politieke_partijen_versus_rekeningrijden (2019/09/03).

Wattleworth, J. A. (1965). Peak-period analysis and control of a freeway system. Technical report, Texas Transportation Institute.

Wu, N. (2002). A new approach for modeling of fundamental diagrams. *Transportation Research Part A*, 36:867—884.

Yang, G., Xu, H., Wang, Z., and Tian, Z. (2016a). Truck acceleration behavior study and acceleration lane length recommendations for metered on-ramps. *International Journal of Transportation Science and Technology*, 5:93–102.

Yang, G., Xu, H., Wang, Z., and Tian, Z. (2016b). Truck acceleration behavior study and acceleration lane length recommendations for metered on-ramps. *International journal of transportation science and technology*, 5(2):93–102.

Yang, H. and Ozbay, K. (2011). Estimation of traffic conflict risk for merging vehicles on highway merge section. *Transportation Research Record*, 2236:58–65.

Yau, K. K. (2004). Risk factors affecting the severity of single vehicle traffic accidents in hong kong. *Accident Analysis & Prevention*, 36:333–340.

Young, W., Sobhani, A., Lenné, M. G., and Sarvi, M. (2014). Simulation of safety: A review of the state of the art in road safety simulation modelling. *Accident Analysis & Prevention*, 66:89–103.

Yuan, K., Knoop, V. L., Leclercq, L., and Hoogendoorn, S. P. (2017). Capacity drop: a comparison between stop-and-go wave and standing queue at lane-drop bottleneck. *Transportmetrica B: transport dynamics*, 5(2):145–158.

Zhang, H. M. and Ritchie, S. G. (1997). Freeway ramp metering using artificial neural networks. *Transportation Research Part C: Emerging Technologies*, 5:273–286.

A VARIABLES EXPLANATION

In this appendix all variables that are present in either the main report of the appendices are summarised.

Variable	Units	Short Description
A	m^2	The area of the object that encounters the air resistance
a	$\frac{m}{s^2}$	Acceleration
a_{av}	unitless	Acceleration fraction, indicating the average acceleration for the acceleration distance
a_{max}	$\frac{m}{s^2}$	The maximum acceleration of the merging vehicle
a_{max}	$\frac{m}{s^2}$	The maximum acceleration
a_t^{eff}	$\frac{m}{s^2}$	The effective acceleration at time t
a_t^f	$\frac{m}{s^2}$	Calculated acceleration as a results of the applied force at time t
C_d	unitless	The drag coefficient
$\Delta \frac{X_i^m}{X_i^f}$	unitless	The linear increase of X in meters over X in frames between data points i and $i-1$
dt	s	The chosen time-step
$d\tau$	minutes	The chosen time-step
DTT_{system}	s	Total travel time delay for the entire system
DTT_i	s	Total travel time delay for route i
DTT_i^n	s	Average travel time delay per vehicle for route i
f_{des}	unitless	Fraction of the speed on the main lane that is deemed desired when merging
F	N	Force
F_a	N	The acceleration force
F_e	N	The force produced by the engine
F_{eff}	N	The effective force
F_{res}	N	The total resistance force
F_p	N	The delivered force
F_t^a	N	The acceleration force at time t
F_t^e	N	The force delivered by the engine of the vehicle at time t
F_t^r	N	Force due to the air resistance (or drag) that applies to the vehicle at time t
F_τ^k	unitless	The fraction of vehicles that have reached their destination at time τ for control strategy k
$FTTD_{[0,130]}^{k,l}$	$\frac{minutes}{vehicle}$	Fractional travel time difference between control strategies k and l for the entire simulation
FTT_i	s	Free flow travel time for route i
I	unitless	Set of origin to destination routes that can be travelled
m	kg	The mass of the vehicle
MSE_n	m^2	Mean squared error for vehicle n
N_{130}^k	#	Number of cumulative vehicles that have passed at simulation end for control strategy k
N_i	#	Total number of vehicles that have travelled route i
N_τ	#	Number of cumulative vehicles that have passed at time τ
$N_{\tau+1}$	#	Number of cumulative vehicles that have passed at time $\tau+1$
$N_\tau^{\text{Cumulative}}$	#	Cumulative number of vehicles that have reached the specific point at time τ
N_τ^k	#	Number of cumulative vehicles that have passed at time τ for control strategy k

Variable	Units	Short Description
P	Watt	Power
P_{eff}	unitless	Effective usable power for the car. This is equal to one minus the resistance of the wheels
P_{horse}	Watt	Horse power of a car at top speed
P^{used}	Watt	The used power by the driver
ϕ	$\frac{kg}{m}$	The combined air resistance components that applies to the vehicle, without the speed
q_o	$\frac{Vehicles}{minute}$	Offset flow
ρ	$\frac{kg}{m^3}$	The density of the air
s	m	Distance
s_i	m	Distance between origin and destination for route i
s_{eff}	m	The effective acceleration distance of the merging vehicle
s_{main}	m	The travelled distance on the main road of the desired merging point
s_{max}	m	The maximum distance that can be used to accelerate to the desired speed
s_{merg}	m	The acceleration distance of the merging vehicle following the desired merging speed
s_{min}	m	The minimum acceleration distance of the merging vehicle
t	s	Time value
$t+1$	s	Time value
t_{acc}	s	The acceleration time of the merging vehicle
t_{eff}	s	The effective time the measured desired merging point will travel on the main road
t_{gap}	s	The gap time necessary before the traffic light is set to green
t_{lead}	s	Desired time headway for the merging vehicle to the measured gap leading vehicle
τ	minutes	Time value
$\tau+1$	minutes	Time value
T_i^f	frames	The time at data point i
T_i^s	s	The time at data point i
T_n	unitless	Set of time steps in seconds for an individual vehicle n
$TTD^{k,l}_{[0,130]}$	minutes	Total travel time difference between control strategies k and l for the entire simulation
TTT_i	s	Total measured travel time for route i
TTT_i^{n}	s	Total measured travel time for route i for vehicle n
v	$\frac{m}{s}$	Speed
v_{des}	$\frac{m}{s}$	Desired speed for the merging vehicle when merging onto the main road
v_i^{max}	$\frac{m}{s}$	Maximum speed between for route i
v_{main}	$\frac{m}{s}$	The speed on the main lane
v_{merg}	$\frac{m}{s}$	The actual speed of the merging vehicle when performing the merging manoeuvre
v_{top}	$\frac{m}{s}$	Top speed of a vehicle
v_t	$\frac{m}{s}$	The speed of the vehicle at time t
v_{t+1}	$\frac{m}{s}$	The speed of the vehicle at time $t+1$
V_c	$\frac{m}{s}$	The constant speed of the 'controlled' vehicle
x_{loop}	m	The longitudinal distance the loop detector should be placed upstream of the RMI
x_t	m	The location of the vehicle at time t
x_{t+1}	m	The location of the vehicle at time $t+1$
$x_{t,n}^{calc}$	m	The computed position of vehicle n at time t
$x_{t,n}^{obs}$	m	The measured position of vehicle n at time t
$X_i^{'f}$	pixels	The inverse distance (from low to high) at data point i
X_i^f	pixels	The distance (from high to low) at data point i
X_i^m	m	The distance at data point i
y^{truck}	s	The acceleration time of the truck until the predicted merging point for the passenger car
z^{truck}	$\frac{m}{s}$	The speed of the truck when it reaches the predicted merging point for the passenger car

Variable	Units	Short Description
Activation	s	The time in the simulation when the RMI is activated
AvDMain	$\frac{s}{vehicle}$	Average computed delay for the main road flow (A to D)
AvDOff	$\frac{s}{vehicle}$	Average computed delay for the off-ramp flow (A to B)
AvDOn	$\frac{s}{vehicle}$	Average computed delay for the on-ramp flow (C to D)
AvDSys	$\frac{s}{vehicle}$	Average computed delay compared to free flow conditions for the entire system
Deactivation	s	The time in the simulation when the RMI is deactivated
GotGreen	#	Number of controlled on-ramp vehicles that received a green traffic light
Success	%	Percentage of the controlled on-ramp vehicles that merged in the measured gap
WaitLong	%	Percentage of controlled on-ramp vehicles that had to wait longer than 15 seconds while being first in line

B DETAILED ACCELERATION MATHEMATICS

In this appendix all mathematical steps to get to the computation of the position and speed for every time step of an individual vehicle are outlined. An overview of all used variables, their units and a short description regarding these variables can be found in Appendix A.

Power equals force times the speed.

$$P = Fv \tag{B.1}$$

Moreover, the force is equal to the acceleration times the mass of an object.

$$F = ma \tag{B.2}$$

Additionally, the produced power at top speed can be calculated by multiplying the effective power at top speed with the horse power of the vehicle at top speed. Then, this outcome is divided by the top speed, resulting in the produced power. The effective power of a vehicle at top speed is normally equal to 0.9. This is due to the fact that the wheel resistance is approximately 10% at top speed for vehicles.

$$P = \frac{P_{\text{eff}} P_{\text{horse}}}{v_{\text{top}}} \tag{B.3}$$

The force that can be used for the acceleration of a vehicle is the force produced by the engine minus the force that is 'wasted' with the resistance.

$$F_a = F_e - F_{\text{res}} \tag{B.4}$$

In other words, the effective force for the acceleration of the vehicle is equal to the powered force minus the resistance force.

$$F_{\text{eff}} = F_p - F_{\text{res}} \tag{B.5}$$

The resistance force that applies to the vehicle at time t can be calculated by the formula for calculating the air resistance (or drag).

$$F_t^r = \frac{1}{2} C_d \rho A v_t^2 \tag{B.6}$$

In order to make the calculations a bit more clear, a new variable is introduced. This variable stands for the combined air resistance components that applies to the vehicle, without the speed.

$$\phi = \frac{1}{2} C_d \rho A \tag{B.7}$$

With this component, the resistance force that applies to the vehicle at time t can be calculated. Namely, this force is equal to the air resistance component times the squared speed at time t.

$$F_t^r = \phi v_t^2 \tag{B.8}$$

The force delivered by the engine at time t can be calculated by dividing a used power value by the speed at time t. The used power is kept the same for the entire acceleration distance. For every vehicle trajectory, this used power is fitted by means of the least square method as explained in Section 3.4.

$$F_t^e = \frac{P^{\text{used}}}{v_t} \tag{B.9}$$

Knowing both the resistance force at time t and the force delivered by the engine, the force that remains for the acceleration at time t can be computed. This is done by subtracting the resistance force at time t from the force delivered by the engine at time t.

$$F_t^a = F_t^e - F_t^r \tag{B.10}$$

Combining this equation with Equation B.2 enables the calculation of the acceleration of the vehicle at time t. Namely, this is equal to the acceleration force at time t divided by the mass of the vehicle. The mass of the vehicle is kept constant for the entirety of the acceleration trajectory.

$$a_t^f = \frac{F_t^a}{m} \tag{B.11}$$

However, the computed acceleration is not supposed to be higher than a certain maximum accepted acceleration by the driver. Therefore, an effective acceleration at time t is introduced. This effective acceleration is equal to the minimum of the calculated acceleration at time t and a maximum acceleration. This maximum acceleration is fitted for every individual vehicle. For the individual vehicles, this maximum acceleration is kept constant for the entire trajectory.

$$a_t^{eff} = \min\left(a_t^f, a_{\max}\right) \tag{B.12}$$

All this leads to the final to equation which calculate the speed at time $t+1$ and the position of the vehicle at time $t+1$. The speed can be calculated by adding the speed of the current time step (t) to the calculated effective acceleration at time t. This effective acceleration is equal to the calculated effective acceleration at time t times the time step.

$$v_{t+1} = v_t + a_t^{eff} dt \tag{B.13}$$

When the speeds at t and $t+1$ are known, the position of the vehicle at $t+1$ can be determined. This position is equal to the position at time t added to the average speed between t and $t+1$ times the time step.

$$x_{t+1} = x_t + \frac{v_t + v_{t+1}}{2} dt \tag{B.14}$$

These formulae and variables are used to fit the individual used power and maximum acceleration for the various observed vehicles.

C DETAILED CUMULATIVE CURVES MATHEMATICS

In this appendix all mathematical steps to get to the mathematically computed travel time savings by means of the cumulative curves are outlined. An overview of all used variables, their units and a short description regarding these variables can be found in Appendix A.

As stated in Section 3.5.2, a linear increase is assumed between two adjacent data points. A formula describing such a linear increase is shown in Equation C.1.

$$f(\tau) : N = u\tau + b \tag{C.1}$$

As stated in Section 3.5.2, the area under the graphs needs to be calculated. This can be done by taking the integral of the original formula. For a linear equation, this integral reads:

$$\int f(\tau)d\tau = \frac{1}{2}u\tau^2 + b\tau \tag{C.2}$$

The linear increase per time interval can be calculated by dividing the vertical increase by the horizontal increase.

$$u = \frac{\Delta y}{\Delta \tau} \tag{C.3}$$

Then, the starting point (b-value) of Equation C.1 can be calculated by subtracting the linear increase from zero until a considered specific point on the line from the vertical value of the same specific point on the linear line.

$$b = y - u\tau \tag{C.4}$$

So, two measured data points on the line have to be known. Two adjacent points (with a separation of one minute) are taken. These points will be called K and L.

$$K\Big(\tau, N_\tau\Big) \wedge L\Big(\tau + 1, N_{\tau+1}\Big) \tag{C.5}$$

The linear increase on the time interval of these two data points can be characterised as follows:

$$f(\tau)_{[\tau,\tau+1]} : y = u\tau + b \tag{C.6}$$

In this equation, the value for u can be determined by dividing the difference in the total number of vehicles that have passed between points L and K by the time difference between points L and K.

$$u = \frac{N_{\tau+1} - N_\tau}{\tau + 1 - \tau} \tag{C.7}$$

Since the difference in time between two adjacent points is always equal to one in these calculations, the value of u can be reduced to the difference in number of vehicles passed between L and K.

$$u = N_{\tau+1} - N_\tau \tag{C.8}$$

With the known linear increase value, the starting point of the linear formula (b-value) can be computed. This can be done for point K and for point L. It leads to effectively the same formula, but the corresponding b-value are calculated for both points, since this enables reducing the calculations later on. In Equation C.9 the left hand side shows the b-value for point K and the right hand side shows the b-value for point L.

$$b = N_\tau - (N_{\tau+1} - N_\tau)\tau \vee b = N_{\tau+1} - (N_{\tau+1} - N_\tau)(\tau + 1) \tag{C.9}$$

Now that the values for u and b for points K and L are known, Equation C.2 can be used to calculated the area under the graph between L and K. This area is equal to the difference in the area underneath the start of the linear equation ($\tau = 0$) to L and the start of the linear equation to K.

$$\int_\tau^{\tau+1} f(\tau)d\tau = \left[\frac{1}{2}u\tau^2 + b\tau\right]_\tau^{\tau+1} = \left[\frac{1}{2}u\tau^2 + b\tau\right]_0^{\tau+1} - \left[\frac{1}{2}u\tau^2 + b\tau\right]_0^{\tau} \tag{C.10}$$

Firstly, the area under the graph between the start of the linear equation ($\tau = 0$) to L will be calculated. This is equal to the equation with the values of point L minus the equation with the values of point $\tau = 0$. The value that results of filling in the latter data point results in 0. Therefore, this is left out. This leads to the area under the graph from $\tau = 0$ to L calculation.

$$\left[\frac{1}{2}u\tau^2 + b\tau\right]_0^{\tau+1} = \frac{N_{\tau+1} - N_\tau}{2}(\tau + 1)^2 + \Big(N_{\tau+1} - (N_{\tau+1} - N_\tau)(\tau + 1)\Big)(\tau + 1) \tag{C.11}$$

This can be simplified to:

$$\left[\frac{1}{2}u\tau^2 + b\tau\right]_0^{\tau+1} = N_{\tau+1}(\tau + 1) - \frac{N_{\tau+1} - N_\tau}{2}(\tau + 1)^2 \tag{C.12}$$

The area under the graph between $\tau = 0$ and point K can be calculated in a similar fashion.

$$\left[\frac{1}{2}u\tau^2 + b\tau\right]_0^{\tau} = \frac{N_{\tau+1} - N_\tau}{2}(\tau)^2 + \Big(N_\tau - (N_{\tau+1} - N_\tau)(\tau)\Big)(\tau) \tag{C.13}$$

This can be simplified too.

$$\left[\frac{1}{2}u\tau^2 + b\tau\right]_0^{\tau} = N_\tau\tau - \frac{N_{\tau+1} - N_\tau}{2}\tau^2 \tag{C.14}$$

Subtracting Equation C.14 from Equation C.12 results in the area under the line between points L and K. This can be reduced to the following equation:

$$\int_\tau^{\tau+1} f(\tau)d\tau = N_{\tau+1}(\tau + 1) - N_\tau\tau + \frac{N_{\tau+1} - N_\tau}{2}\Big(\tau^2 - (\tau + 1)^2\Big) \tag{C.15}$$

Then, the area under the graph for the entire simulation can be calculating by taking the sum over the areas under the graphs of all adjacent points in this interval.

$$\int_0^{130} f(\tau)d\tau = \sum_0^{130} \int_\tau^{\tau+1} f(\tau)d\tau \tag{C.16}$$

Similarly, the difference in the computed travel times between two control alternatives can be computed by subtracting the area under the graph of control strategy l for the entire simulation from the area under the graph of control strategy k for the entire simulation.

$$TTD^{k,l}_{[0,130]} = \int_0^{130} f_k(\tau)d\tau - \int_0^{130} f_l(\tau)d\tau \tag{C.17}$$

In order to adjust for the variation between the total number of vehicles that originate (and reach their destination) between the different control strategies as a result of randomness in the simulation, the fractional cumulative vehicle values can be used instead of the total number of cumulative vehicles. The fraction of cumulative vehicles that have reached their destination at time τ can be calculated as follows:

$$F_{\tau}^{k} = \frac{N_{\tau}^{k}}{N_{130}^{k}} \tag{C.18}$$

Replacing the actual cumulative vehicles in Equation C.15 with the fractional number of cumulative vehicles (see Equation C.18) leads to the equation that determines the area under a graph for the fractional cumulative curves.

$$\int_{\tau}^{\tau+1} g(\tau)d\tau = F_{\tau+1}(\tau+1) - F_{\tau}\tau + \frac{F_{\tau+1} - F_{\tau}}{2}\left(\tau^2 - (\tau+1)^2\right) \tag{C.19}$$

This in turn can be used to calculate the difference in the average travel travel time between control strategy l for the entire simulation and control strategy k for the entire simulation.

$$FTTD_{[0,130]}^{k,l} = \int_{0}^{130} g_k(\tau)d\tau - \int_{0}^{130} g_l(\tau)d\tau \tag{C.20}$$

D DETAILED GAP MEASUREMENT DETECTOR LOCATION MATHEMATICS

In this appendix all mathematical steps to determine the gap measurement loop detectors are outlined. Additionally, the calculations for determining the minimum waiting time for a passenger vehicle succeeding a truck at the RMI is repeated in this appendix. An overview of all used variables, their units and a short description regarding these variables can be found in Appendix A.

The travelled distance can be calculated multiplying a constant acceleration with the squared time divided by two.

$$s = \frac{1}{2}at^2 \tag{D.1}$$

Moreover, the speed can be calculated by multiplying a constant acceleration with time.

$$v = at \tag{D.2}$$

Additionally, the travelled distance can be calculated by multiplying a constant speed with the time

$$s = vt \tag{D.3}$$

Combining Equation D.1 with Equation D.2, it is found that the travelled distance can be computed by dividing the squared constant speed by two times a constant acceleration.

$$s = \frac{v^2}{2a} \tag{D.4}$$

Therefore, a constant speed can be calculated by taking the square root of two times the travelled distance times a constant acceleration

$$v = \sqrt{2sa} \tag{D.5}$$

The desired merging speed for the on-ramp vehicles can be calculated by multiplying the speed of the main lane vehicles with a fraction indicating the relative desired merging speed.

$$v_{\text{des}} = f_{\text{des}} * v_{\text{main}} \tag{D.6}$$

The acceleration distance as a result of this desired merging speed can now be calculated. This acceleration distance is equal to the squared desired merging speed divided by two times acceleration over the entire acceleration distance. This acceleration in turn is equal to the maximum acceleration (i.e. the acceleration in the beginning of the acceleration trajectory) times a fraction indicating the average acceleration over the entire acceleration distance.

$$s_{\text{merg}} = \frac{v_{\text{des}}^2}{2 * a_{\text{max}} * a_{\text{av}}} \tag{D.7}$$

However, the merging vehicles can not have an acceleration distance that exceeds the distance of the traffic light to the end of the merging area with the main lane. Moreover, there is a minimum acceleration distance. This minimum acceleration distance is equal to the distance between the traffic light of the RMI and the start of the merging area with the main lane. Thus, the effective acceleration distance is equal to the calculated acceleration distance, or the minimum or the maximum acceleration distance, depending on which constraint is violated with the computed acceleration distance.

$$s_{\text{eff}} = \min\Big(s_{\text{merg}}, s_{\text{max}}\Big) \wedge \max\Big(s_{\text{merg}}, s_{\text{min}}\Big) \tag{D.8}$$

With this actual (or effective) merging distance in mind, the speed of the merging vehicle when performing the merging manoeuvre can be determined. This is equal to the square root of the two times the effective merging distance times the actual acceleration of the merging vehicle for the acceleration trajectory.

$$v_{\text{merg}} = \sqrt{2 * s_{\text{eff}} * a_{\text{max}} * a_{\text{av}}} \tag{D.9}$$

Then, the time it takes for the merging vehicle from the moment it starts to accelerate to the point of merging can be computed. This is equal to the merging distance divided by the average speed of the acceleration trajectory. This average speed is equal to half the actual merging speed, assuming a constant acceleration.

$$t_{\text{acc}} = \frac{s_{\text{eff}}}{\frac{1}{2} v_{\text{merg}}} \tag{D.10}$$

The time the measured gap on the main lane travels before the on-ramp vehicles merges into the gap is for the main part equal to the acceleration time of the merging vehicle. However, the required time gap has to be added, since the gap has already travelled this time before the on-ramp vehicle receives a green light. When using this value, the merging vehicle will merge exactly at the rear of the leading vehicle of the gap however. So, a time variable indicating the time headway between the rear of the leading vehicle of the measured gap and the merging vehicle is introduced. Combining all this information leads to the equation for determining the effective time the measured gap can travel during the process. This time is equal to the acceleration time of the merging vehicle added to the minimum required gap time, minus the time headway to the rear of the leading vehicle of the measured gap.

$$t_{\text{eff}} = t_{\text{acc}} + t_{\text{gap}} - t_{\text{lead}} \tag{D.11}$$

The distance the measured gap has travelled during this time is equal to the effective travel time of the measured gap times the speed of the measured gap. The speed of this measured gap is assumed to be equal to the average speed of the main lane vehicles in this research. This could be adjusted in later iterations to the measured speed of the leading vehicle of the measured gap for example. Nonetheless, the speed is assumed to remain constant for the effective travelling time.

$$s_{\text{main}} = t_{\text{eff}} * v_{\text{main}} \tag{D.12}$$

Using the travelled distance of the measured gap and of the merging vehicle, the location of the gap measurement detector can be determined. This location is equal to the distance travelled by the measured gap minus the travelled acceleration distance of the merging vehicle.

$$x_{\text{loop}} = s_{\text{main}} - s_{\text{eff}} \tag{D.13}$$

To ascertain that the same gap for a single vehicle is not used for both a truck and a passenger vehicle, the minimum waiting time is put in place. This minimum waiting time is used when a passenger vehicle follows up on a truck. This waiting time can be computed by dividing the difference in the location of the gap measurement loop detectors by the travelling speed of the measured gap added to the required minimum gap time.

$$t_{\text{wait}} = \frac{x_{\text{loop}}^{truck} - x_{\text{loop}}^{car}}{v_{\text{main}}} + t_{\text{gap}}^{truck} \tag{D.14}$$

This should also prevent the need for a passenger vehicle to overtake a truck to reach the gap in time. However, to make sure these situations do not occur, an additional minimum waiting time can be computed. This additional minimum waiting time is dependent on the speed of the truck when reaching the estimated merging point for the passenger vehicle and the time it takes for the truck to get to that location with the average speed between zero and that location. The speed of the truck at the merging location of the passenger vehicle can be calculated taking the square root of the two times the acceleration distance of the passenger car times the average acceleration of the truck for that distance. The average acceleration for the truck in turn can be computed by multiplying the maximum truck acceleration (i.e. at the beginning of the acceleration trajectory) by a factor indicating the average acceleration over the entire acceleration trajectory.

$$z^{\text{truck}} = \sqrt{2 * s_{\text{eff}}^{car} * a_{\text{max}}^{truck} * a_{\text{av}}^{truck}} \tag{D.15}$$

Then, the time it takes the truck to get to the assumed merging location of the passenger car can be determined. This time is equal to the distance of the acceleration of the passenger vehicle divided by the average speed of the truck. The average speed of the truck in turn is equal to half the speed of the truck when reaching the location of the merging manoeuvre of the passenger car, assuming a constant acceleration.

$$y^{\text{truck}} = \frac{s_{\text{eff}}^{car}}{\frac{1}{2} z^{\text{truck}}} \tag{D.16}$$

The used minimum waiting time for a passenger car that succeeds a truck can then be calculated by taking the maximum of the original t_{wait} and the waiting time that is obtained by subtracting the acceleration time of the car to their merging point from the acceleration time of the truck to the assumed acceleration point of the passenger car.

$$t_{\text{wait}} = \max\left(\frac{x_{\text{loop}}^{truck} - x_{\text{loop}}^{car}}{v_{\text{main}}} + t_{\text{gap}}^{truck}, y^{\text{truck}} - t_{\text{acc}}^{car} \right) \tag{D.17}$$

Again, this should always be equal to the originally calculated minimum waiting time following the calculations regarding the differences in the gap measurement loop detectors. Nevertheless, this way it is ensured that a passenger car is not hindered by a truck in such a way that it can not merge in the measured gap for the passenger car.

E ADDITIONAL OUTPUT FIGURES AND TABLES

In this appendix some additional outputs that are specifically referenced in the text of Chapter 7 are displayed. First off all, the base case OTS output is repeated. This is done in order to make this table more accessible to the reader when comparing the various results to this base case scenario. An overview of the KPIs that are reported in the tables can be found in Appendix A.

Table E.1: Mean OTS output values of the base case scenario

Base case scenario									
Mean									
Control settings	AvDSys	AvDMain	AvDOn	AvDOff	GotGreen	WaitLong	success	Activation	Deactivation
No control	88	75	254	58					
Rijkswaterstaat	48	37	176	31	558			650	6054
Microscopic 1	47	35	186	30	537	12	42	536	6070
Microscopic 2	57	45	203	35	635	7	27	1026	6114
Total	60	48	205	38	577	9	34	740	6080

The first explicitly mentioned conclusions regarding these outputs are with regards to the semi-permeable lane demarcation sensitivity analysis. This table is displayed in Table E.2.

Table E.2: Mean OTS output values of the first sensitivity analysis

Semi-permeable lane demarcation sensitivity analysis									
Mean									
Control settings	AvDSys	AvDMain	AvDOn	AvDOff	GotGreen	WaitLong	success	Activation	Deactivation
No control	109	93	306	73					
Rijkswaterstaat	52	42	181	34	566			556	6090
Microscopic 1	46	34	196	27	525	13	35	524	6075
Microscopic 2	96	81	281	64	610	9	14	812	6226
Total	76	62	240	49	567	11	24	631	6130

Thereafter, the sensitivity analysis regarding the various truck percentages is mentioned. The corresponding tables are displayed in Table E.3 and Table E.4

Table E.3: Mean OTS output values of the 0% truck percentage sensitivity analysis

0% **truck percentage at the on-ramp**									
Mean									
Control settings	AvDSys	AvDMain	AvDOn	AvDOff	GotGreen	WaitLong	success	Activation	Deactivation
No control	76	61	258	45					
Rijkswaterstaat	46	35	178	30	562			456	6052
Microscopic 1	54	42	200	33	638	6	28	830	6090
Microscopic 2	48	35	195	29	535	12	42	752	6082
Total	56	43	208	34	578	9	35	679	6077

Table E.4: Mean OTS output values of the 10% truck percentage sensitivity analysis

10% **truck percentage at the on-ramp**									
Mean									
Control settings	AvDSys	AvDMain	AvDOn	AvDOff	GotGreen	WaitLong	success	Activation	Deactivation
No control	105	90	284	70					
Rijkswaterstaat	54	44	176	36	570			484	6114
Microscopic 1	61	49	198	41	530	12	35	862	6139
Microscopic 2	82	68	242	55	608	8	18	1359	6161
Total	75	63	224	50	569	10	27	897	6132

The next explicitly mentioned conclusions regarding these outputs are with regards to the main lane demand sensitivity analyses. Therefore, the lower main lane demand outputs are displayed in Table E.5 and the outputs for the increased main lane demand are shown in Table E.6.

Table E.5: Mean OTS output values of the lower main lane demand scenario

−10% **main lane demand scenario**									
Mean									
Control settings	AvDSys	AvDMain	AvDOn	AvDOff	GotGreen	WaitLong	success	Activation	Deactivation
No control	58	45	200	32					
Rijkswaterstaat	36	24	158	17	652			588	6028
Microscopic 1	34	20	179	14	540	11	42	850	6043
Microscopic 2	45	33	177	25	626	5	28	1122	6026
Total	43	31	179	22	606	8	35	853	6031

Table E.6: Mean OTS output values of the higher main lane demand scenario

+10% **main lane demand scenario**									
Mean									
Control settings	AvDSys	AvDMain	AvDOn	AvDOff	GotGreen	WaitLong	success	Activation	Deactivation
No control	120	105	332	82					
Rijkswaterstaat	54	43	189	37	484			324	6134
Microscopic 1	59	47	212	39	522	14	36	640	6189
Microscopic 2	84	71	260	57	645	9	19	882	6416
Total	79	67	248	54	550	11	28	615	6247

Besides these outputs, the main lane slanted cumulative curves are mentioned in Chapter 7. The corresponding slanted cumulative curves are illustrated in Figure E.1, Figure E.2 and Figure E.3. These correspond respectively with the decreased main lane demand scenario, the base case scenario and the increased main lane demand scenario. The axis for all figures are kept identical.
The next sensitivity analyses in Chapter 7 which refers to the additional tables is the sensitivity analysis regarding the changes in the on-ramp demand adjustments. Firstly, in Table E.7 the outputs for the decreased on-ramp demand are displayed. Secondly, the results regarding the increased on-ramp demand are shown in Table E.8.

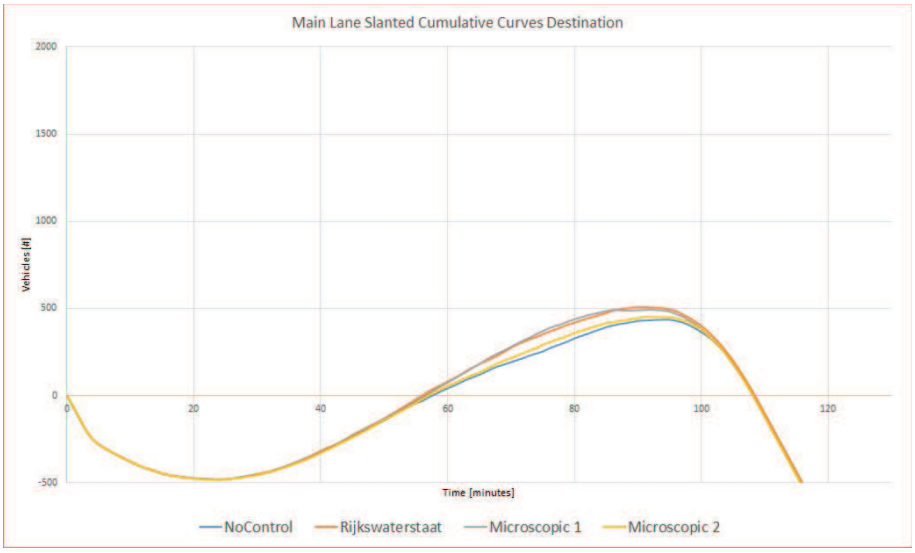

Figure E.1: Decreased main lane scenario main lane Slanted Cumulative Curves

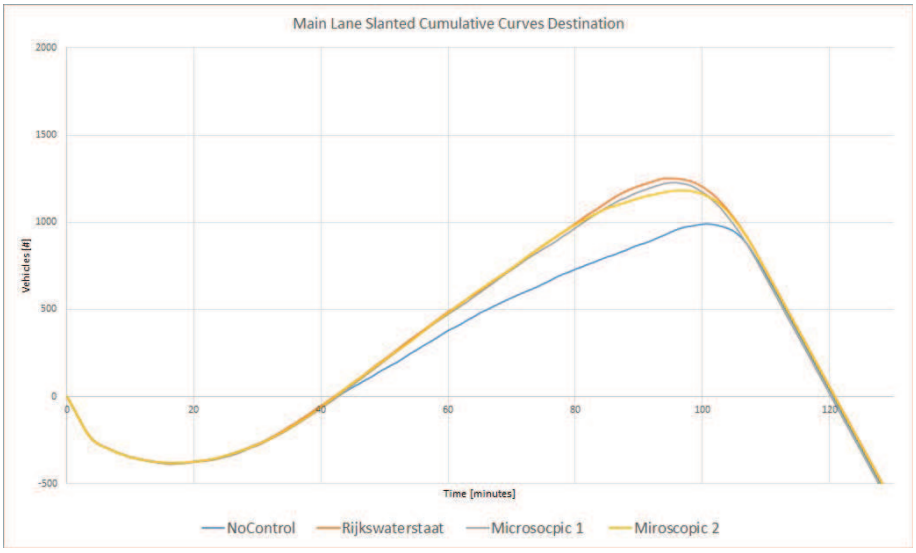

Figure E.2: Base case scenario main lane Slanted Cumulative Curves

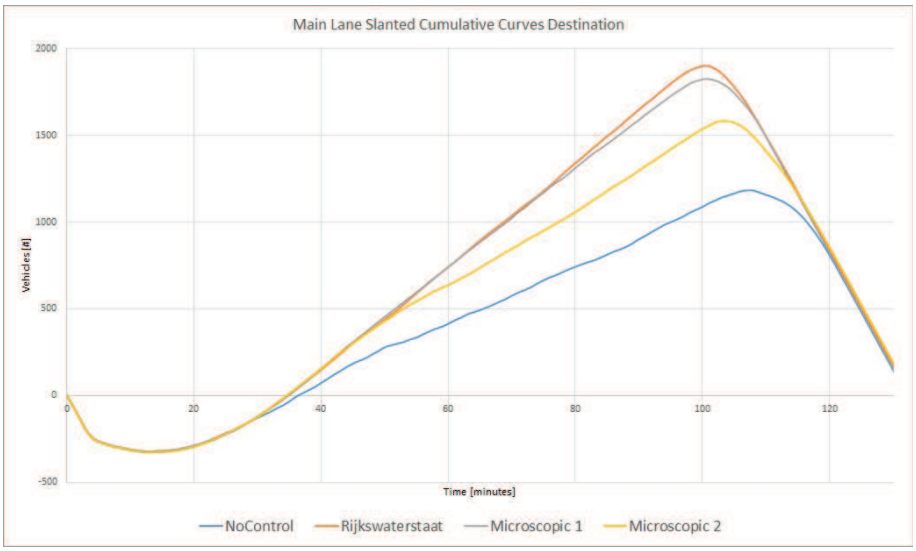

Figure E.3: Increased main lane scenario main lane Slanted Cumulative Curves

Table E.7: Mean OTS output values of the lower on-ramp demand scenario

−10% **on-ramp demand scenario** **Mean** Control settings	AvDSys	AvDMain	AvDOn	AvDOff	GotGreen	WaitLong	success	Activation	Deactivation
No control	78	67	231	51					
Rijkswaterstaat	53	42	193	35	544			834	6102
Microscopic 1	52	40	200	34	530	12	39	690	6094
Microscopic 2	61	50	214	40	609	7	23	918	6132
Total	61	50	209	40	561	10	31	814	6109

Table E.8: Mean OTS output values of the higher on-ramp demand scenario

+10% **on-ramp demand scenario** **Mean** Control settings	AvDSys	AvDMain	AvDOn	AvDOff	GotGreen	WaitLong	success	Activation	Deactivation
No control	97	82	268	63					
Rijkswaterstaat	50	39	165	32	585			466	6074
Microscopic 1	54	41	188	33	540	12	38	918	6096
Microscopic 2	70	57	208	46	634	7	24	927	6128
Total	68	55	207	44	586	9	31	768	6097

The following sensitivity analyses in Chapter 7 which refers to the additional tables is the sensitivity analysis regarding the changes in the off-ramp demand adjustments. Firstly, in Table E.9 the outputs for the decreased off-ramp demand are displayed. Secondly, the results regarding the increased off-ramp demand are shown in Table E.10.

Table E.9: Mean OTS output values of the lower off-ramp demand scenario

−10% **off-ramp demand scenario** **Mean**									
Control settings	AvDSys	AvDMain	AvDOn	AvDOff	GotGreen	WaitLong	success	Activation	Deactivation
No control	93	78	273	59					
Rijkswaterstaat	42	30	177	23	579			410	6074
Microscopic 1	48	35	201	28	522	13	38	676	6098
Microscopic 2	50	37	206	27	606	8	25	844	6074
Total	58	45	215	34	568	10	32	644	6083

Table E.10: Mean OTS output values of the higher off-ramp demand scenario

+10% **off-ramp demand scenario** **Mean**									
Control settings	AvDSys	AvDMain	AvDOn	AvDOff	GotGreen	WaitLong	success	Activation	Deactivation
No control	99	87	257	70					
Rijkswaterstaat	59	49	179	42	544			512	6114
Microscopic 1	56	45	189	39	548	11	41	776	6098
Microscopic 2	74	61	226	50	640	6	22	1104	6162
Total	72	60	213	50	577	8	31	797	6122

The final analyses which refers to the additional tables in this appendix, is the sensitivity analysis revolving around the various speed limits. In Table E.11, the results regarding a decreased maximum speed limit to $80\frac{km}{hour}$ is illustrated. The results regarding a maximum speed limit of $120\frac{km}{hour}$ are shown in Table E.12.

Table E.11: Mean OTS output values of the $80\frac{km}{hour}$ speed limit scenario

$80\frac{km}{hour}$ **speed limit scenario** **Mean**									
Control settings	AvDSys	AvDMain	AvDOn	AvDOff	GotGreen	WaitLong	success	Activation	Deactivation
No control	108	90	320	79					
Rijkswaterstaat	69	58	196	55	575			860	6340
Microscopic 1	94	77	287	68	612	8	20	1014	6443
Microscopic 2	101	84	312	74	602	11	11	1429	6508
Total	93	77	278	69	596	10	16	1094	6432

Table E.12: Mean OTS output values of the $120\frac{km}{hour}$ speed limit scenario

$120\frac{km}{hour}$ **speed limit scenario** **Mean**									
Control settings	AvDSys	AvDMain	AvDOn	AvDOff	GotGreen	WaitLong	success	Activation	Deactivation
No control	81	70	222	50					
Rijkswaterstaat	49	38	173	30	572			492	6034
Microscopic 1	64	53	204	40	646	6	23	712	6111
Microscopic 2	70	59	208	43	662	5	16	1246	6090
Total	66	55	202	41	627	6	20	817	6079